Geo-ν & Earth electricity

L.B. Bezrukov (INR, Moscow)

the work done with cooperation I.Karpikov, A.Mezokh, S.Silaeva, V.Sinev (INR, Moscow)

12th Zatsepin Seminar at INR, 27 May 2022

Владимир Николаевич Ларин
– создатель модели
«Изначально богатая водородом Земля» или «Гидридная модель Земли» (НЕ)

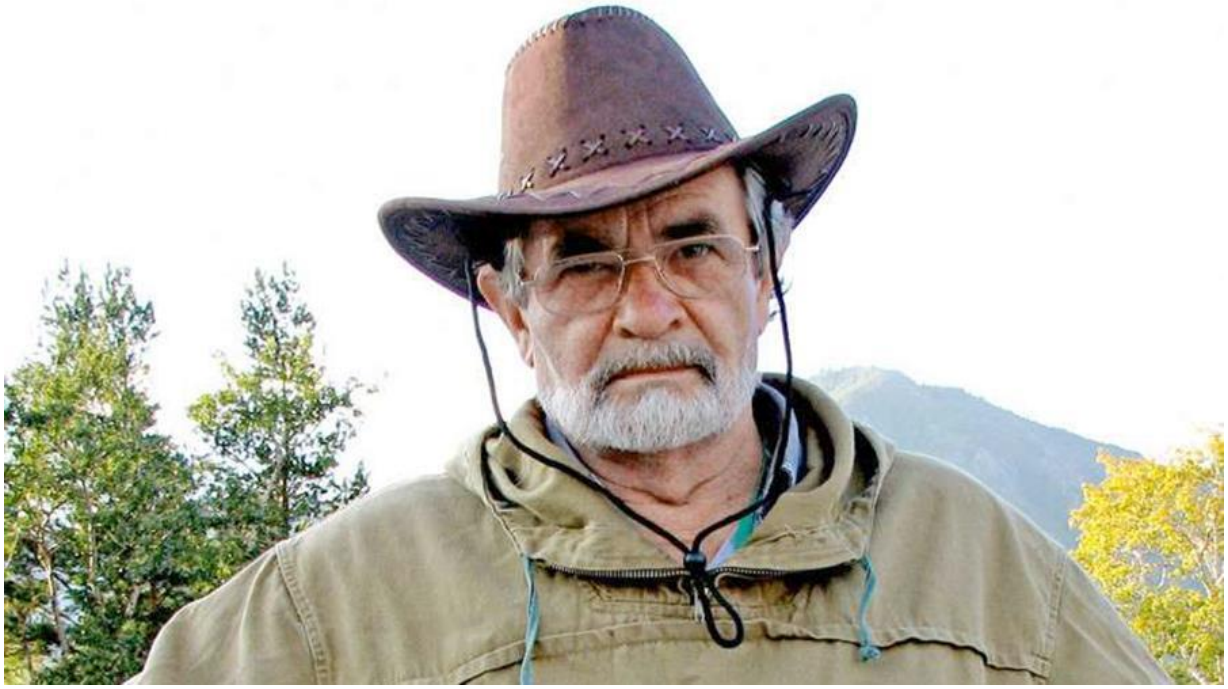

Он выступал в ИЯИ РАН.

Он завещал нам борьбу за правильную модель Земли.

Chemical Differentiation of Planets: A Core Issue.
Hervé Toulhoat and Viacheslav Zgonnik. The Astrophysical Journal, 924:83 (18pp), 2022 January 10 https://doi.org/10.3847/1538-4357/ac300b

Predicted Overall Compositions of the Earth in wt% for Major and Minor Elements

Element	Initially wt%	H Escaped wt%	H Retained wt%	Crust wt%	BSE wt%
H	83.28	0	4.050	1	
C	1.098	**6.579**	6.323	0.35	
N	0.046	0.275	0.264		
O	0.701	4.200	**4.037**	**49**	**30**
Na	0.858	**5.141**	4.941	2.4	
Mg	3.214	**19.249**	18.499	2.35	10 -16
Al	0.864	***5.176***	4.974	7.49	
Si	2.622	**15.702**	15.091	26	12 - 18
S	0.308	1.845	1.773		
K	0.161	0.966	**0.929**	**2.35**	**$2 \cdot 10^{-2}$**
Ca	0.837	**5.015**	4.820	3.52	
Ti	0.026	0.158	0.152		
V	0.0034	0.020	0.0196		
Cr	0.156	0.935	0.898		
Mn	0.076	0.455	0.437		
Fe	5.310	31.804	30.566	4.2	40
Co	0.015	0.093	0.089		
Ni	0.374	2.241	2.153		

Связь потоков гео-антинейтрино с внутренним теплом Земли.

- ^{238}U, ^{235}U, ^{232}Th, ^{40}K decays in the Earth body are the source of heat and geoneutrinos.

- $^{238}U \rightarrow {}^{206}Pb + 8\alpha + 6e + 6\tilde{\nu}_e + 51{,}7$ MeV (47,7)
- $^{232}Th \rightarrow {}^{208}Pb + 6\alpha + 4e + 4\tilde{\nu}_e + 42{,}7$ MeV(40,4)
- $^{40}K \rightarrow {}^{40}Ca + e + \tilde{\nu}_e + 1.31$ MeV prob.0,893

  $\rightarrow {}^{40}Ar + \Upsilon + \nu_e + 1.51$ MeV prob.0,1066

НЕ модель: $H_U + H_{Th} \approx 40$ TW, 1% ÷ 1.5% → $H_K = 177 \div 265$ TW.

BSE модель: $H_U + H_{Th} \approx 20$ TW, $H_K \approx 4$ TW.

В гео-науку внедрён результат усреднения измерения потока внутреннего тепла Земли: 47 ± 2 TW.

Prediction 2015, 2020: Borexino will observe 6 ÷ 9 cpd/100tons as CNO-ν events. Expected from CNO-ν in SSM is 4.9 cpd/100tons

Geoneutrino and Hydridic Earth model. Version 2. **Leonid Bezrukov**. INR Preprint: 1378/2014, January 2014, Moscow. **arXiv:1308.4163v2** [astro-ph.EP]

V.V.Sinev, L.B.Bezrukov, E.A.Litvinovich, I.N.Machulin, M.D.Skorokhvatov, S.V.Sukhotin. Looking for Antineutrino Flux from ^{40}K with Large Liquid Scintillator Detector, Physics of Particles and Nuclei.46 (2015) 186, doi:10.1134/S1063779615020173; arXiv:1405.3140 [physics.ins-det].

L.B.Bezrukov, I.S.Karpikov, A.S.Kurlovich, A.K.Mezhokh, S.V.Silaeva, V.V.Sinev, V.P.Zavarzina, On the contribution of the ^{40}K geo-antineutrino to single Borexino events. (2020) arXiv:2004.02533v2 [hep-ex]

On first detection of solar CNO neutrinos. arXiv:2007.07371v2 [hep-ex physics.ins-det] L. B. Bezrukov, I. S. Karpikov, A. S. Kurlovich, A. K. Mezhokh, S. V. Silaeva, V. V. Sinev, V. P. Zavarzina. Интерпретация первой регистрации солнечных нейтрино CNO цикла детектором БОРЕКСИНО. *Л. Б. Безруков, В. П. Заварзина, И. С. Карпиков, А. С. Курлович, А. К. Межох, С. В. Силаева, В. В. Синёв.* Известия Российской Академии Наук, Серия физическая. № 4, том 85**,** *с.566-569***.** 2021.
DOI: 10.3103/S1062873821040067

Энергетический спектр электронов отдачи при рассеянии нейтрино (или антинейтрино) на электронах сцинтиллятора а детекторе Borexino. Красным – солнечные CNO нейтрино, зелёным и синим – CNO нейтрино + ^{40}K гео-антинейтрино.

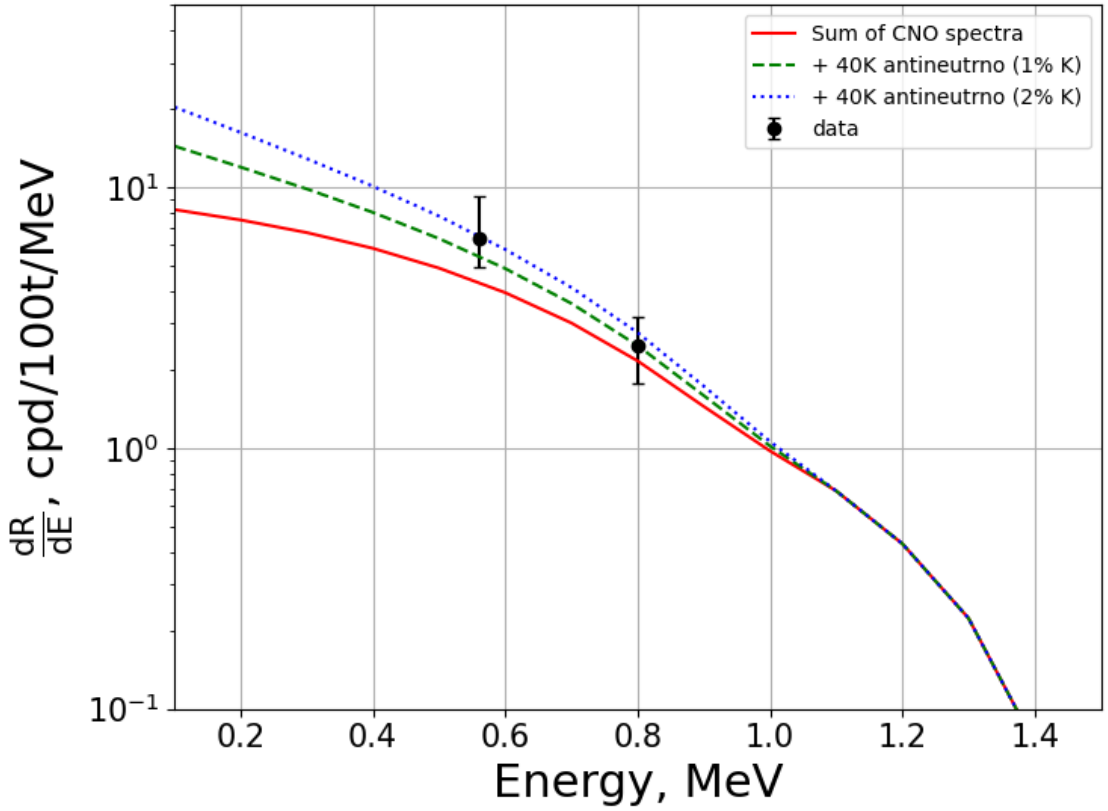

Potassium abundance in the Earth and Borexino data. L.Bezrukov, A.Gromtseva, I.Karpikov, A.Kurlovich, A.Mezhokh, P.Naumov, Ya.Nikitenko, S.Silaeva, V.Sinev, V.Zavarzina. arXiv:2202.08531 [physics.ins-det]

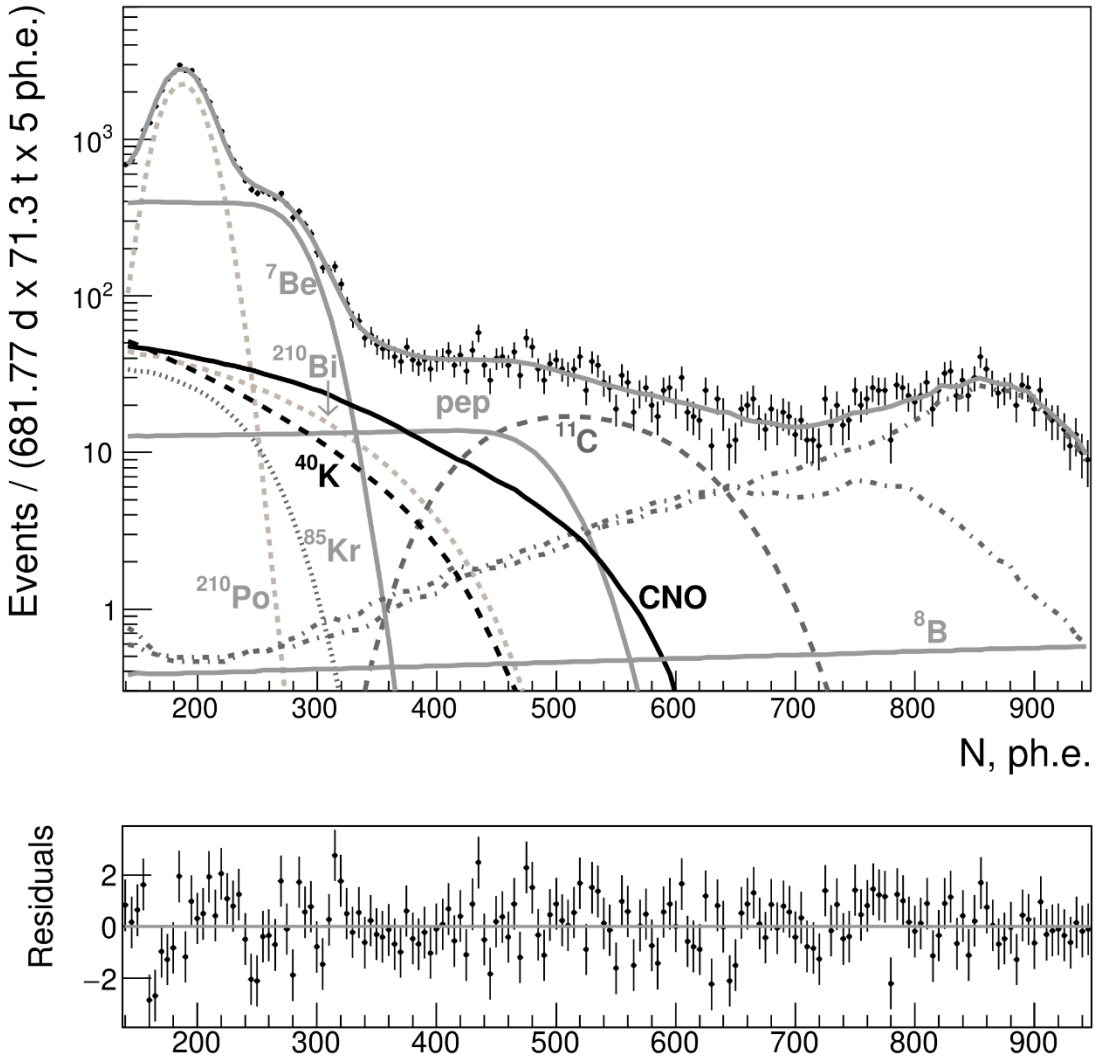

K-geo-ν. Выводы

- Добавление событий от ^{40}K-geo-ν при анализе данных Борексино позволяет улучшить согласие экспериментального и фитированного спектров при скоростях счёта событий: $R(^{40}\text{K-geo-}\nu)$ = 7.05 cpd/100t, $R(^{210}\text{Bi})$ = 6 cpd/100t и $R(^{85}\text{Kr})$ = 3.76 cpd/100t. Скорости счёта событий от CNO-ν и остальных источников не изменяются. Полученная скорость счёта от ^{40}K-geo-ν соответствует 3.9% калия от массы Земли.

- Можно предложить детектор нового поколения, который сможет зарегистрировать поток калийных гео-антинейтрино с высокой достоверностью. Это – детектор типа Борексино, но с очищенным от радиоактивности нейлоновым внутренним мешком. Это позволит измерить концентрацию ^{210}Bi в сцинтилляпоре и увеличит статистику.

На основе Гидридной модели Земли мы создали новую модель земного электричества.

Эта новая модель единым образом объясняет:

1. Механизм образования электрического поля Земли.
2. Природу теллурических токов.
3. Унитарную вариацию атмосферного электрического поля хорошей погоды.
4. Изменение земного электрического поля в момент землетрясения.
5. Электродный эффект и положительный заряд земной коры.
6. Отвечает на вопрос о месте расположения отрицательного электроды Земного конденсатора.
7. Природу высыпания электронов из магнитных поясов Земли в момент землетрясения.
8. Устанавливает связь между электрическим и магнитным полями Земли.

Negative charge is under lithosphere. L.B.Bezrukov.

The International Astroparticle Physics Workshop
July 22 - 27, 2012. Ulan-Ude, Baikal, Russia

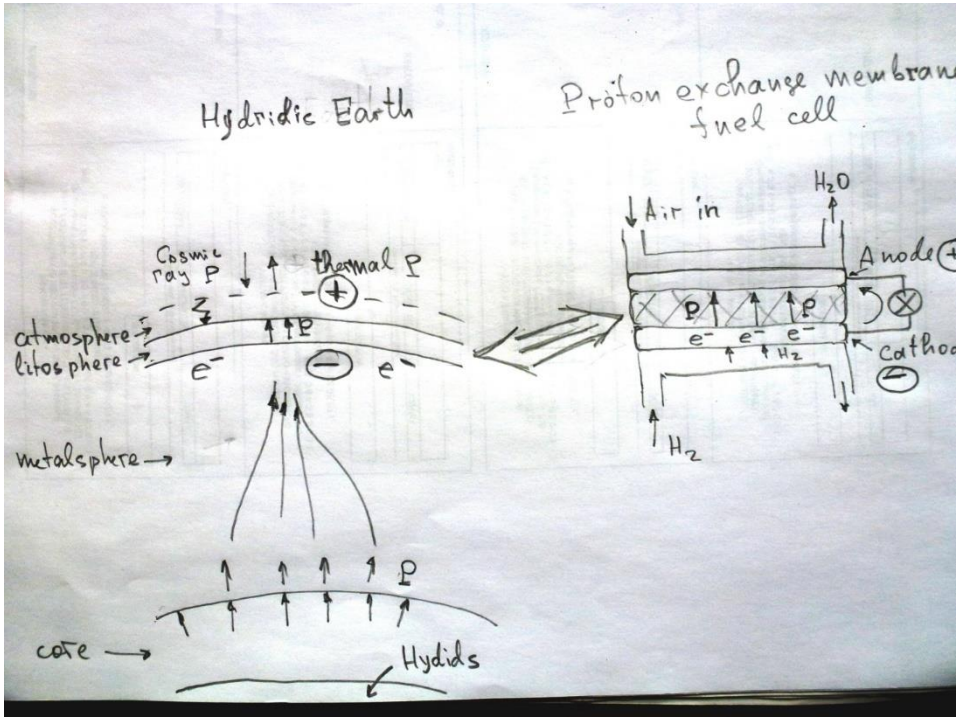

Доклады Академии наук. 2018.

Л. Б. Безруков, В. П. Заварзина, А. С. Курлович, Б. К. Лубсандоржиев, А. К. Межох, В. П. Моргалюк, В. В. Синёв.

ОБ ОТРИЦАТЕЛЬНО ЗАРЯЖЕННОМ СЛОЕ ЭЛЕКТРИЧЕСКОГО ПОЛЯ ЗЕМЛИ // Доклады Академии наук. 2018. Т. 480. № 2. С. 155-157.

Фото автономного стенда по долговременному наблюдению за избытком положительно заряженных аэроионов, расположенного в подземной невентилируемой лаборатории НИИЯФ МГУ с глубиной 12.7 м.

Фото модифицированного счётчика ионов Сапфир-3М

Фото серийного счётчика ионов Сапфир-3М, расположенного в подземной (слабовентиллируемой) лаборатории Центра подземной физики частиц (CUPP) университета Оулу (Финляндия) в медной шахте Пюхясалми (Pyhäsalmi) на глубине 1440 м.

Зависимость плотности аэроионов обоих знаков от времени. Измерения проводились с 03 декабря 2021 г. до 19 декабря 2021 г. в подземной невентилируемой лаборатории НИИЯФ МГУ с глубиной 12.7 м. Измерения проводились у потолка.

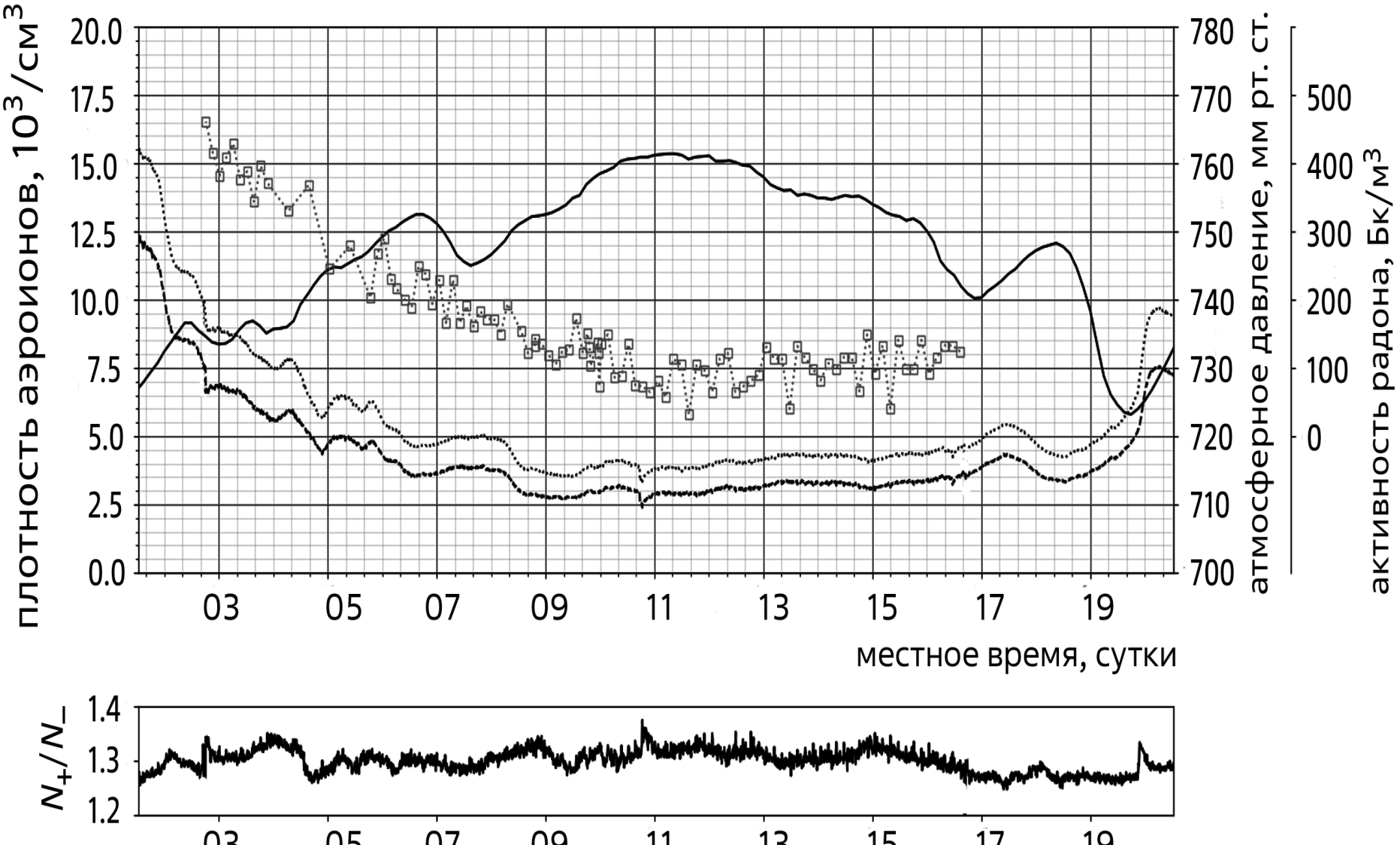

Гидридная модель электрического поля Земли. Выводы

- Приведены исследования плотностей аэроионов в подземной лаборатории НИИЯФ МГУ и в медной шахте Пюхясалми. Во всех проведённых измерениях в невентилируемых подземных помещениях зарегистрирован избыток положительных аэроионов.

- Предложен вариант объяснения наличия избытка положительного заряда в подземных полостях как наличие избытка положительного заряда в коре Земли.

New

- 300 TW
- We observed the predicted fact: The Earth crust (continents and ocean) saturates by positive ions (protons).
- New Earth electric field Новая модель model on the base of HE model is the instrument for earthquake predictions.

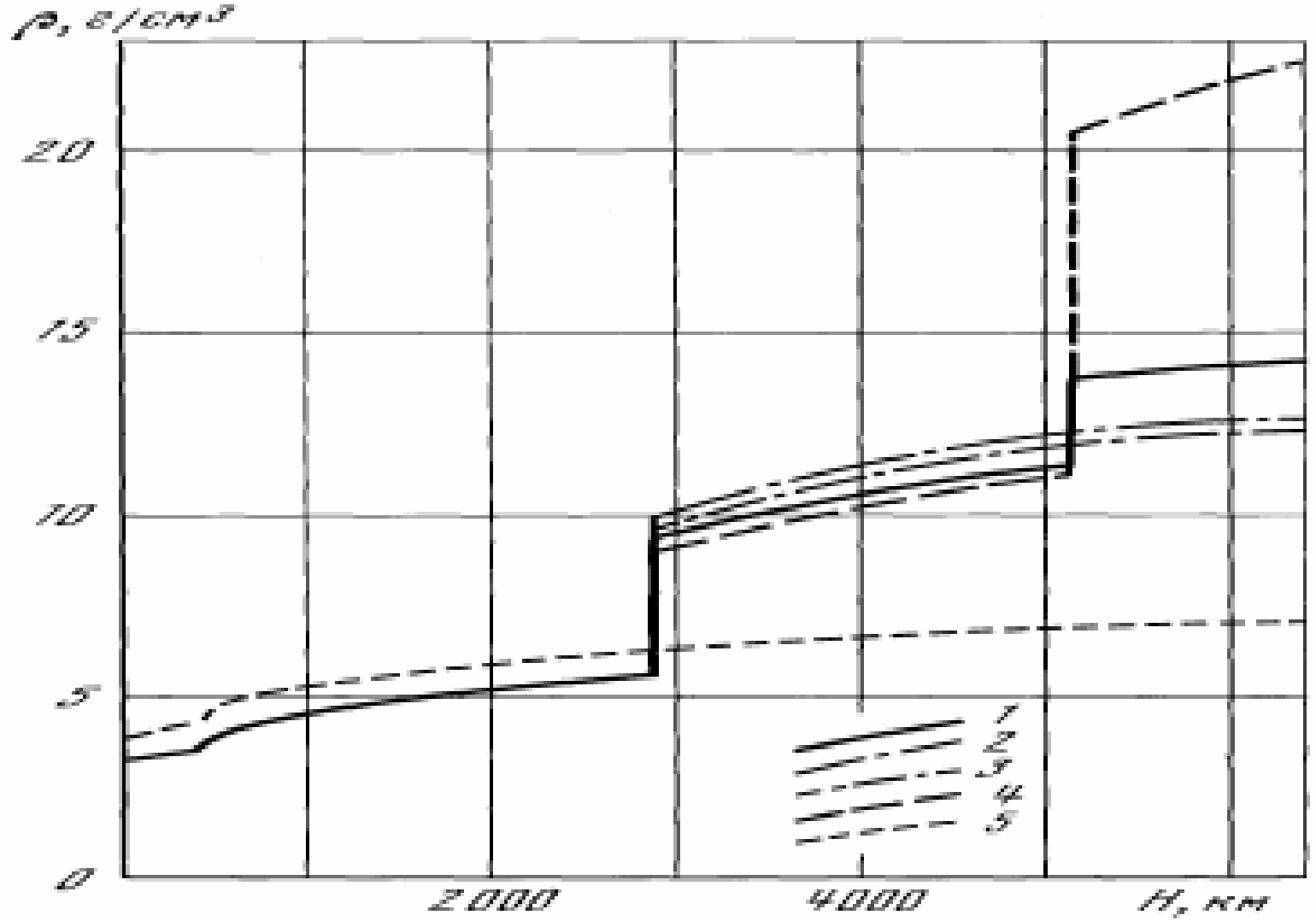
ρ, г/см³
20
15
10
5
0
2000
4000
H, км
1
2
3
4
5

Earth structure

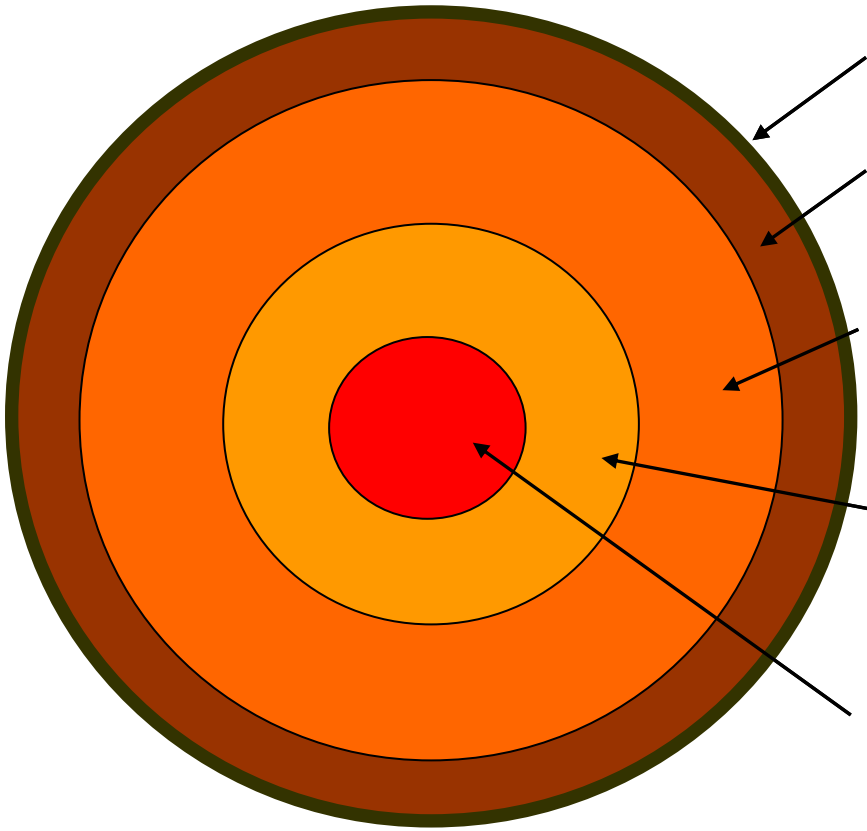

Crust: 7-10 km at ocean bottom and 30-60 km at continents, ρ=~3-3.5 g/cm^3

Upper mantle: ~660-670 km, ρ=~3.5-4 g/cm^3

Lower mantle: ~2900 km, ρ=~5 g/cm^3

Outer core, ~5140 km, ρ=~10-11 g/cm^3

Inner core, ~6371 km, ρ=~12-13 g/cm^3, t = 6000° C

At site http://igppweb.ucsd.edu/~gabi/ data for 2° x 2° were available. (Now 1°x1°)

Seismology

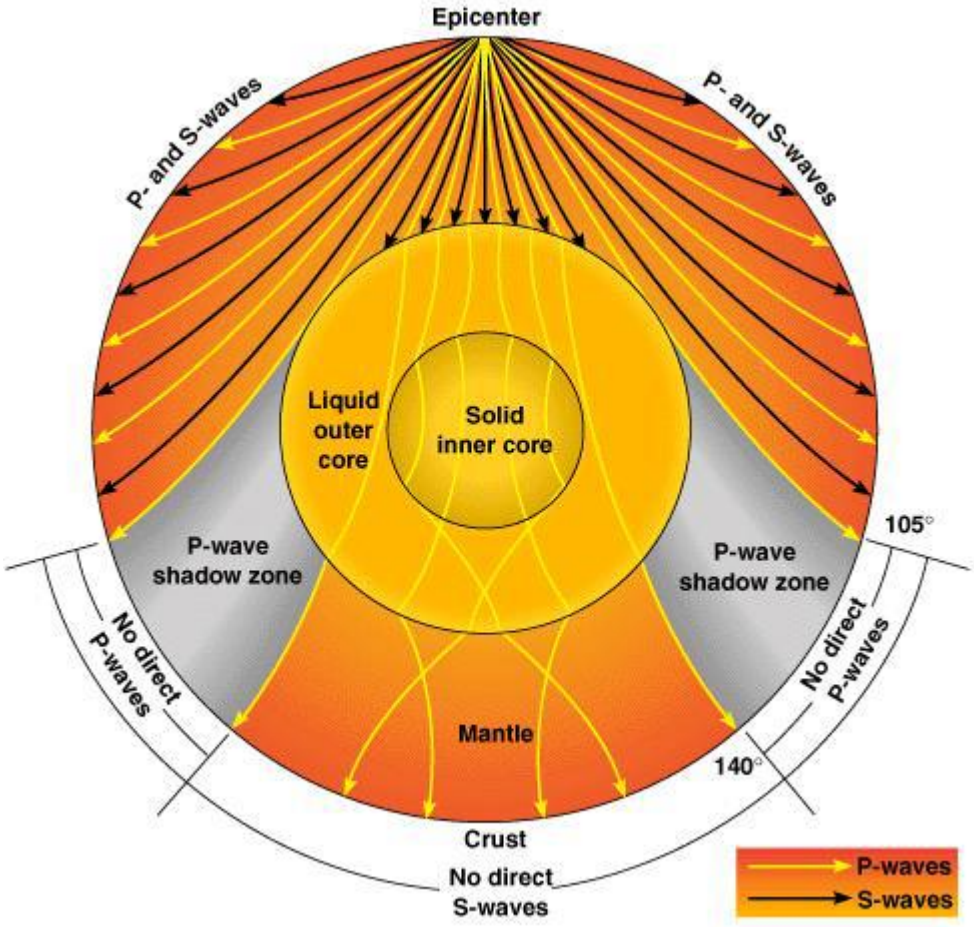

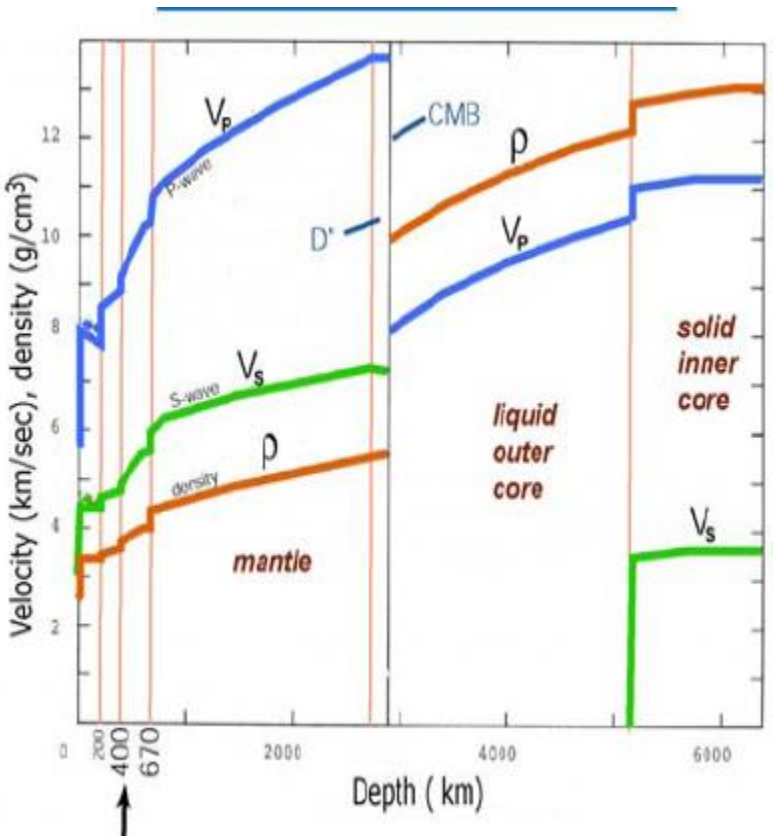

P – primary, longitudinal waves

S – secondary, transverse/shear waves

Bulk Silicate Earth (BSE)

Basic idea:

Earth chemical composition ≡

meteorite chemical composition ≡

Asteroid Belt (AB) chemical composition

Bulk Silicate Earth (BSE)

- **There are no any U, Th, K in Lower mantle and Core**
- **Mantle → oxides**
- **Core → Fe**
- **BSE introduced the problem: The calculated radiogenic heat 20 TW is not enough to explain the experimentally measured one 47 TW**

The asteroid belt (shown in white) is located between the orbits of Mars and Jupiter.

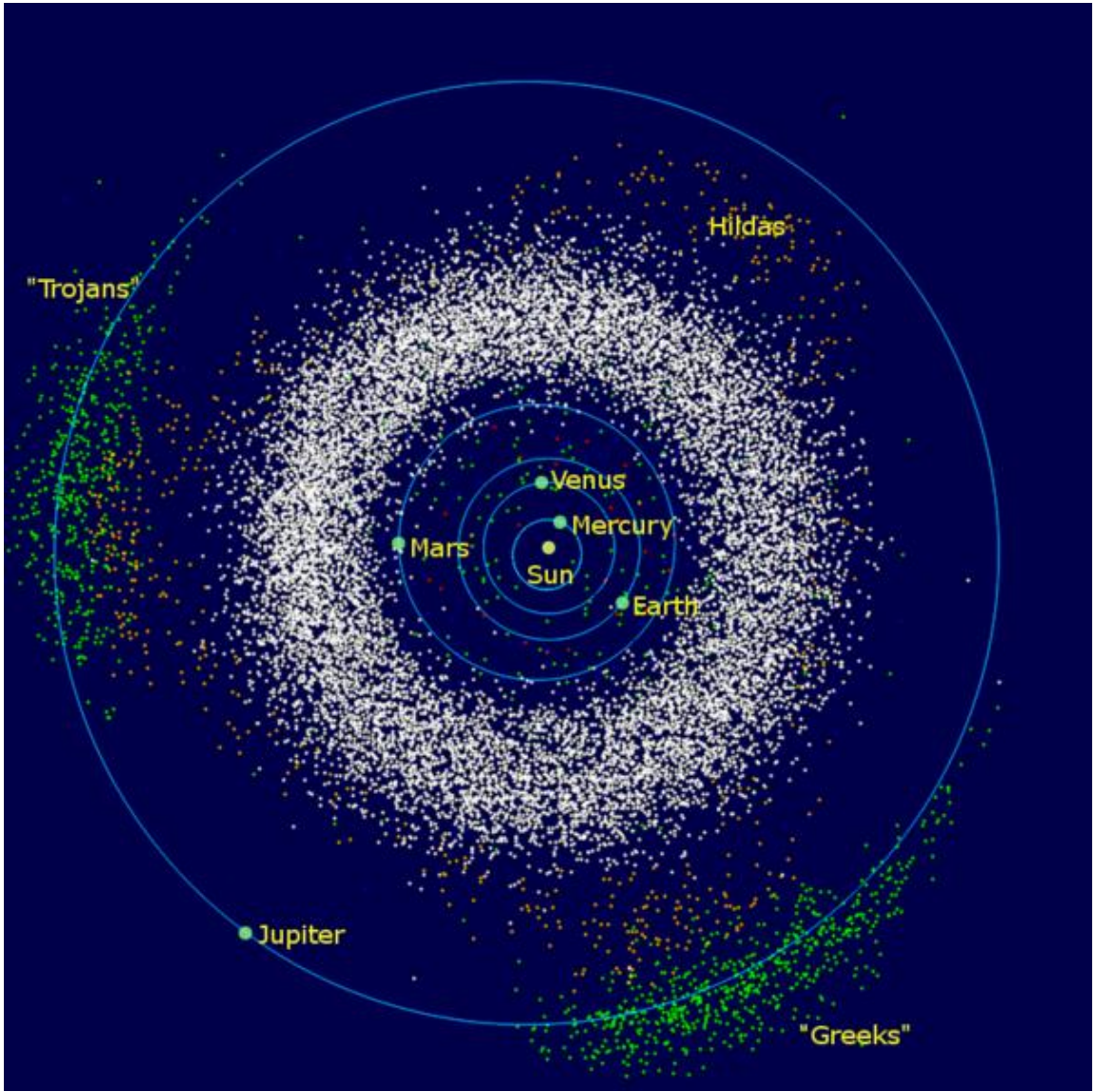

Hydridic Earth (HE) model (primordially Hydrogen-Rich Planet)

was born 40 years ago and does not killed up to now

- Basic idea:

Planet chemical composition depends on distance from the Sun.

Earth chemical composition ≠ Asteroid Belt (AB) chemical composition.

Hydridic Earth
Гидридная Земля

Hydrid Earth model can explain the hydrogen degassation of the Earth.

The Earth hydrogen degassation – the hydrogen starts from surface of the Earth core and goes to the cosmos space through the long chain of processes.

Металлогидридная теория строения Земли В. Н. Ларина позволила объяснить явление водородной дегазации Земли.

1. Ларин В.Н. Гипотеза изначально гидридной Земли (новая глобальная концепция). М., «Недра», 1975, 101 с., (АН СССР. Министерство геологии СССР. ИМГРЭ).

2. Ларин В.Н. Гипотеза изначально гидридной Земли. 2-е изд., перераб. и доп.. - М., Недра. 1980, 216 с

3. Ларин В.Н. Наша Земля (происхождение, состав, строение и развитие изначально гидридной Земли). М. «Агар» 2005, 248 с.

4. Larin,V. N., ed. C. Warren Hunt. Hydridic Earth: the New Geology of Our Primordially Hydrogen-Rich Planet. Polar Publishing, Calgary, Alberta, Canada, 1993.

Larin's law.

- $(X_M/X_{Si})_{Earth} = (X_M/X_{Si})_{Sun} \cdot F(E_{IP}(M))$;

where X_M is the mass fraction in the planet mass of the chemical element with atomic number M,
$E_{IP}(M)$ is the ionization potential of the chemical element with atomic number M in eV,

$F_{Earth}(E_{IP}(M))$ is the law of chemical element differentiation for the Earth.

- $F(E_{IP}(M)) = A \cdot \exp\{- B \cdot E_{IP}(M)\}$

Chemical differentiation of planets: a core issue. Herve Toulhoat, Valerie Beaumont, Viacheslav Zgonnik, Nikolay Larin, Vladimir N. Larin. Aug 2012. 15 pp. e-Print: arXiv:1208.2909 [astro-ph.EP]

Ratio of Earth crust
chemical element abundances
to Sun
chemical element abundances
versus
first ionization potential
of these elements
(normalize to Si)

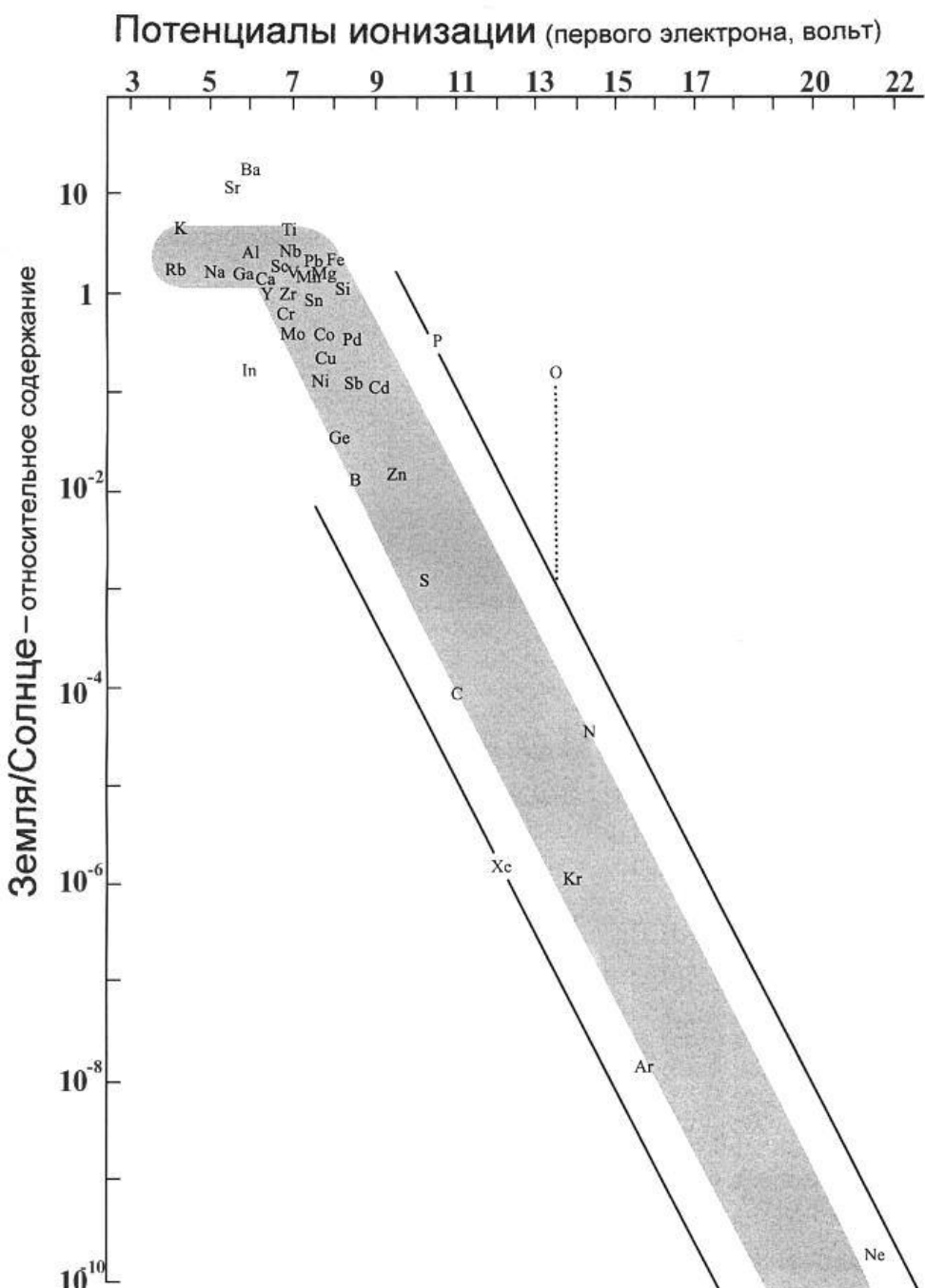

ratio of meteorite chemical element abundances to Earth crust chemical element abundances

Ratio Moon /Earth

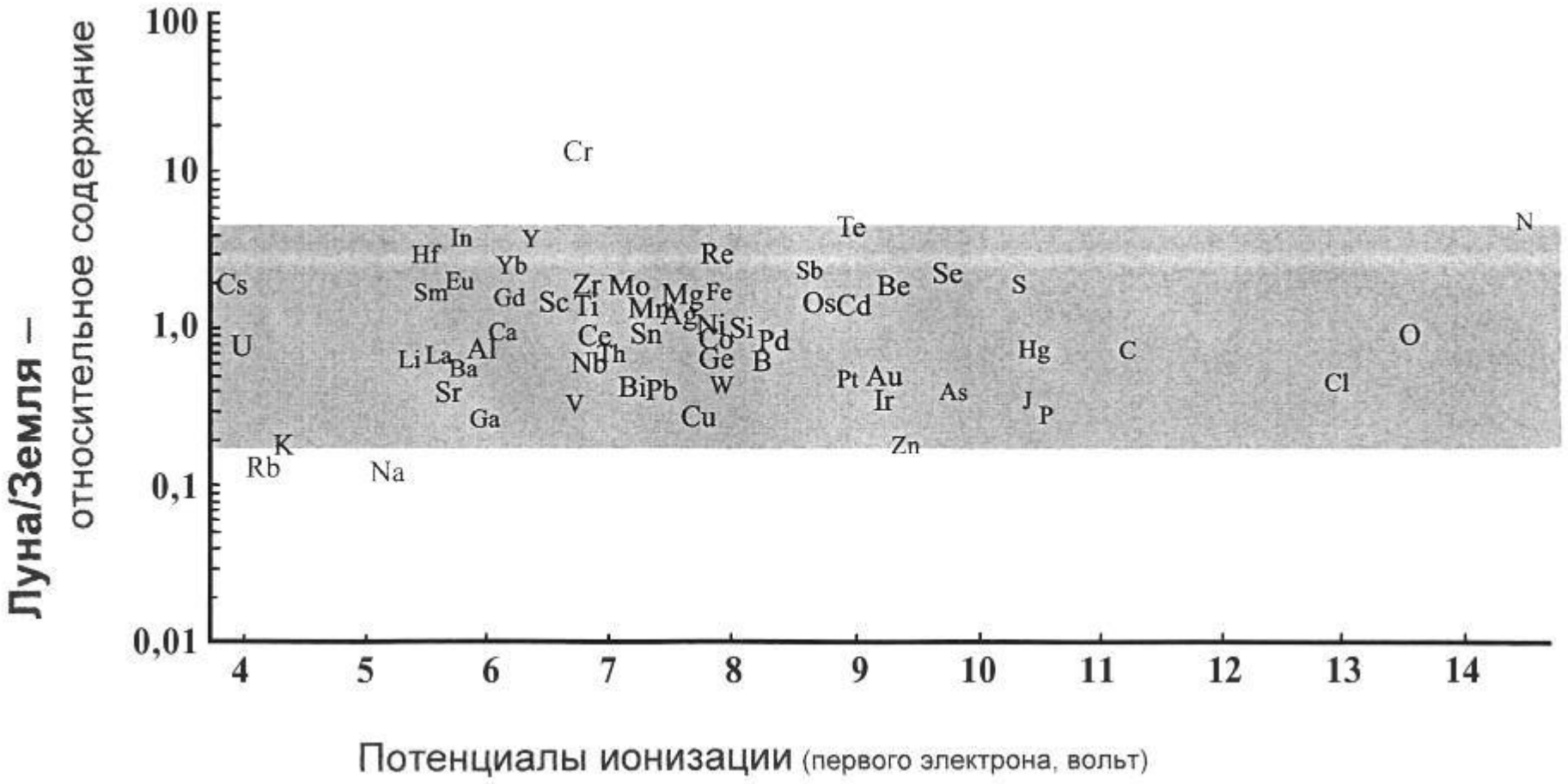

Predicted overall initial composition of the Earth. Major elements are typed in bold (mass fraction larger than 0.1%).

Chemical differentiation of planets: a core issue. Herve Toulhoat, Valerie Beaumont, Viacheslav Zgonnik, Nikolay Larin, Vladimir N. Larin. Aug 2012. 15 pp. e-Print: arXiv:1208.2909 [astro-ph.EP]

Element	wt %	mol %	Element	wt %	mol %	Element	wt %	mol %
H	**1.830E+01**	**87.43**	**Mg**	**1.389E+01**	**2.75**	Sc	3.601E-03	<0.01
He	1.856E-05	<0.01	**Al**	**8.769E+00**	**1.57**	**Ti**	**2.100E-01**	**0.02**
B	4.220E-05	<0.01	**Si**	**9.028E+00**	**1.55**	V	2.329E-02	<0.01
C	**7.550E-01**	**0.30**	P	5.715E-03	<0.01	**Cr**	**1.046E+00**	**0.10**
N	5.562E-03	<0.01	**S**	**3.793E-01**	**0.06**	**Mn**	**4.518E-01**	**0**.04
O	**1.391E-01**	**0.04**	Cl	4.210E-04	<0.01	**Fe**	**1.942E+01**	**1.67**
F	1.260E-07	<0.01	Ar	1.883E-04	<0.01	Co	6.153E-02	0.01
Ne	2.675E-06	<0.01	**K**	**3.760E+00**	**0.46**	**Ni**	**1.627E+00**	**0.13**
Na	**1.341E+01**	**2.81**	**Ca**	**8.792E+00**	**1.06**			
					Balance		1,00E+02	100

Geochemical model of primordial Earth

Geosphere	Depth range, km	Composition
Lithosphere	0 - 30	CaO;MgO; Al_2O_3; SiO_2;Na_2O; Fe_2O_3;H_2O
External core	30 - 2360	$MgH_{0,1}$; $SiH_{0,1}$; $FeH_{0,1}$ +MgH_n; SiH_n; FeH_n (n = 10)
Fe Core	2360 - 3730	Fe; Ni; Cr

Geochemical model of modern Earth

Geosphere	Depth range, km	Composition
Lithosphere	0 - 150	CaO;MgO; Al_2O_3; SiO_2;Na_2O; Fe_2O_3;H_2O
Asthenosphere	150	Thin layer of Metalsphere with high hydrogen concentration
Metalsphere	150 - 2900	Mg_2Si : Si : FeSi = 6 : 3 : 1
External core	2900 - 5000	$MgH_{0,1}$; $SiH_{0,1}$; $FeH_{0,1}$ +MgH_n; SiH_n; FeH_n (n = 10)
Inernal core	5000 - 6371	Fe; Ni; Cr

Hydride Earth (HE)

- **There are U, Th, K in Lower mantle and Core**
- **Mantle → metallic**
- **Core → FeH_{10} + MgH_{10} + NaH_{10} + …**
- **Percentage of K in Earth mass is 2 %– 4 %**
- **HE model introduced the opposite problem: The calculated radiogenic heat can be up to 650 TW. ^{40}K decay give the main contribution in Earth heat flux.** Leonid Bezrukov. Geoneutrino and Hydridic Earth model. Preprint INR 1378/2014. arXiv:1308.4163
- **HE model predicts that Earth heat flux is not stationary.**

Temperature changes in Earth center and on the surface

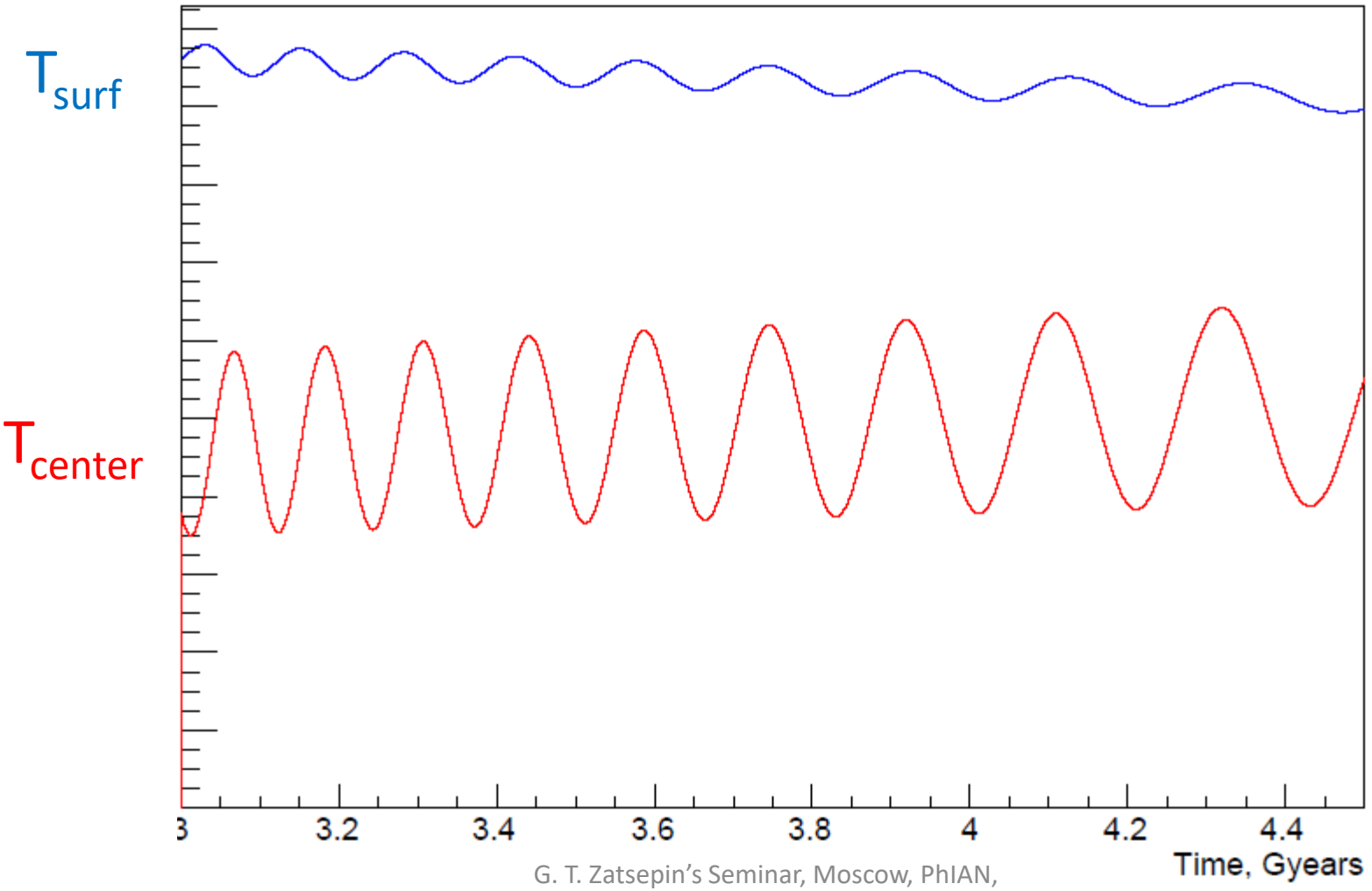

Intrinsic Earth heat + Geoneutrinos

- ^{238}U, ^{235}U, ^{232}Th, ^{40}K decays in the Earth body are the source of heat and geoneutrinos.

- $^{238}U \rightarrow {}^{206}Pb + 8\alpha + 6e + 6\tilde{\nu}_e + 51{,}7$ MeV (47,7)
- $^{232}Th \rightarrow {}^{208}Pb + 6\alpha + 4e + 4\tilde{\nu}_e + 42{,}8$ MeV(40,4)
- $^{40}K \rightarrow {}^{40}Ca + e + \tilde{\nu}_e + 1.32$ MeV(0,598)prob.0,89

  $\rightarrow {}^{40}Ar + \gamma + \nu_e + 1.5$ Mev (1.46) prob.0,1066

Bezrukov L. and Sinev V. report at MIAPP, 2014, Munich

- **We introduce the new problem: where and how the Earth radiogenic heat is lost?**
- **We support the idea that the Earth heat flux can be not stable.**

http://users.ph.tum.de/ga24wax/2014_W2_slides/BezrukovL_MIAPP.pdf

Leonid Bezrukov. Geoneutrino and Hydridic Earth model. Preprint INR 1378/2014. arXiv:1308.4163

Conductive Heat Flux: F = æΔT/h

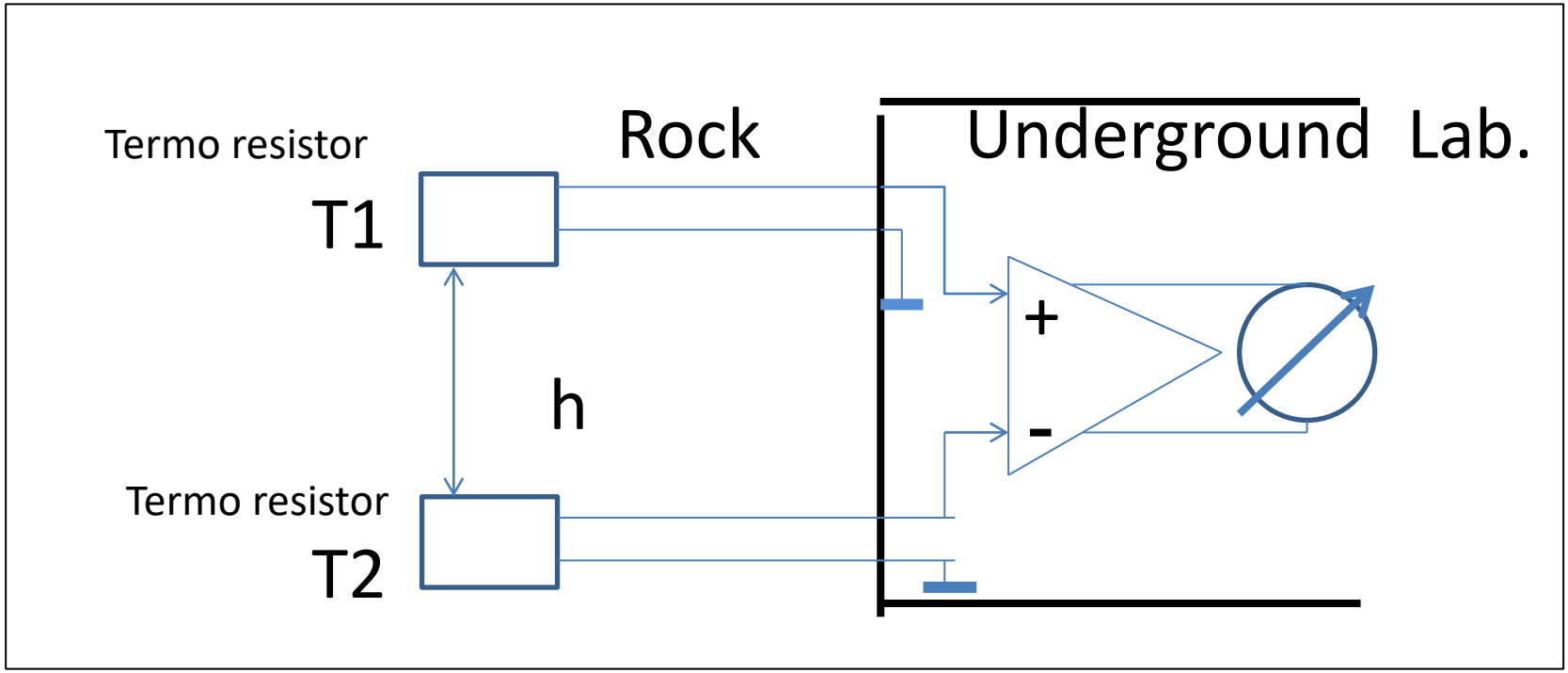

Surface heat flux

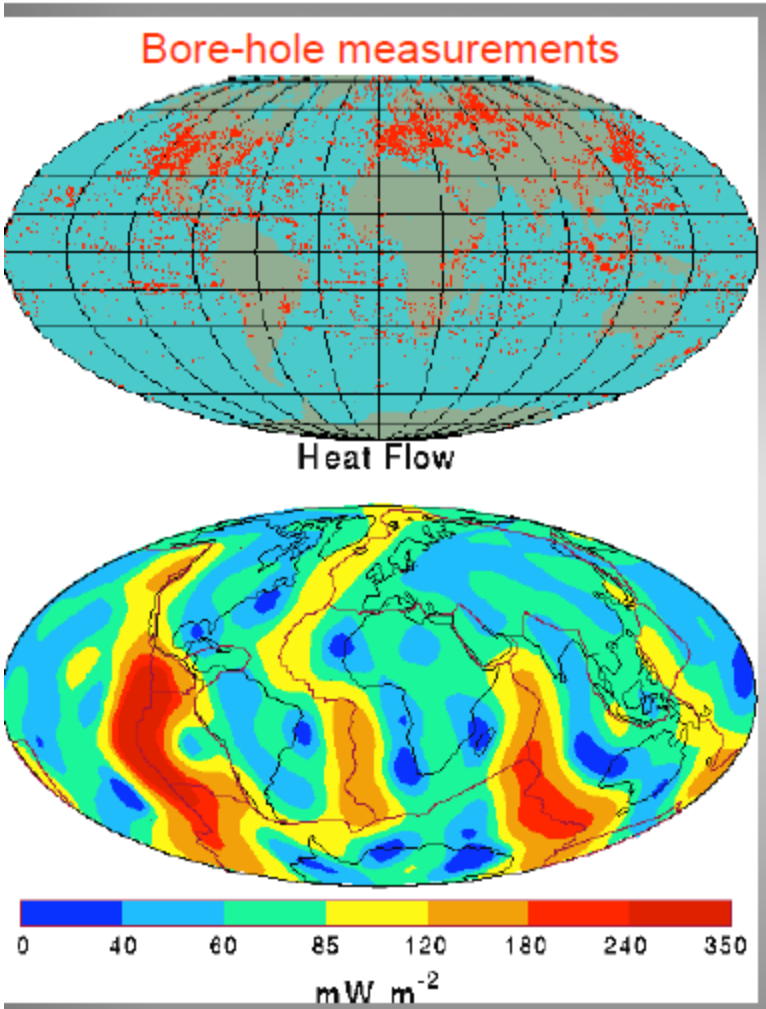

Global Heat Flow Data (Pollack *et al.*)

- Conductive heat flow from bore-hole temperature gradient;
- **Total surface heat flux:**
  31 ± 1 TW (Hofmeister&Criss 2005)
  46 ± 3 TW (Jaupart et all 2007)
  47 ± 2 TW (Davis&Davies 2010)
  (same data, different analysis)

SYSTEMATIC ERRORS

Different assumptions concerning the role of fluids in the zones of mid ocean ridges.

Результаты измерения температуры в скважине «Рукхоуп» (Станоп, Северная Англия).

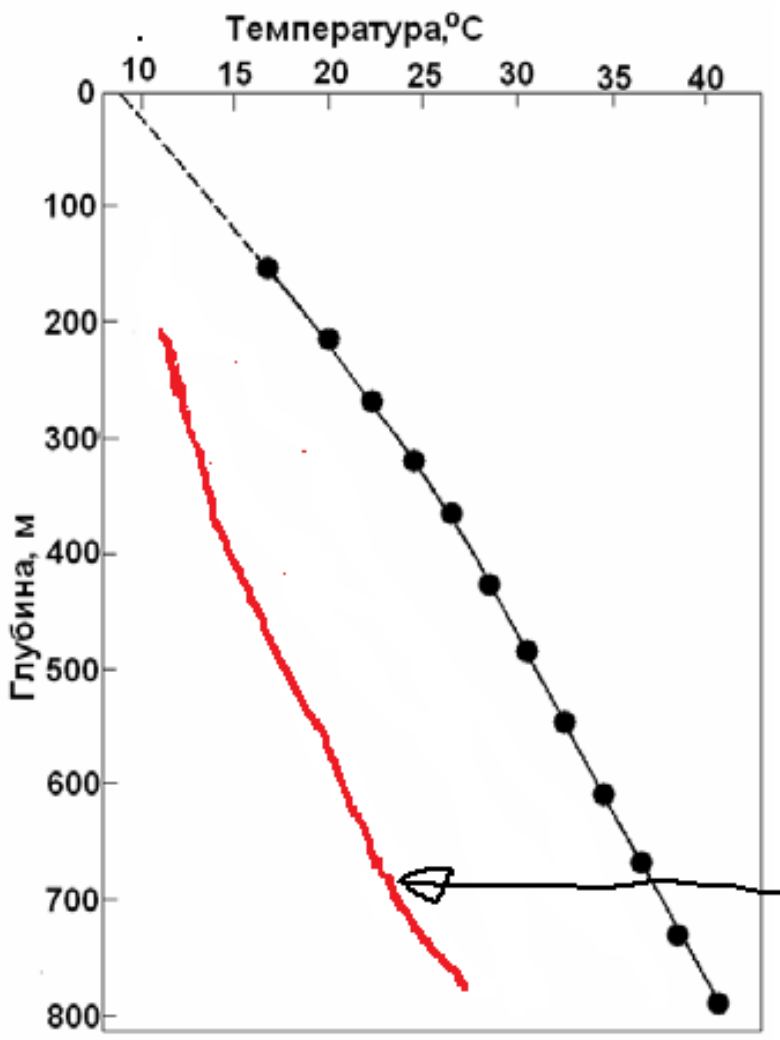

$$\frac{\partial}{\partial z}\left(\lambda \frac{\partial T}{\partial z}\right) = -P(z)$$

$$P(z) = 0, \quad \lambda = \lambda_0 \frac{T_0}{T}$$

$$\frac{1}{T}\frac{\partial T}{\partial z} = \text{const}$$

$$T = e^{\text{const} \cdot z}$$

The way of heat transfer in HE model: the gas carries up the binding energy

- Silane - SiH_4 - gas from -112 to 450 °C

Formation: $Mg_2Si + 4H^+ = 2Mg^{2+} + SiH_4 \uparrow - Q$

Decomposition: $SiH_4 + 2H_2O = SiO_2 + 4H_2 \uparrow + Q$

SiH_4 slowly dissolves in water and the decomposition reaction goes slowly under normal conditions – 20% per day.

ARGO PROJECT: Global array of free-drifting profiling floats that will measure the temperature of the upper 2000 m of the ocean in real-time

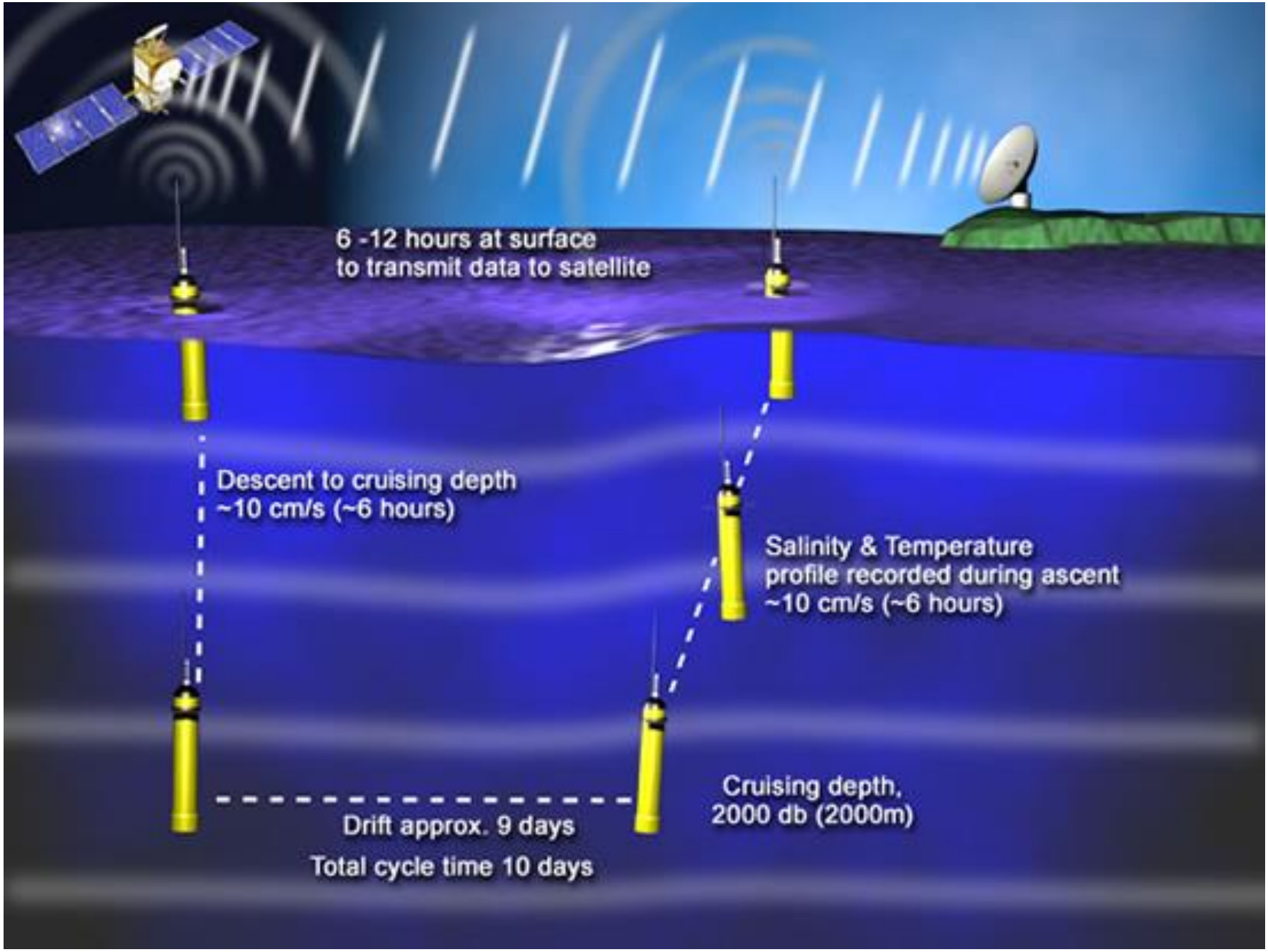
6 -12 hours at surface
to transmit data to satellite
Descent to cruising depth
~10 cm/s (~6 hours)
Salinity & Temperature
profile recorded during ascent
~10 cm/s (~6 hours)
Cruising depth,
2000 db (2000m)
Drift approx. 9 days
Total cycle time 10 days

Argo Project

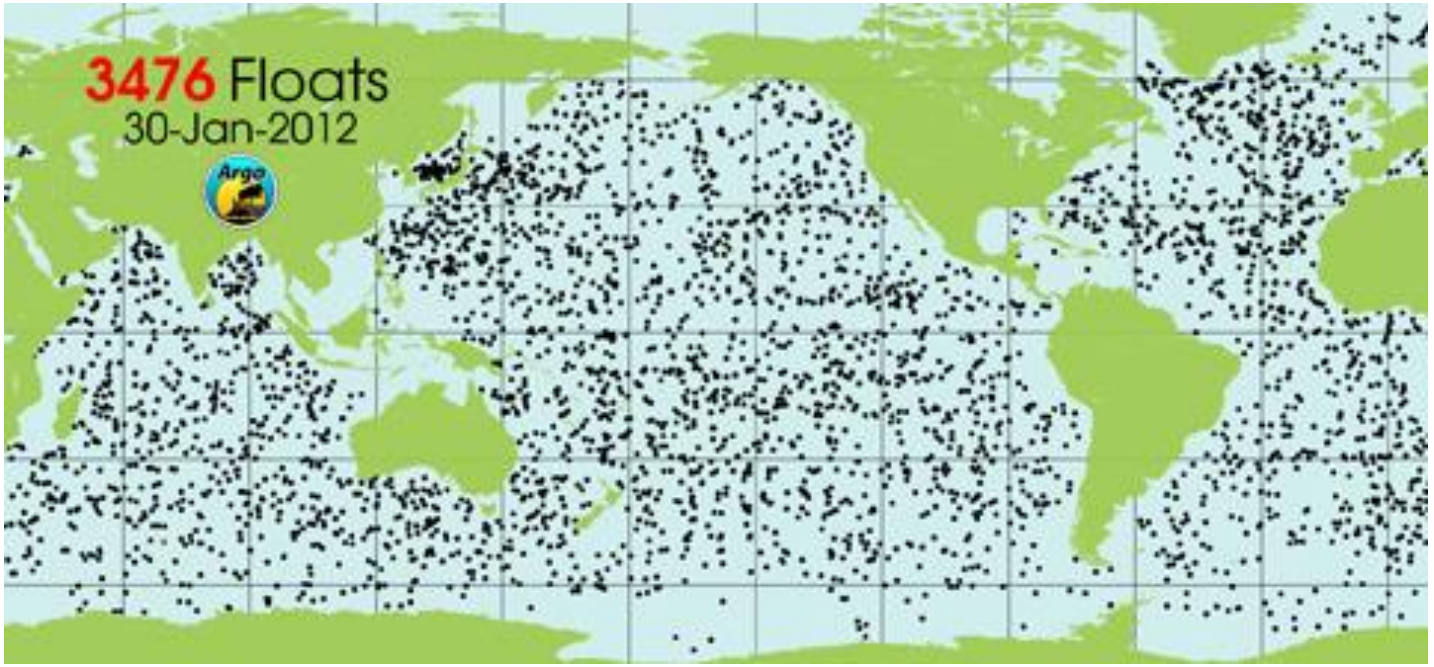

Positions of the floats that have delivered data within the last 30 days : 3476 Floats

$$H = \rho c_p \int_{h2}^{h1} T(z)dz$$

ρ - water density, Cp- sea water specific heat capacity, h2 - bottom depth, h1 - top depth, T(z)- temperature profile.

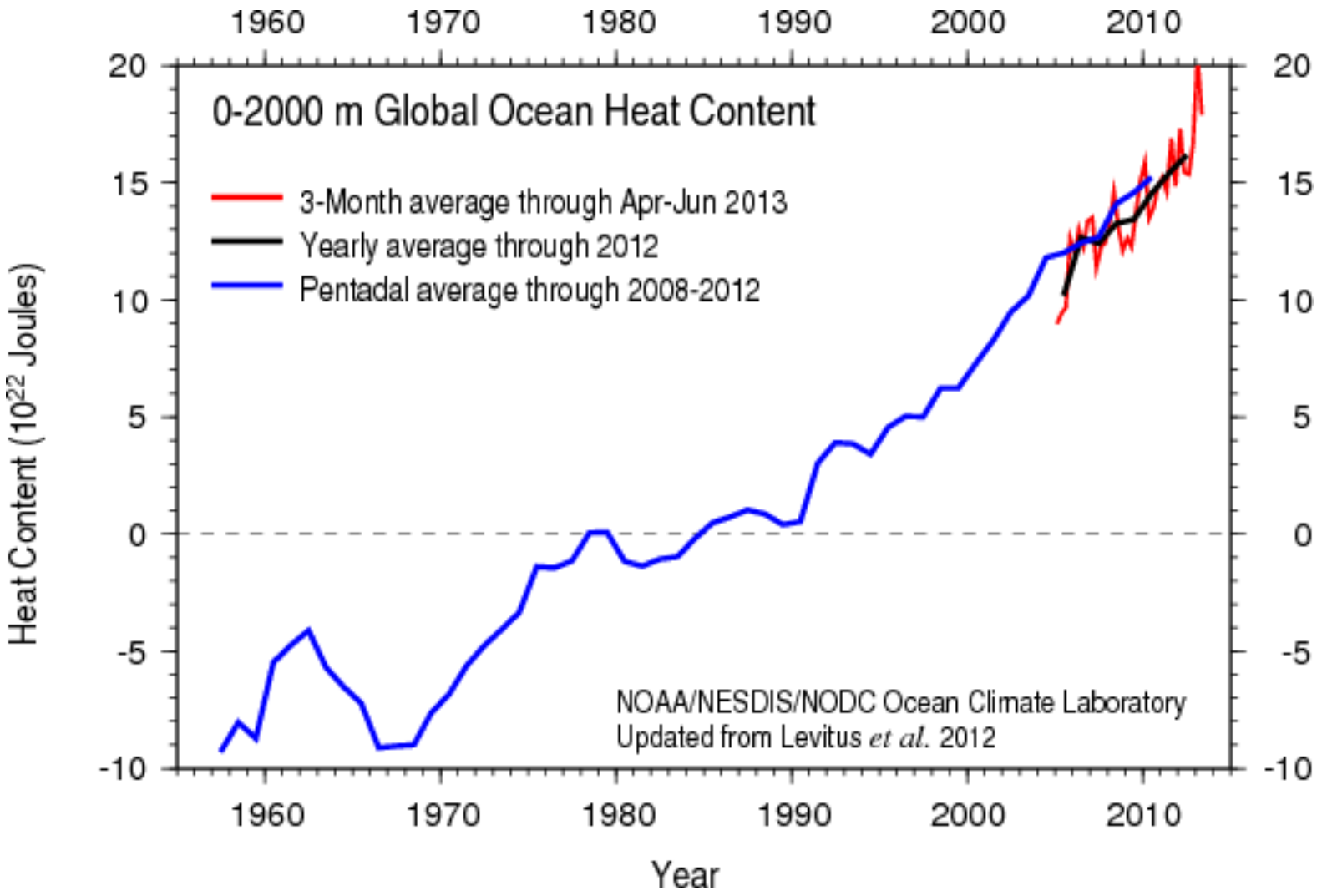

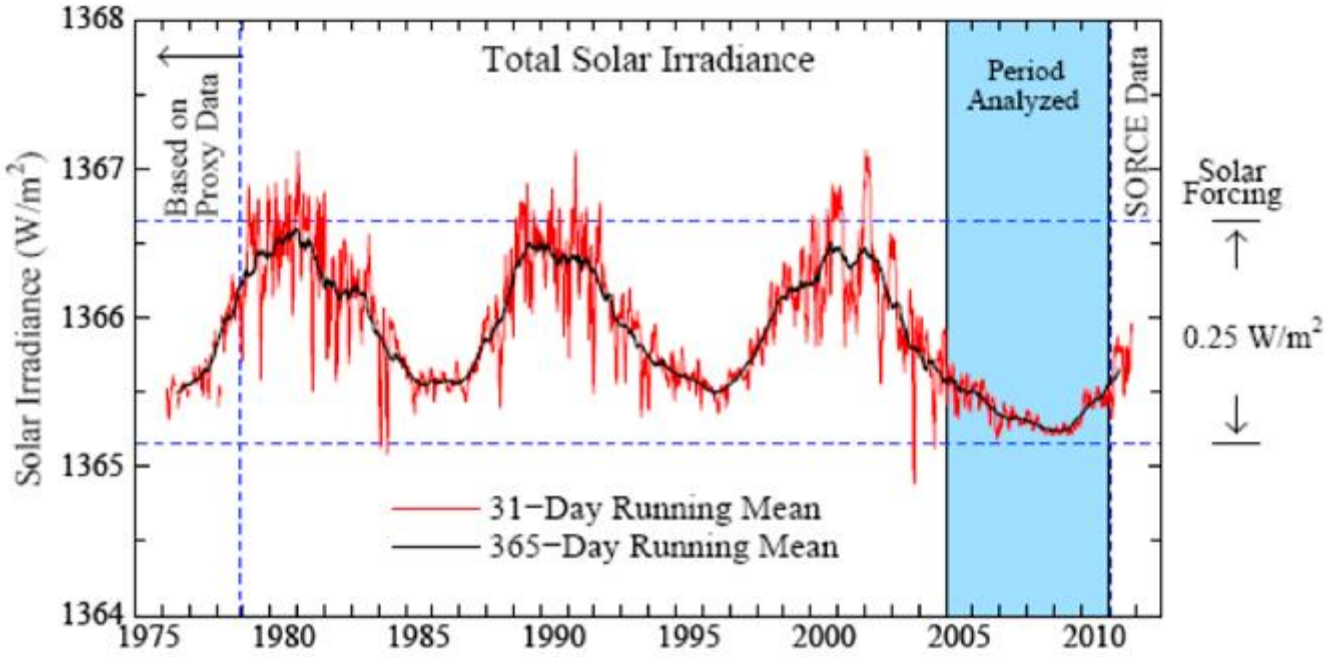

- ***A graph of the sun's total solar irradiance shows that in recent years irradiance dipped to the lowest levels recorded during the satellite era. The resulting reduction in the amount of solar energy available to affect Earth's climate was about .25 watts per square meter, less than half of Earth's total energy imbalance.***

Earth's energy imbalance

Atmos. Chem. Phys., 11, 13421-13449, 2011
www.atmos-chem-phys.net/11/13421/2011/

- **J. Hansen[1,2], M. Sato[1,2], P. Kharecha[1,2], and K. von Schuckmann[3]**
  [1]NASA Goddard Institute for Space Studies, New York, NY 10025, USA
  [2]Columbia University Earth Institute, New York, NY 10027, USA
  [3]Centre National de la Recherche Scientifique, LOCEAN Paris, hosted by Ifremer, Brest, France
- Improving observations of ocean heat content show that Earth is absorbing more energy from the Sun than it is radiating to space as heat, even during the recent solar minimum. The inferred planetary energy imbalance is 0.58 ± 0.15 W m^{-2} during the 6-yr period 2005–2010
- H_{Earth} = 0,58 W m^{-2} · 5,1· 10^{14} m^2 = 3 ·10^{14} W = 300 ± 76 TW

Comments on the Paper "Earth's energy imbalance and implications" by J. Hansen, M. Sato, P. Kharecha, and K. von Schuckmann

arXiv:1203.1289v2 [physics.ao-ph]

- Gerhard Kramm, Ralph Dlugi

- Abstract: In our comments we explicitly acknowledge the attempt of Hansen et al. to assess various uncertainties inherent in geophysical data being based on different measuring concepts and observation methods. However, with regard to the planetary energy budget, this paper offers some vulnerable points. We will focus our comments on these vulnerable points only. We will show that the energy imbalance of the entire Earth-atmosphere system is, indeed, based on these inherent uncertainties. We will demonstrate that the accuracy in the quantification of the global energy flux budget as claimed by Hansen et al. is, by far, not achievable in case of the entire Earth-atmosphere system. Using the value of the solar constant of $S_0 = 1361$ W/m^2 recently determined on the basis of total-solar-irradiance (TSI) observation by three different satellite projects (ACRIMSAT/ACRIM3 launched in 2000, SORCE/TIM launched in 2003, and PICARD/PREMOS launched in 2010) we will document that the planetary energy imbalance of $F = 0.58 \pm 0.15$ W/m^2 calculated by Hansen et al. does not exist. Consequently, the implications related to this planetary energy imbalance have no basis.

Under conditions that the element composition of Moon and Earth is just the same the Earth intrinsic heat flux is:

$$H_{Earth} = H_{Moon} \cdot M_{Earth} / M_{Moon}$$

Photo of the Apollo 15 CDR setting up a deep drill.
NASA photo AS15-87-11847.

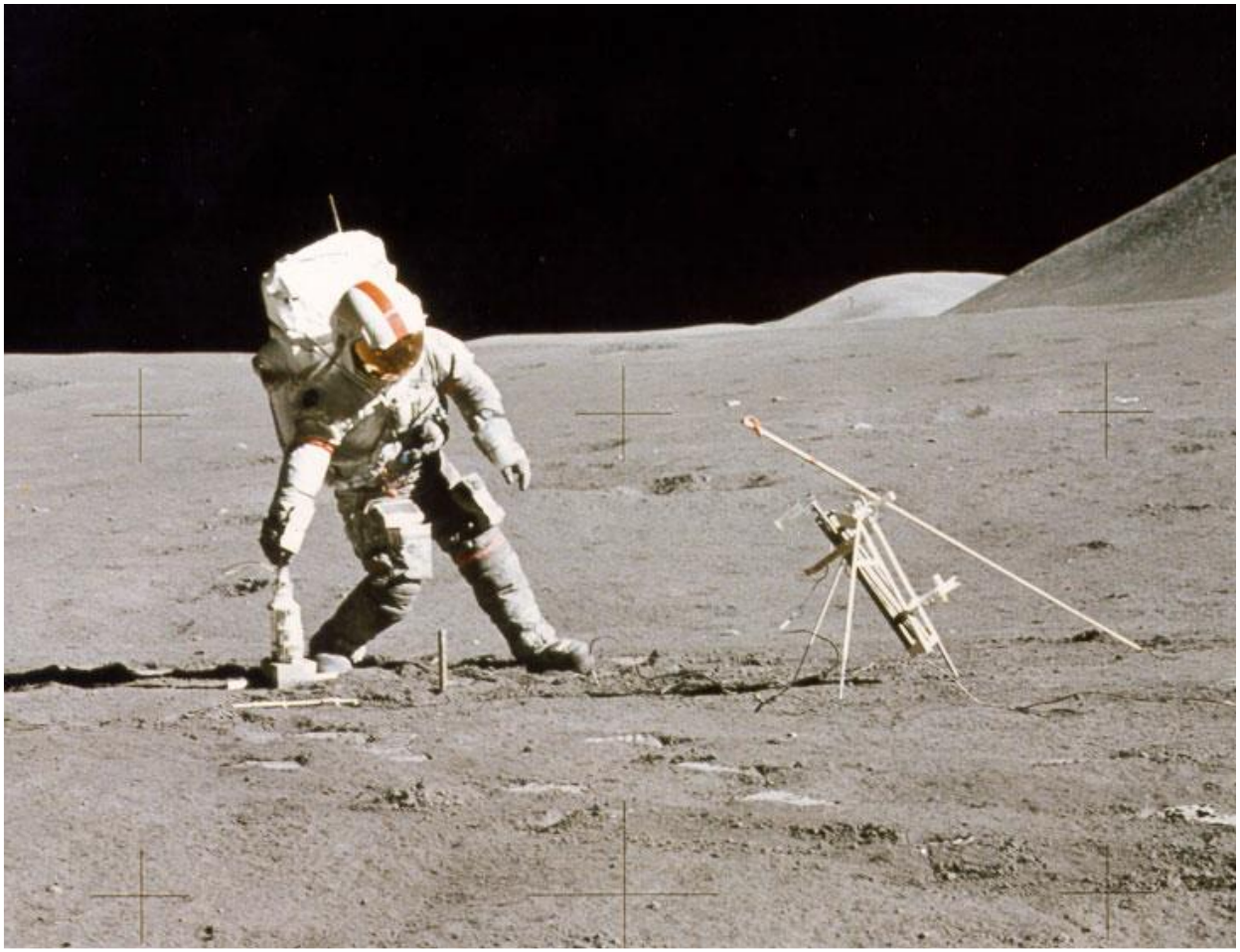

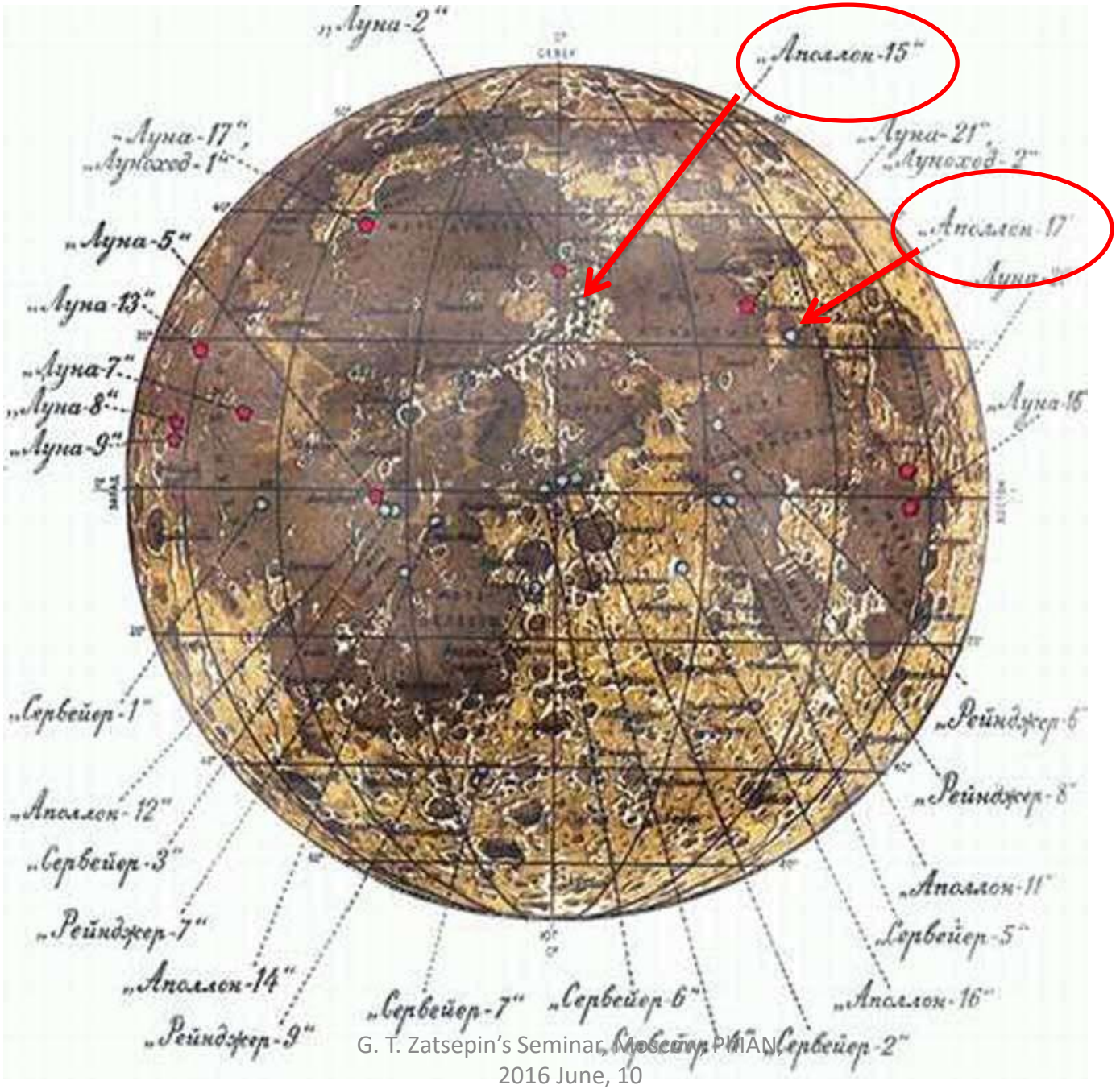
„Луна-2"
„Аполлон-15"
„Луна-17"
„Лунохед-1"
„Луна-21"
„Лунохед-2"
„Аполлон-17"
„Луна-5"
„Луна-13"
„Луна-7"
„Луна-8"
„Луна-9"
„Луна-15"
„Сервейер-1"
„Рейнджер-6"
„Аполлон-12"
„Рейнджер-8"
„Сервейер-3"
„Аполлон-11"
„Рейнджер-7"
„Сервейер-5"
„Аполлон-14"
„Сервейер-7"
„Сервейер-6"
„Аполлон-16"
„Рейнджер-9"
„Сервейер-2"

Infrared photo of the Moon during eclipse

The metal ball covered by old blanket with the holes

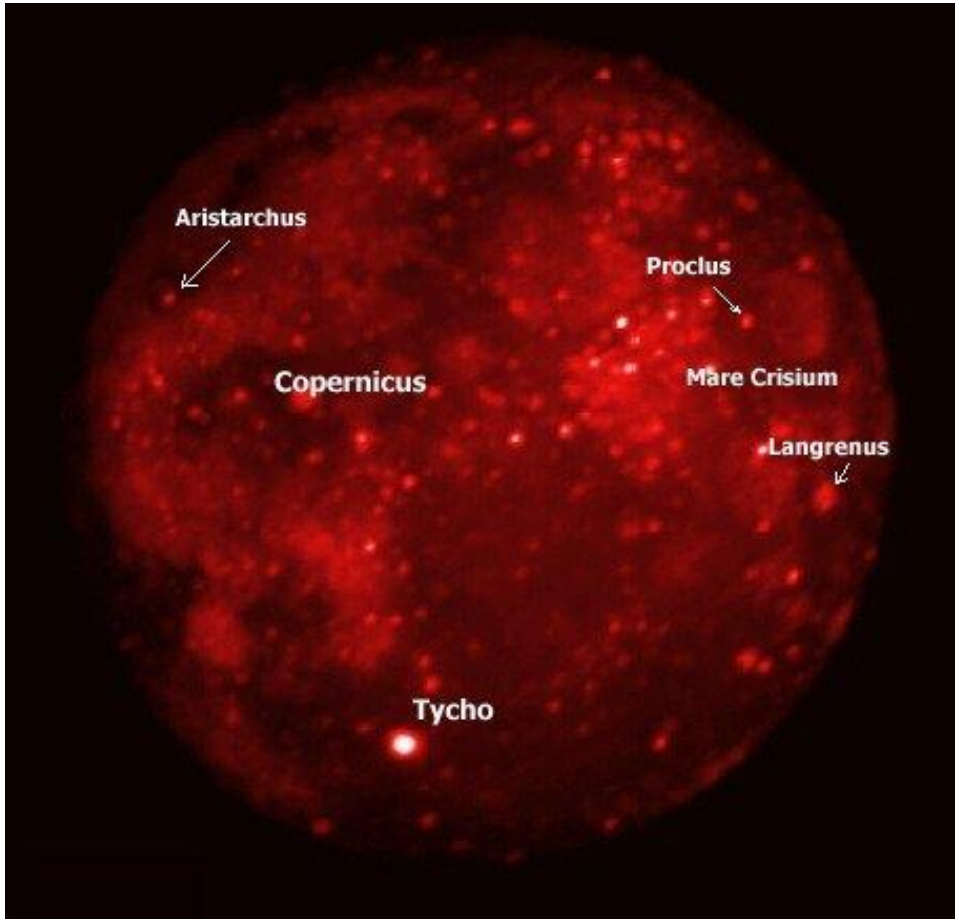

Apollo 15, Apollo 17

$$H_{Earth} = H_{Moon} \cdot M_{Earth} / M_{Moon} = 43 - 65\ TW$$

Effective radiowave emission depth of black body radiation from Moon regolith

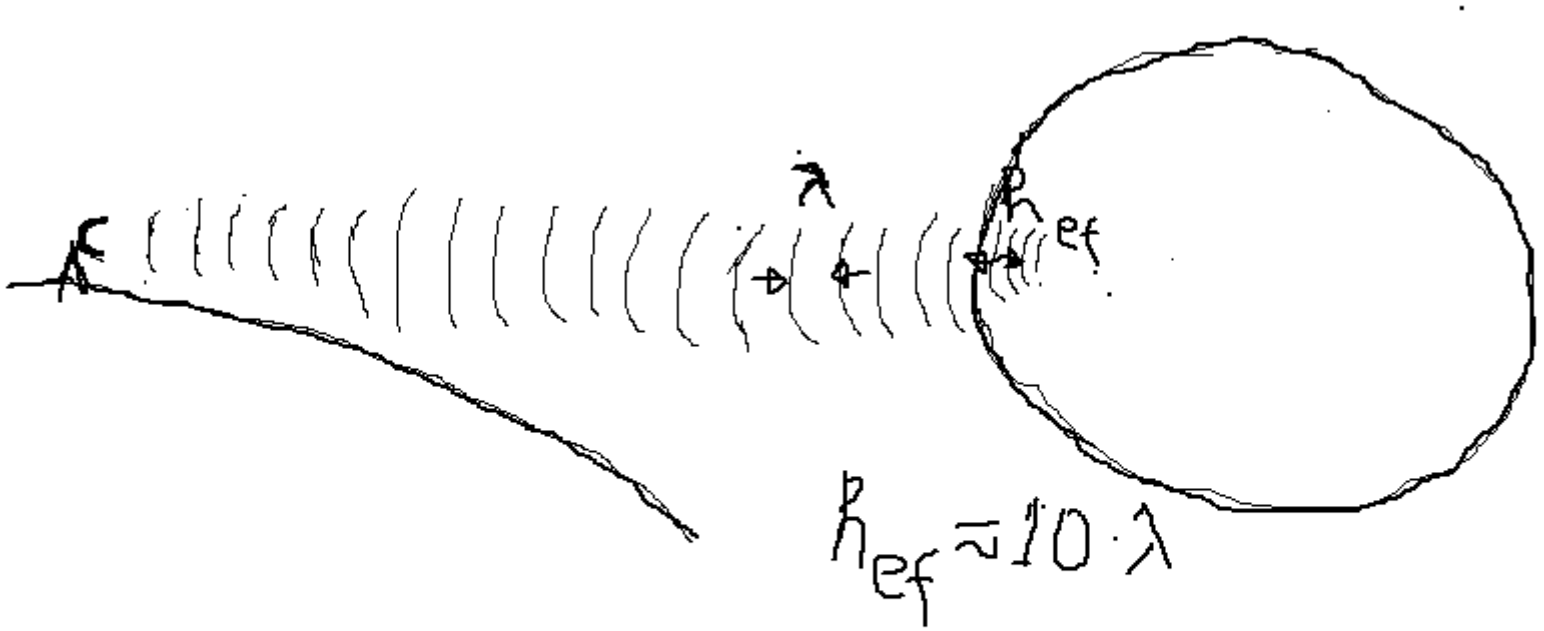

Krotikov V.D., Troitskyi V.S. Radio emission and nature of the Moon. Soviet Phys. Uspekhi. 1964. V.6. pp841-871.

- $\lambda_1 = 10$ cm, $\lambda_2 = 20$ cm
- $H_{Earth} = H_{Moon} \cdot M_{Earth} / M_{Moon} = 170$ TW

This result depends on assumption that Moon crust is non-conductor. If the crust contains metals this result is the low bound of heat flux.

Lunar Reconnaissance Orbiter. 2009

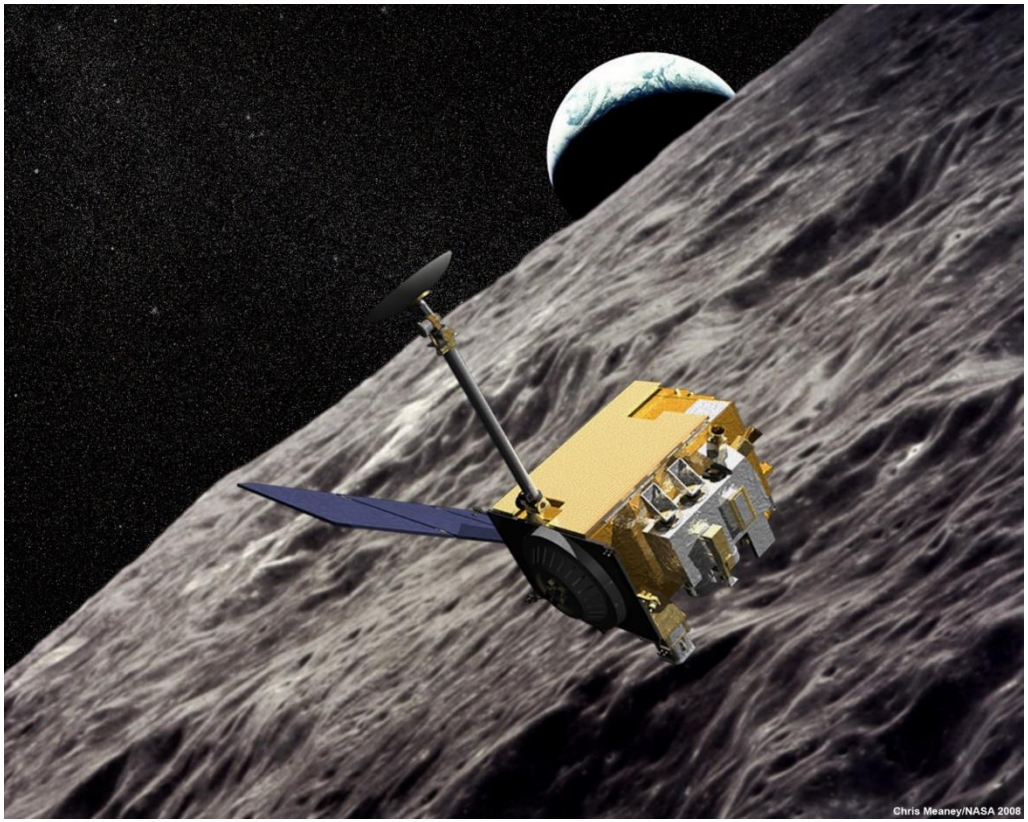

The Diviner Lunar Radiometer Experiment is one of seven instruments aboard NASA's Lunar Reconnaissance Orbiter, which launched on June 18 2009. It is the first instrument to create detailed day and night surface temperature maps of the Moon.

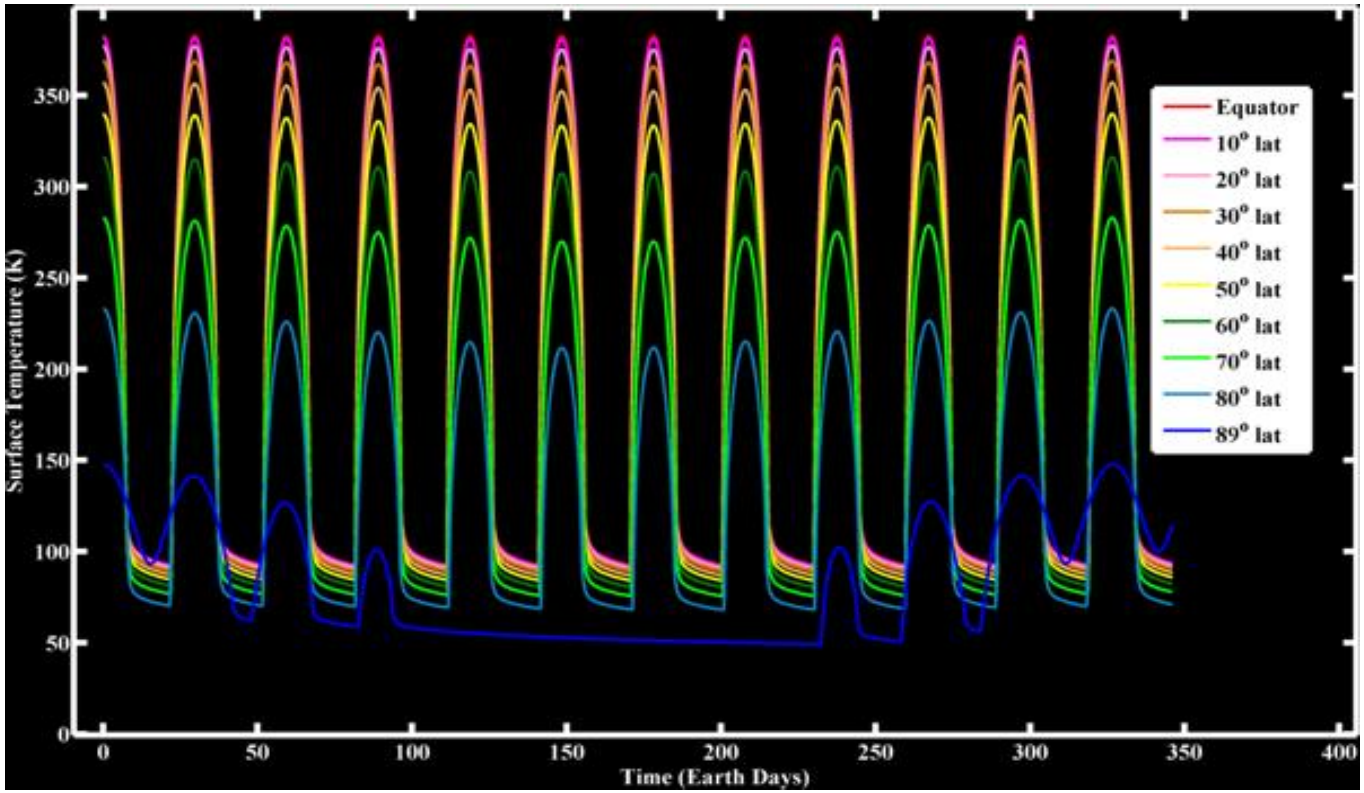

Diviner Daytime Temperature (K) on South Pole.

T_{min} = 40 K

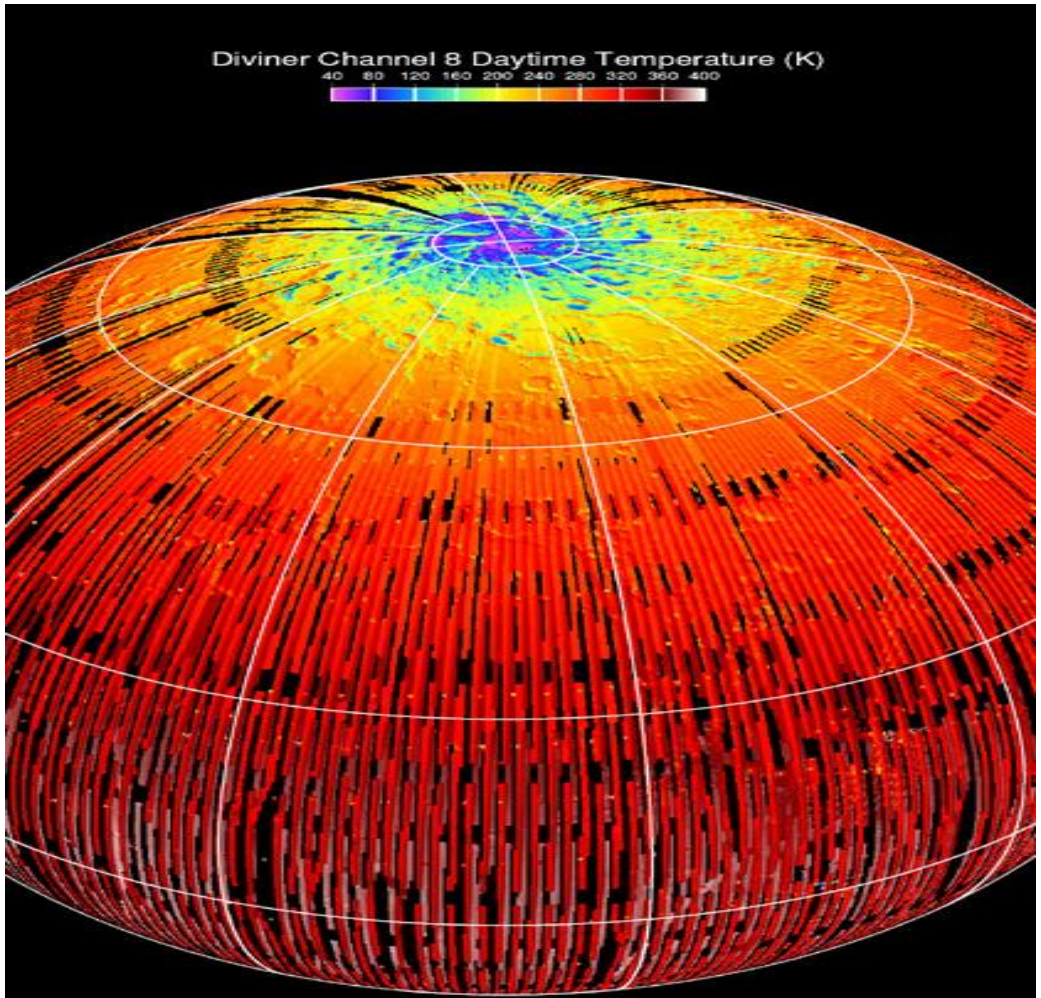

Diviner photo.
Permanent dark places in South Luna Pole.

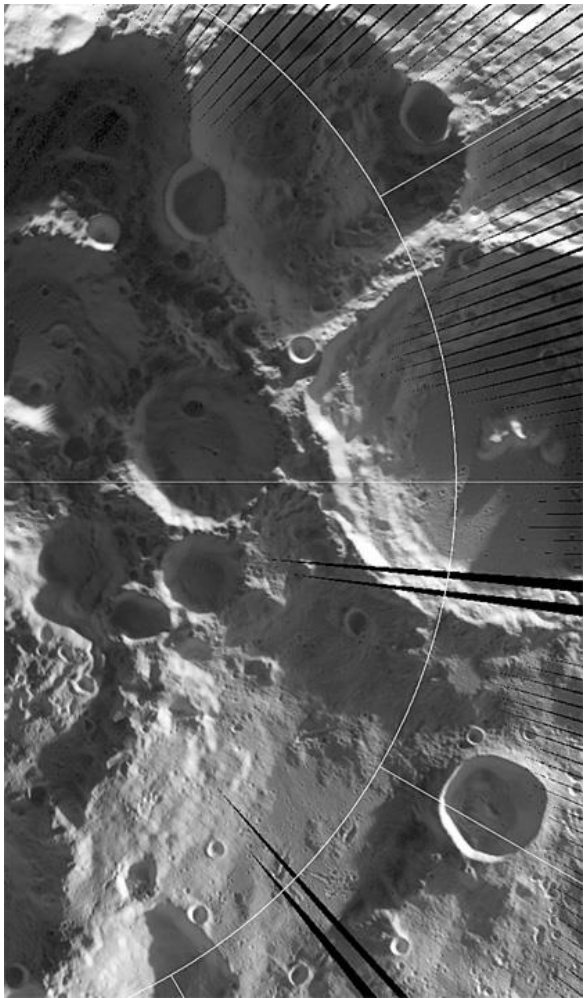

Diviner Nighttime Temperature (K) on South Pole.

T_{min} = 40K

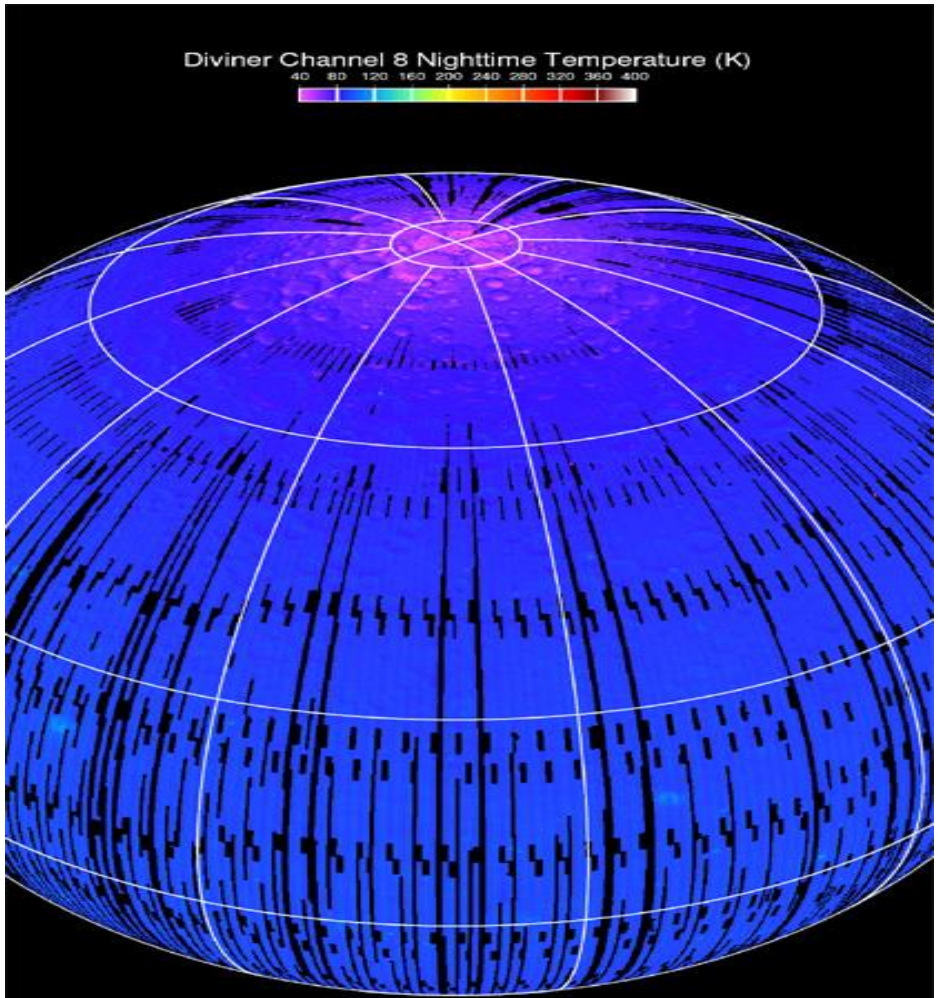

Equilibrium condition for the permanent dark places on Lunar surface

$$F_{rad} = \varepsilon \cdot \sigma' \cdot T^4$$

F_{rad} – radiogenic heat flux,

$\varepsilon = 0{,}95$ – emissivity of lunar surface,

$\sigma' = 5{,}67 \cdot 10^{-8}\ W \cdot m^{-2} \cdot K^{-4}$ - Stefan-Boltzmann constant.

$$F_{rad}\ (T=40K) = 0{,}138\ W \cdot m^{-2}$$

$$H_{Moon} = F_{rad}\ (T=40K) \cdot S_{Moon} = 5{,}2\ TW$$

$$H_{Earth} = H_{Moon} \cdot M_{Earth} / M_{Moon} = 420\ TW$$

The Hydridic Earth model predicts:

$H = H(U) + H(Th) + H(40K) = 300$ TW

for the potassium abundance 1.5% of the Earth mass.

- This heat flux H = 300 TW can explain the observed by ARGO project the heating of the ocean.

$$3 \cdot 10^{14}\ \mathrm{W} / 5 \cdot 10^{14}\ \mathrm{m}^2 = 0{,}6\ \mathrm{W/m}^2$$

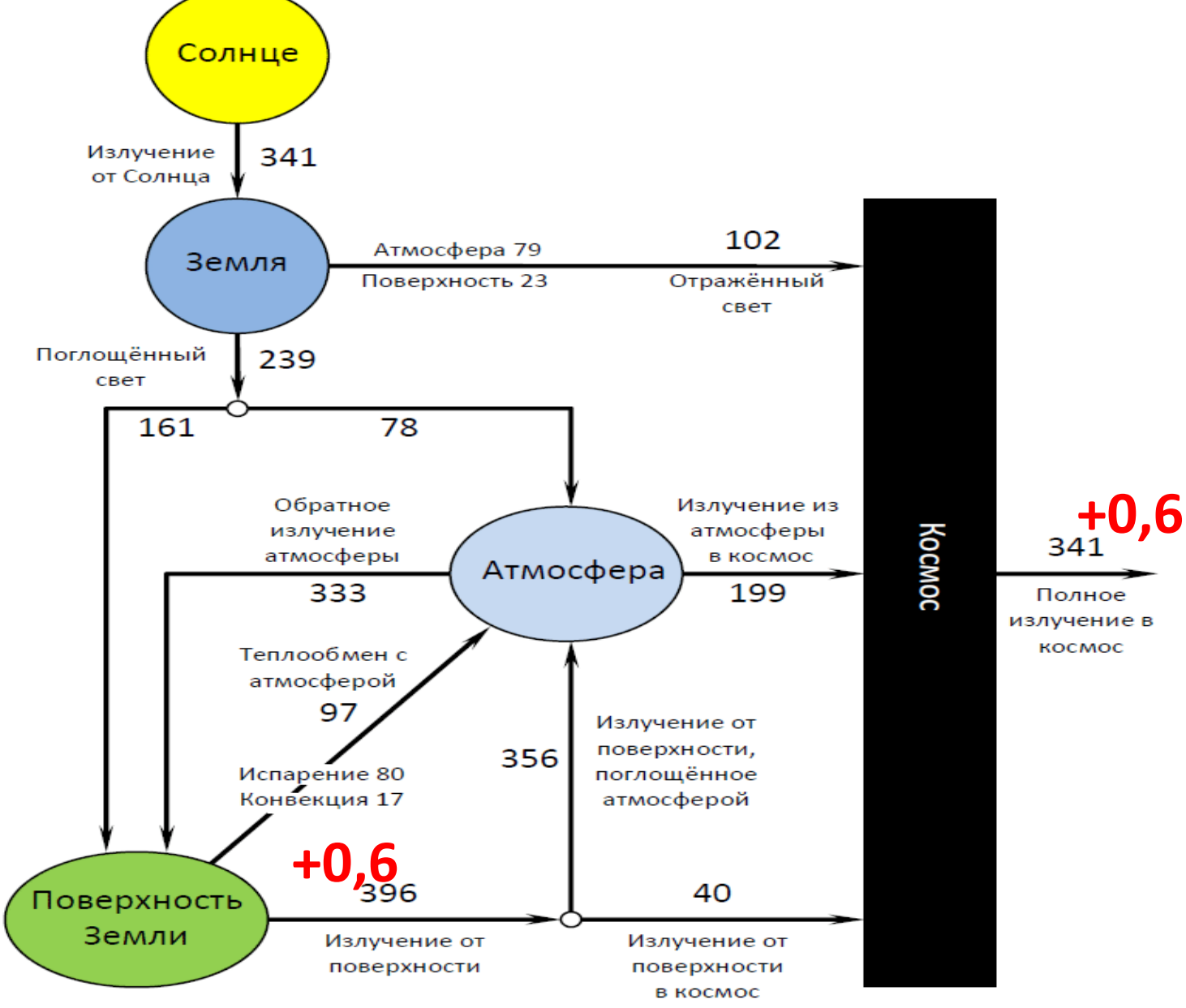

Тепловой баланс Земли (март 2000 – май 2004)

Все тепловые потоки в Вт/м^2, усреднённые по времени и по поверхности Земли
Источник: Trenberth K. T., Fasullo J., Kiehl J. T., 2009: Earth's global energy budget. — *Bull. Amer. Meteor. Soc.*, **90**, 311–323.

AdmiralHood, vladfotki.narod.ru

$$F_{rad} = \varepsilon \cdot \sigma' \cdot T^4$$

F_{rad} – radiogenic heat flux,

$\varepsilon = 0{,}90$ – emissivity of atmosphere,

$\sigma' = 5{,}67 \cdot 10^{-8}\ W \cdot m^{-2} \cdot K^{-4}$ - Stefan-Boltzmann constant.

- $5{,}67 \cdot 10^{-8} \cdot 255^4 = 239{,}7\ W \cdot m^{-2}$

255 K = - 17 °C

- $5{,}67 \cdot 10^{-8} \cdot 255{,}15^4 = 240{,}3\ W \cdot m^{-2}$

257 K = - 16,85 °C

Temperature change in the last 50 years

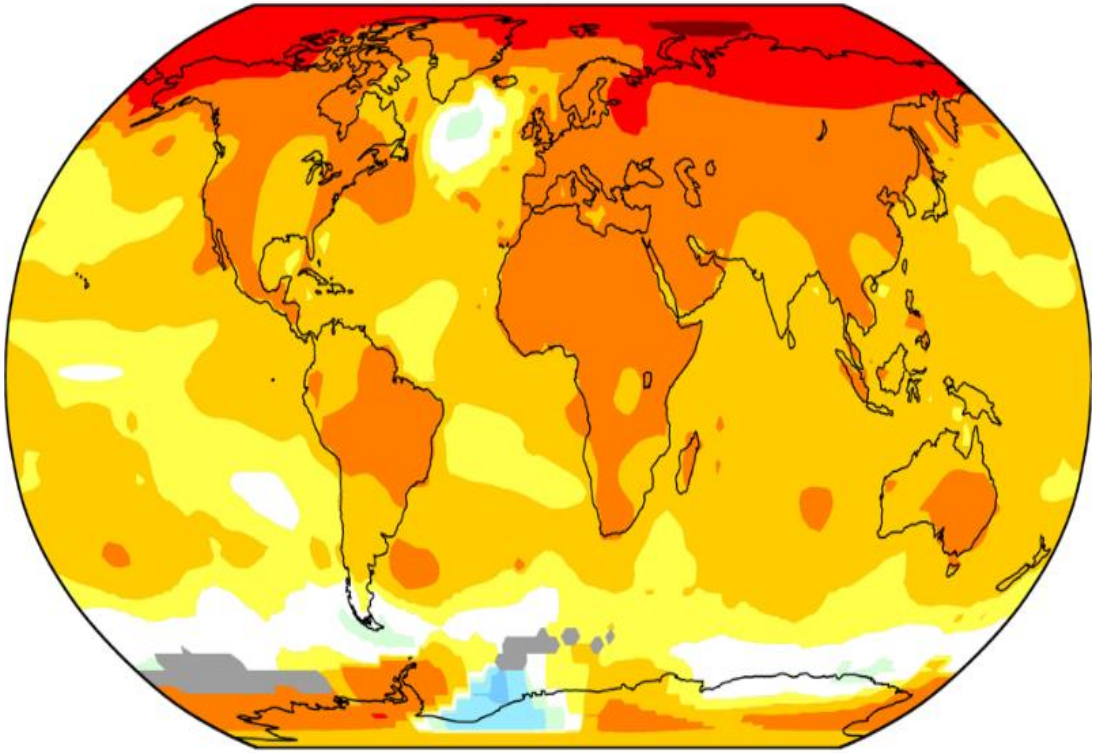

2011-2020 average vs 1951-1980 baseline

Парадокс слабого молодого Солнца

- наблюдаемое противоречие между палеоклиматическими данными и астрофизическими моделями эволюции Солнца. Стандартная модель эволюции звёзд утверждает, что 4 млрд лет назад Солнце излучало приблизительно на 30 % меньше энергии, чем сейчас.
- На Марсе также установлены следы тёплого и влажного климата.

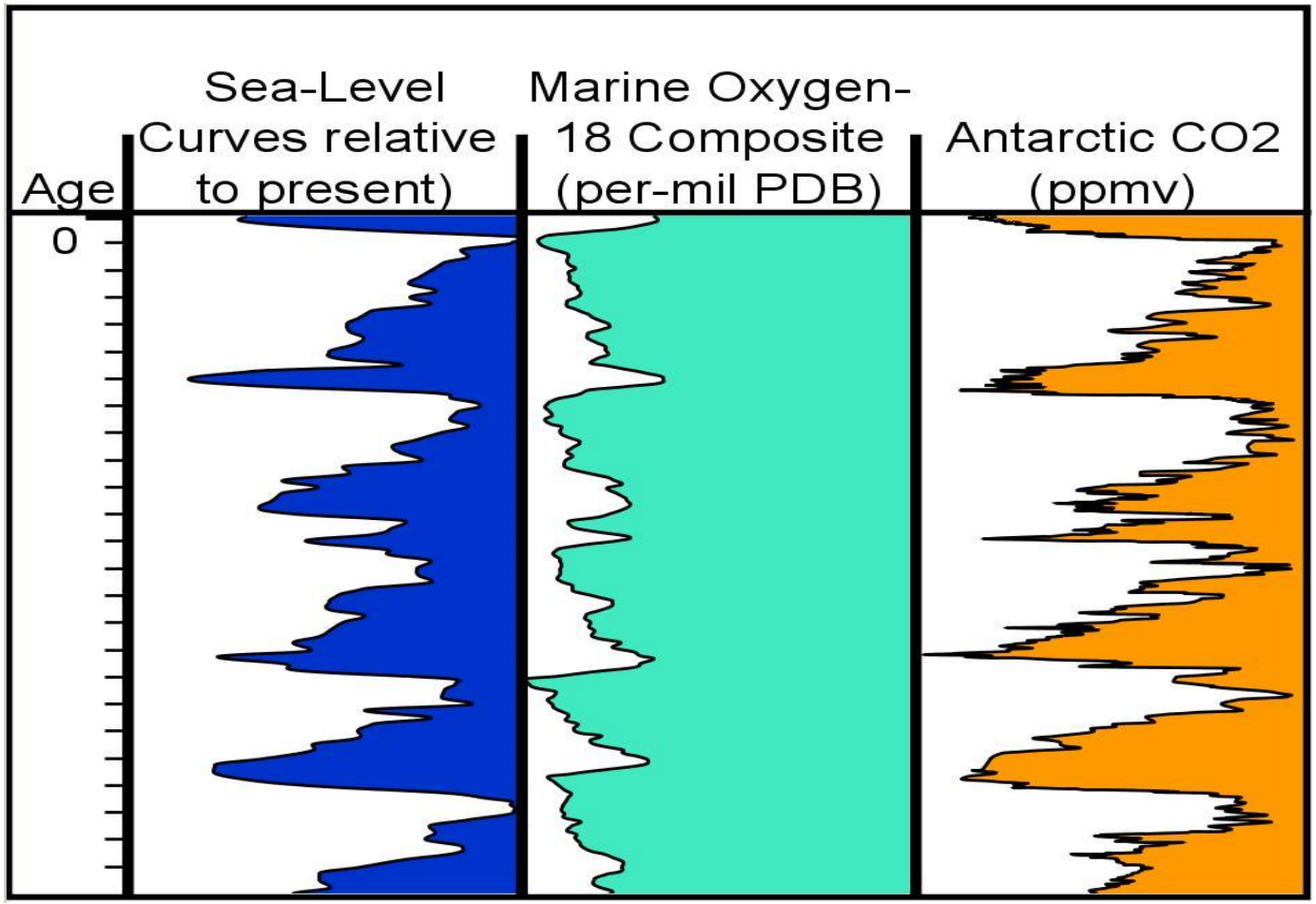

Глобальные изменения климата за последние 0,5 млн лет. Климатические индикаторы: изменение уровня океана (синий), концентрация ^{18}O в морской воде, концентрация CO_2 в антарктическом льду. Деление временной шкалы — 20 000 лет. Пики уровня моря, концентрации CO_2 и минимумы ^{18}O совпадают с межледниковыми температурными максимумами

Повышение температуры поверхности Земли с конца XIX века

Экстраполяция

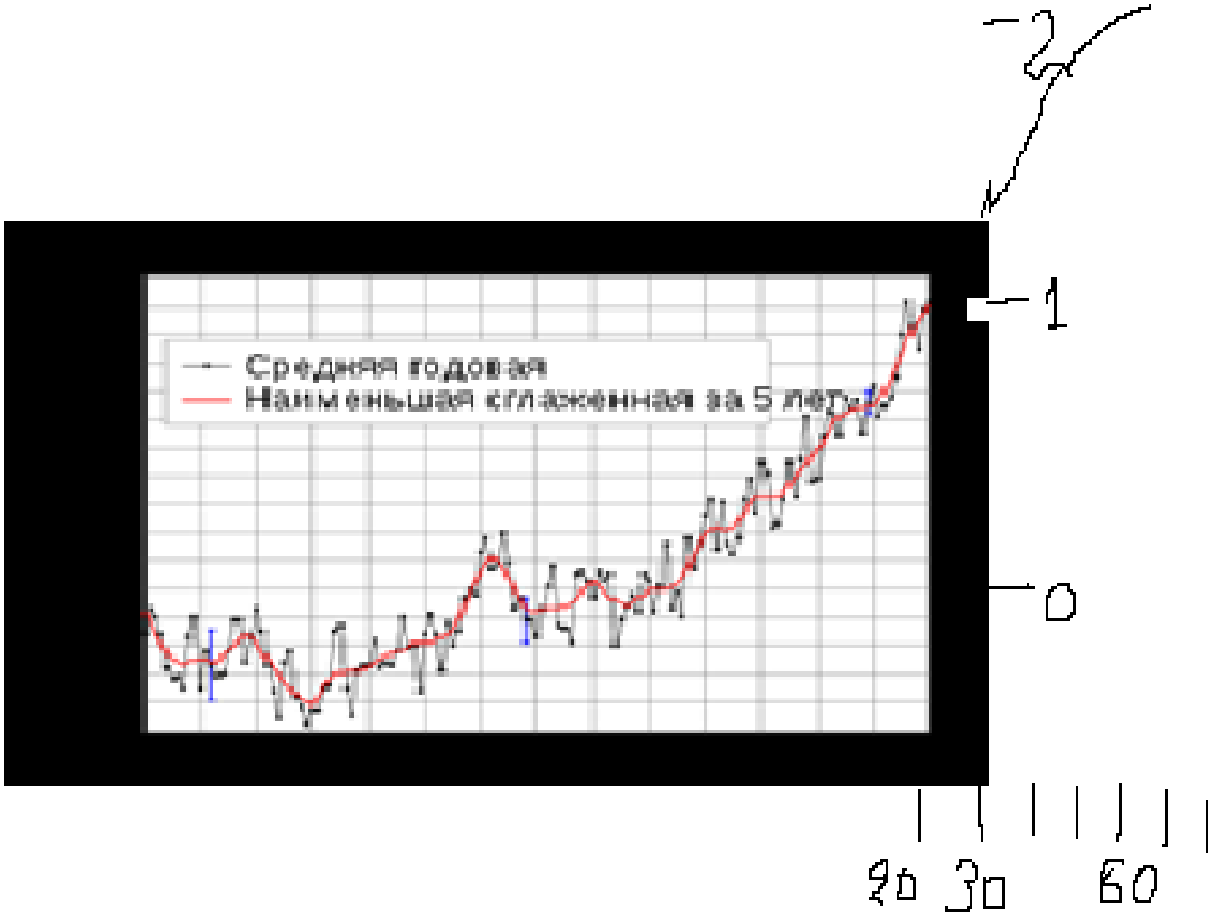

Summary

Earth

- Bore-hole temperature gradient 47±2 TW
- ARGO Earth's energy imbalance 300±76 TW

Moon recalculated to Earth heat flux

- Apollo 15, 17 drilling 43-65 TW
- Russian radio emission exp. 170 TW
- LRO temperature map 420 TW

We consider the value of 300 TW as the most favorable to explain the all experimental data.

300 ± 76 TW

Intrinsic Earth heat + Geoneutrinos

- ^{238}U, ^{235}U, ^{232}Th, ^{40}K decays in the Earth body are the source of heat and geoneutrinos.

- $^{238}U \rightarrow {}^{206}Pb + 8\alpha + 6e + 6\tilde{\nu}_e + 51{,}7$ MeV (47,7)
- $^{232}Th \rightarrow {}^{208}Pb + 6\alpha + 4e + 4\tilde{\nu}_e + 42{,}8$ MeV(40,4)
- $^{40}K \rightarrow {}^{40}Ca + e + \tilde{\nu}_e + 1.32$ MeV(0,598)prob.0,89

  $\rightarrow {}^{40}Ar + \Upsilon + \nu_e + 1.5$ Mev (1.46) prob.0,1066

The new book

Geo-neutrino. Ed. Livia Ludhova.

Open Academic Press. Berlin. Germany. 2016.

ISBN 970-83-944520-1-8

Geoneutrinos energy spectra

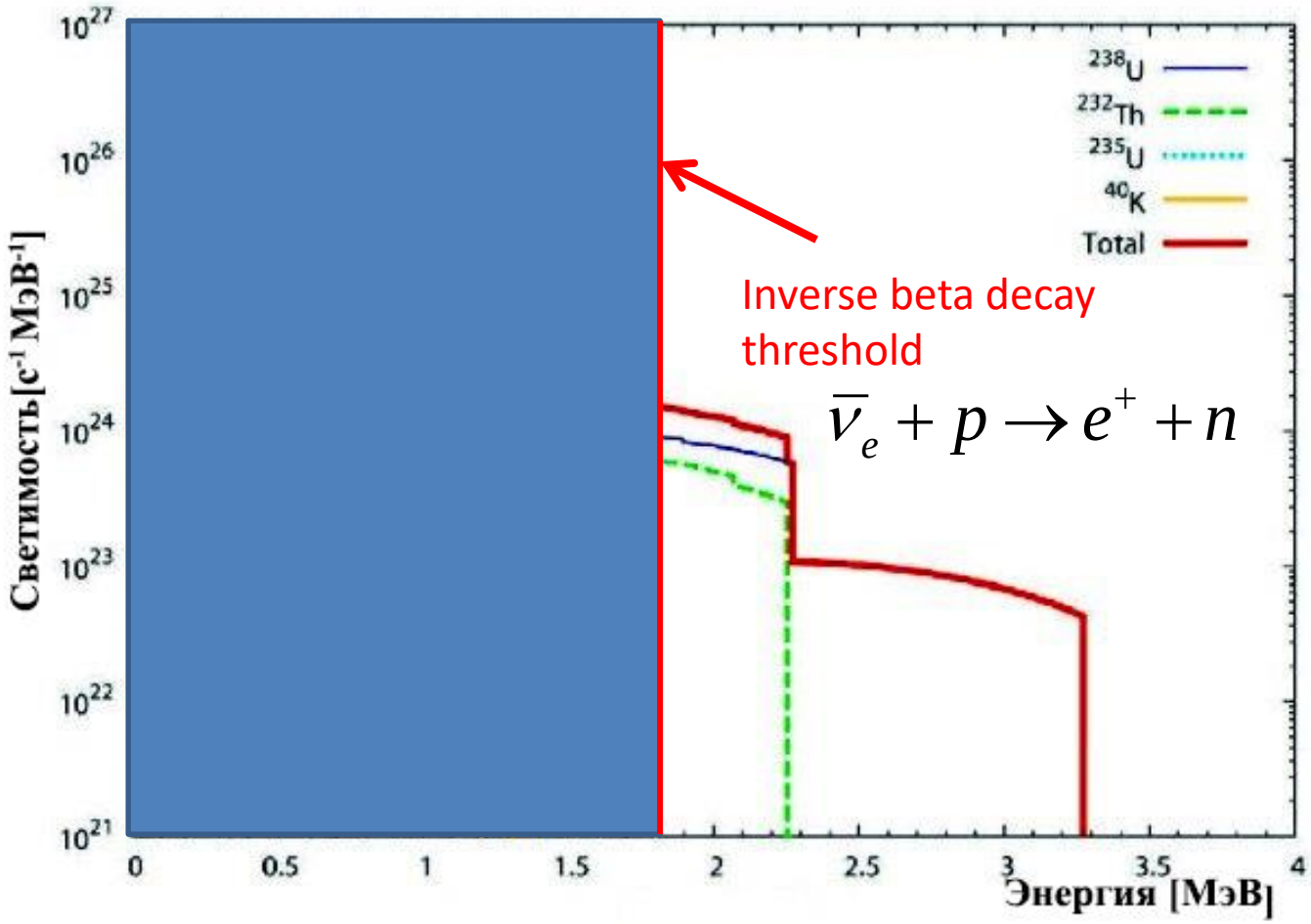

^{238}U and ^{232}Th neutrino spectra observing in a detector via IBD reaction

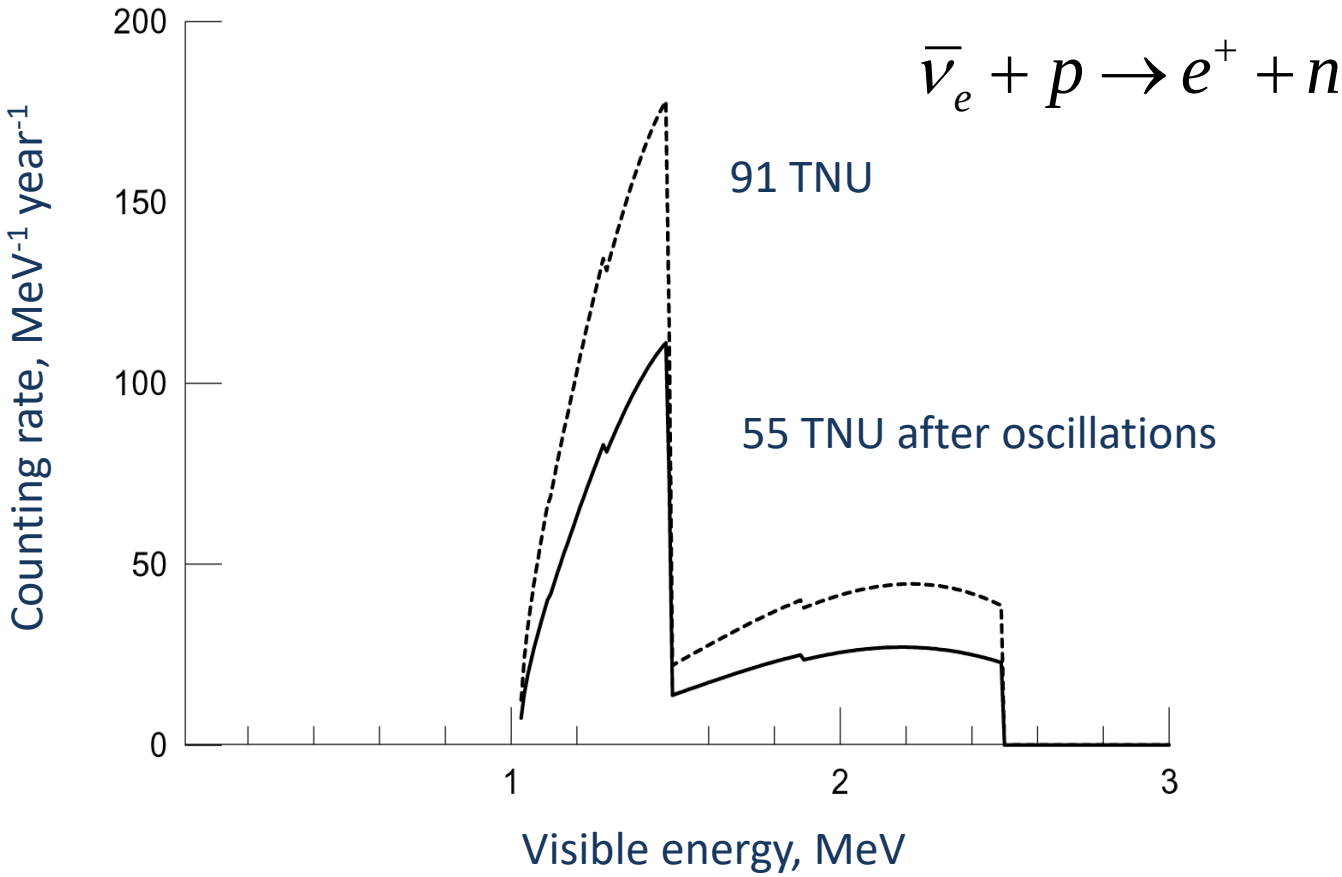

What one can know detecting geoneutrinos?

- What is total amount of radioactive isotopes inside the Earth?
- Is it enough to explain the Earth thermal flux?
- Is the distribution of radioactive elements uniform or not inside the Earth?
- What is thorium and uranium abundances mean ratio? Is it different from meteorites one?
- Is there enough potassium inside the Earth or it is totally distributed in the crust?

Modern detectors sensitive to geoneutrinos from ^{238}U and ^{232}Th

Borexino detector

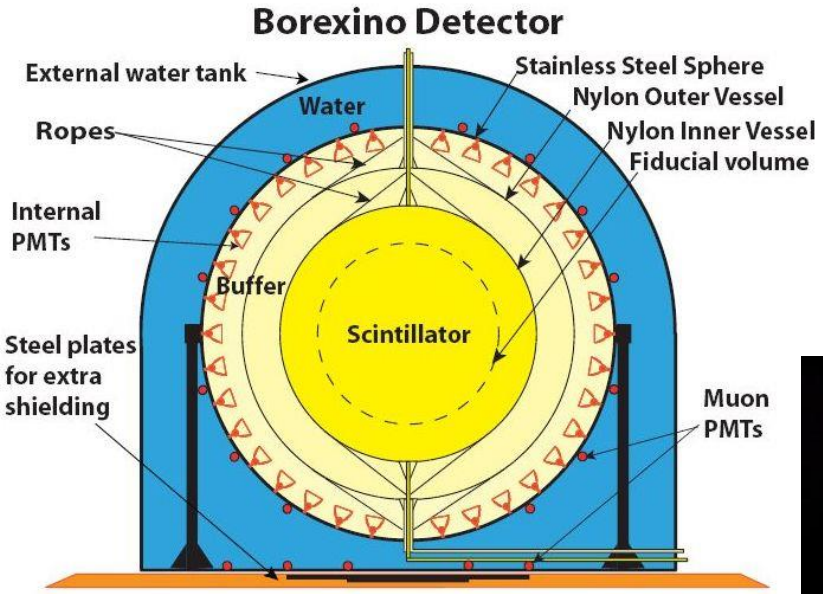

100 t fiducial volume.
Total target mass 300 t.
R ~ 4 events/year

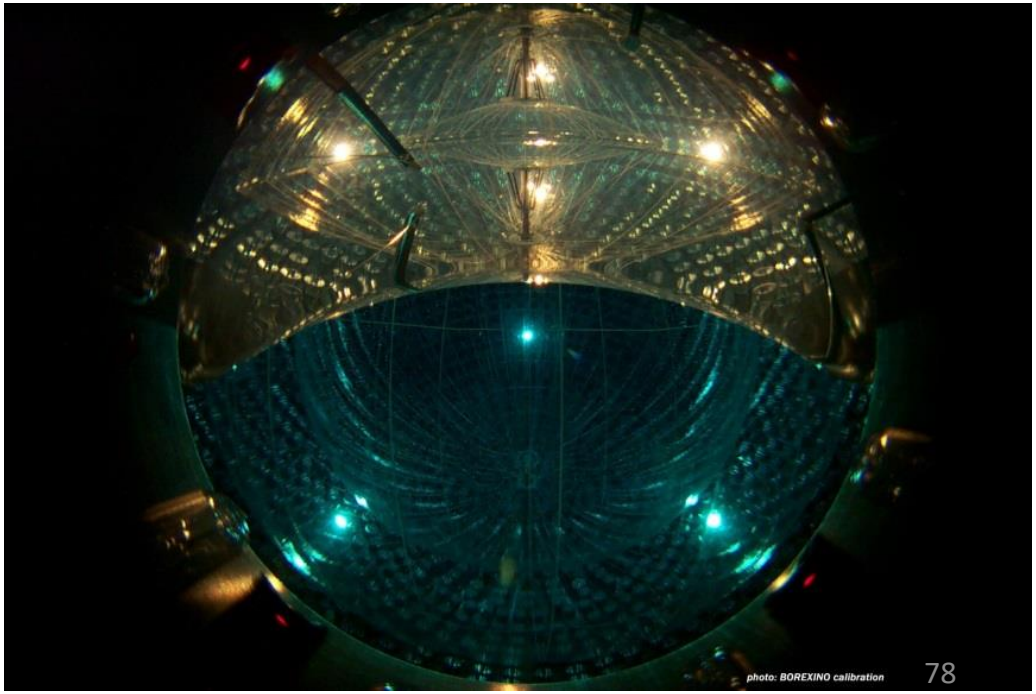

Borexino

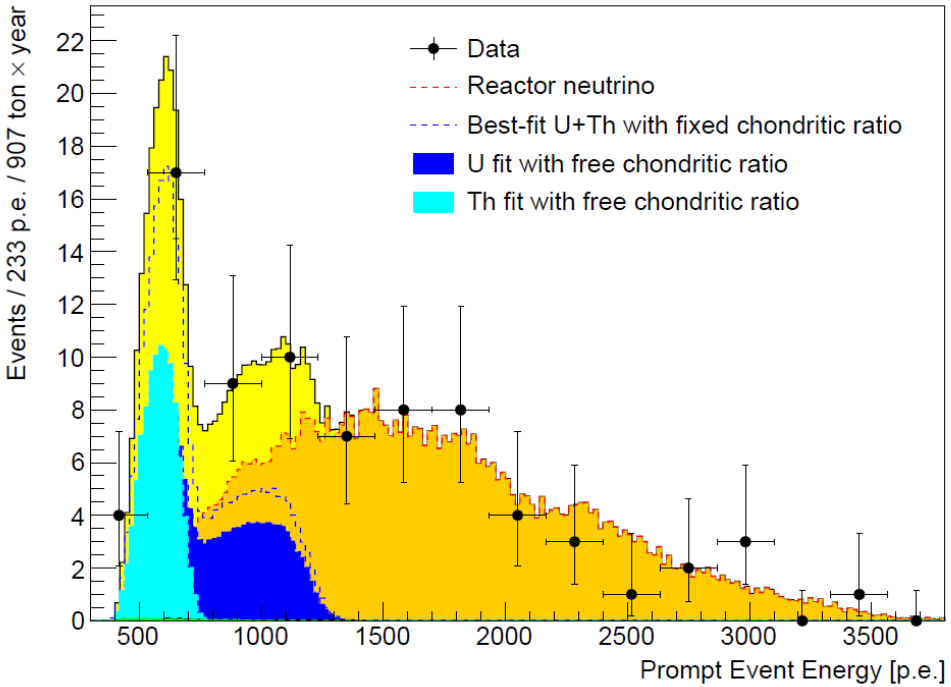

M. Agostini et al. Phys. Rev. D 92, 031101 (2015).

Tmeas = 2056 days (5.6 years)
Np = (0.977±0.05)×10^{31} protons on target
Exposure (5.5±0.3) ×10^{31} proton years
23.7 $^{+6.5(st)+0.8}_{-5.7(st)-0.6}$ geo-nu events

43.5 TNU

KamLAND Detector

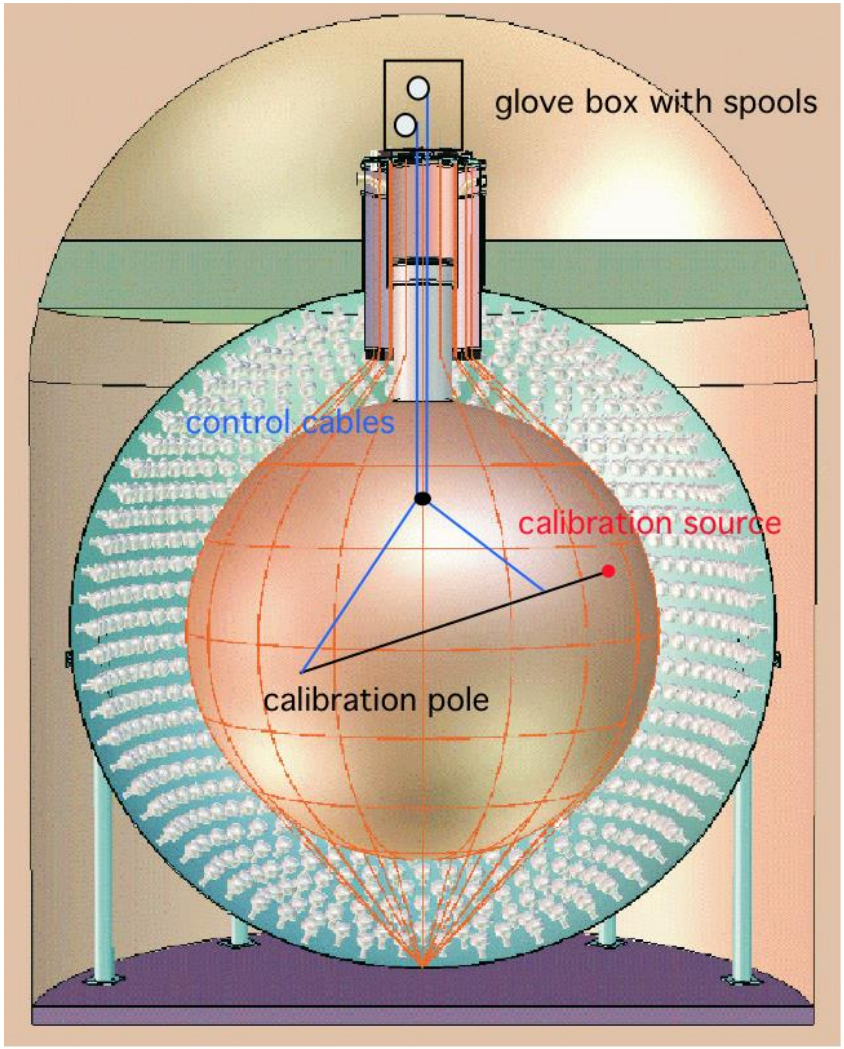

600 t fiducial volume.
Total target mass 1000 t.
R ~12 events/year

KamLAND

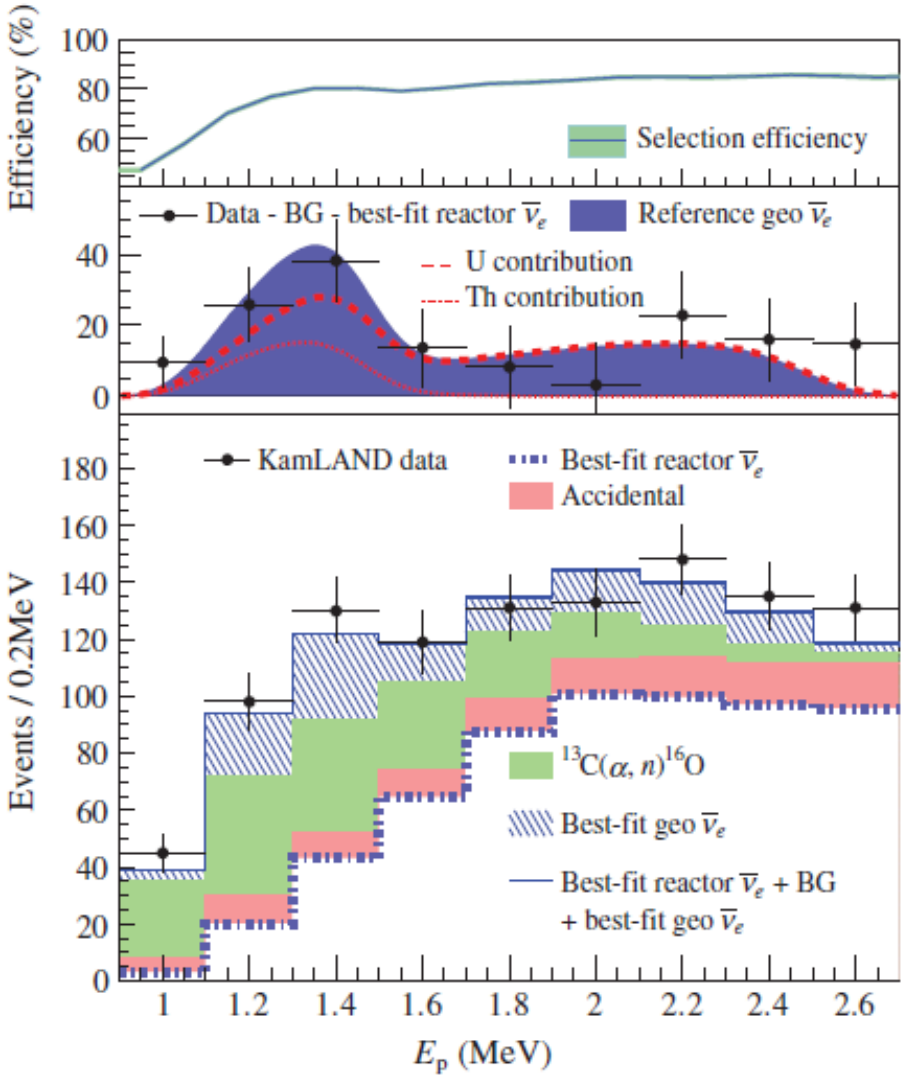

A. Gando et al. Phys. Rev. D 88, 033001 (2013).

Tmeas = 2991 days (8.2 years)
Np = (5.98±0.13)×10^{31} protons on target
Exposure (4.9±0.1) ×10^{32} proton years

116 $^{+28}_{-27}$ geo-nu events

23.67 TNU

How much heat radioactive isotopes produce in the Earth?

Heat production by Uranium and Thorium

(abundance: 2×10^{-6} % 8×10^{-6} %)

branch	Isotope abundance in Natural mixture	Q_eff, MeV	Decays number in 1 kg per s	J/dec	W per kg	Total mass in Earth according BSE, kg	H, TW
^{238}U	0.993	47.7	1.23×10^{7}	7.64×10^{-12}	9.44×10^{-5}	0.806×10^{17}	**7.608**
^{235}U	0.007	44	5.68×10^{5}	7.05×10^{-12}	4.01×10^{-6}	0.58×10^{15}	**0.002**
^{232}Th	1.0	40.4	4.06×10^{6}	6.47×10^{-12}	2.63×10^{-5}	3.2×10^{17}	**8.5**
Total heat							**16.11**

Heat production by Potassium (abundance 0.02% weight)

branch	^{40}K abundance in Natural mixture	Q_eff, MeV	Decays number in 1 kg per s	J/dec	W per kg	Total Potassium mass in Earth, kg	H, TW
0.8914	1.17×10^{-4}	0.595	2.76×10^{4}	9.53×10^{-14}	2.63×10^{-9}	1.194×10^{21}	**3.1**
0.1066		1.46	3.30×10^{3}	2.34×10^{-13}	7.73×10^{-10}		**0.9**
0.002		0.0027	62	4.26×10^{-16}	2.64×10^{-14}		**0.0**
Total heat							**4.0**

Bezrukov-Sinev Model

- M(U) = 1.7×10^{17} kg, M(Th) = 6.7×10^{17} kg
- In the Crust they distributed according BSE (Reference Model)
- In the Mantle and Core they were chosen in abundances not to break observed counting rates (Borexino and KamLAND)

	Experimental counting rate, TNU	Calculated counting rate, TNU
Borexino	**43.5 ± 12.5**	**38.1**
KamLAND	**23.67 ± 5.61**	**31.8**

Looking for antineutrino flux from 40K with large liquid scintillator detector Looking for antineutrino flux from 40K with large liquid scintillator detector

V.V. Sinev, L.B. Bezrukov (Moscow, INR), E.A. Litvinovich, I.N. Machulin, M.D. Skorokhvatov (Kurchatov Inst., Moscow & Moscow Phys. Eng. Inst.), S.V. Sukhotin (Kurchatov Inst., Moscow).

May 13, 2014. 4 pp.
Published in **Phys.Part.Nucl. 46 (2015) 2, 186-189**

Conference: C14-01-26 Proceedings, Valday
e-Print: **arXiv:1405.3140 [physics.ins-det]**

Recoil electrons spectrum from ^{40}K in BOREXINO $\nu_e + e \rightarrow \nu_e + e$

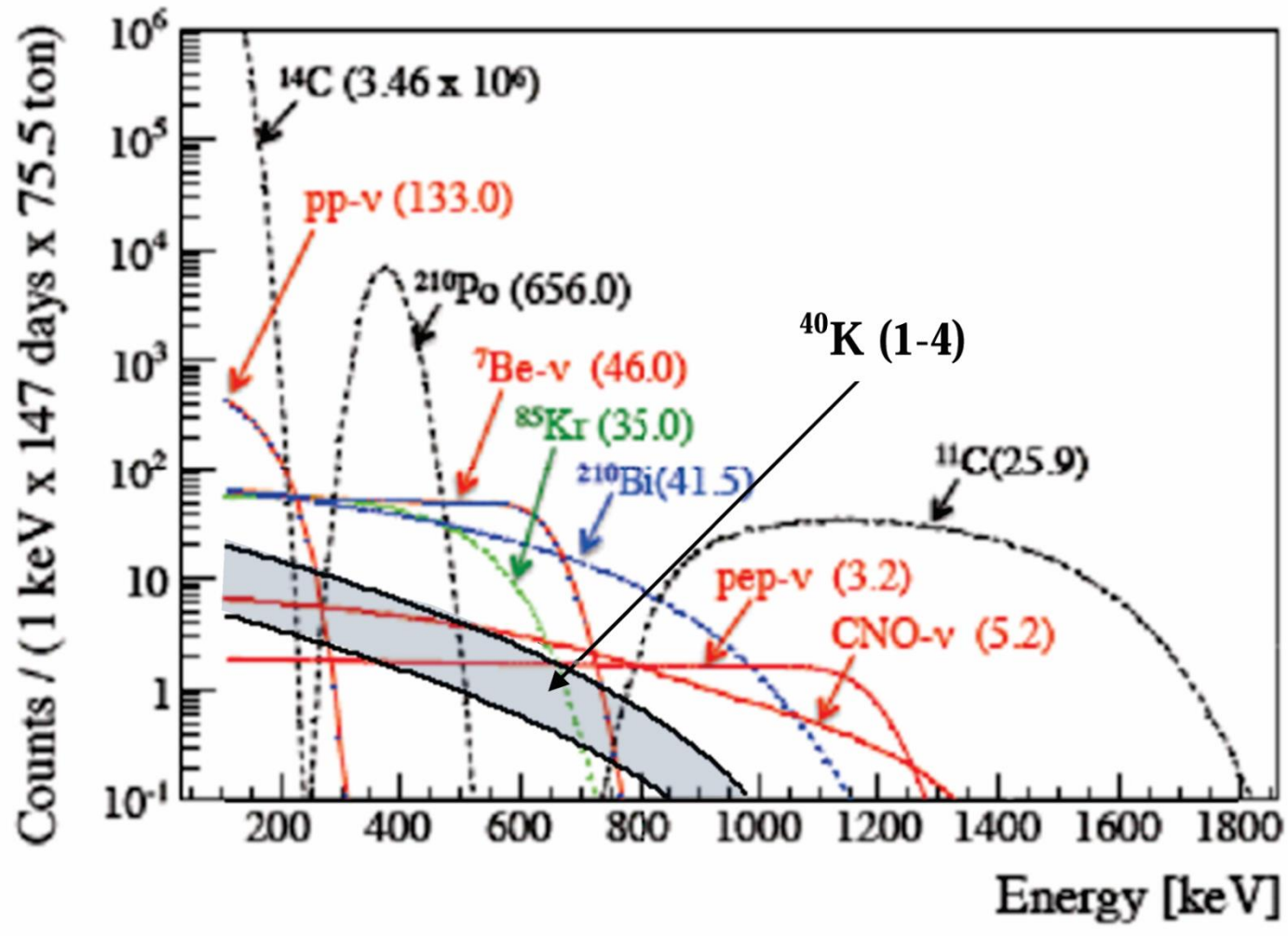

Limits on heat flux from geoν data in the frame of HE model

- U and Th geoν data allow to explain the heat flux up to H = 50 TW without contradiction with data.
- Borexino limit on K geoν flux $M(K)/M_{earth}$ = 4% allow to explain up to H = 600 TW.

Conclusion

- Borexino and KamLAND detectors should be operated more than 1000 and 400 years respectively to get enough statistics for doing appropriate analysis of geoneutrino fluxes.
- It is strongly needed detector with 10 kt target to accumulate at least 4000 events in observable time (10 y.)

- ^{40}K could not be detected by existing detectors.
- Borexino background should be reduced.
- Independent CNO spectrum measurement is desirable to get ^{40}K spectrum.

Our choice

- K → 2%
- H = 300 TW
- Hydride Earth model

Can HE model help to explain the other unusual experimental results and to give unusual predictions?

Yes

- We have developed New model of Earth electric field on the base of HE, which can explain all exp. data and can predict the new facts.
- We observed the predicted fact: The Earth crust (continents and ocean) saturates by positive ions (protons).
- The Pierre Auger telescope registration of Earthquake is the example of unusual result which HE model helps to explain.

Atmospheric electricity

According to Ch. Wilson the Earth and ionosphere compose spherical capacity charged by thunder clouds. Potential difference between them is a source of Earth electric field.

Opened questions

- Where is negative charge of Earth capacity?
- How is it possible to explain unitary variation of fine weather global electric field?
- Why during earthquakes atmospheric electric field is growing? And why high energy electrons are emitted from radiation belt?
- Is there a link between electric and magnetic Earth fields?
- What are the telluric currents?

Earth electrical currents in the HE model

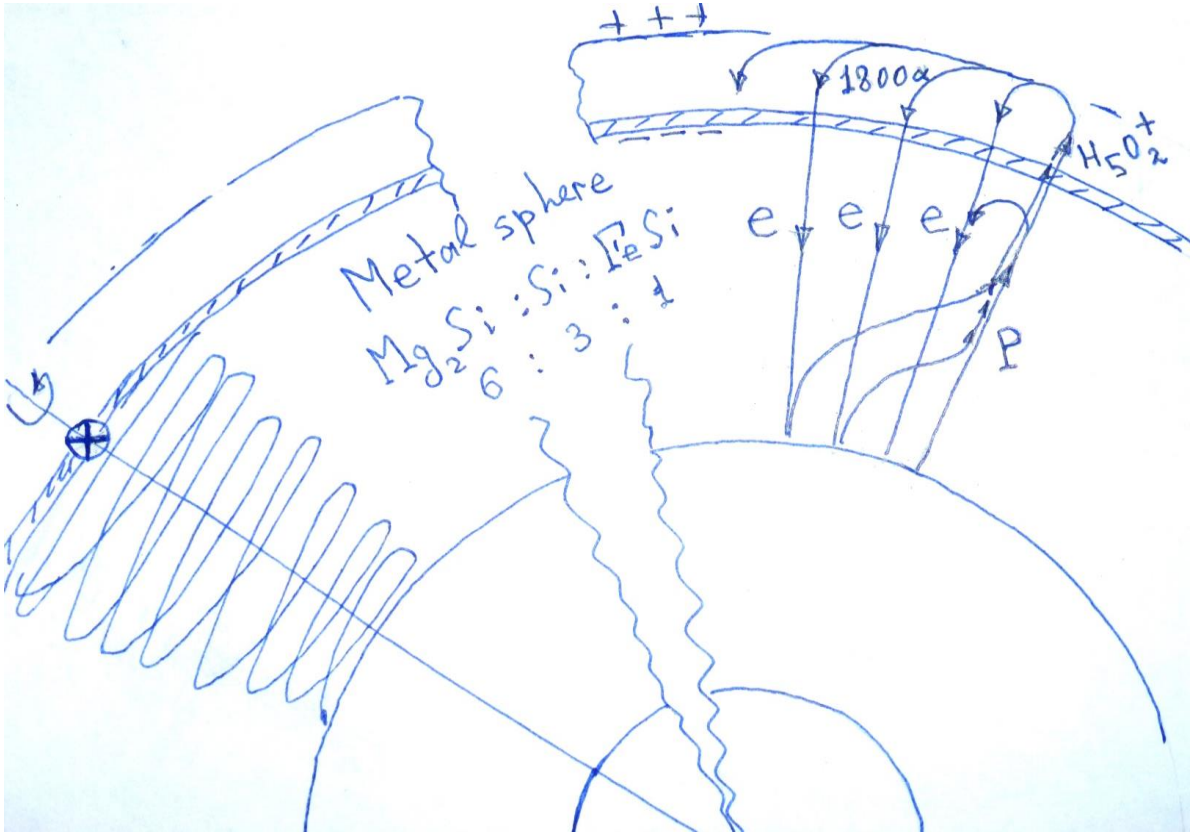

Hydridic theory of Earth electric field

- The negative charge of “Earth capacitor” locates under Earth crust.
- The Earth crust (continents and ocean) saturates by positive ions (protons).
- The gases going up from the Earth crust to atmosphere are positive charged. This gases can charge the “Earth capacitor”.
- The underground discharge can originate the earthquakes.

Hydroxonium ions are created in atmosphere as a result of chemical reactions

- $O_2^+ + (H_2O)_n \rightarrow O_2^+(H_2O)_n$
- $NO^+ + (H_2O)_n \rightarrow NO^+(H_2O)_n$

- $O_2^+(H_2O)_n \rightarrow H_3O^+(OH^\cdot)(H_2O)_{n-2} + O_2$
- $NO^+(H_2O)_n \rightarrow H_3O^+(H_2O)_{n-2} + HNO_2$

Mozumander, Y.Hatano Charged particles and photon interactions with matter, CRC Press 2003.

H.Dolezalek, R.Reiter Electrical Processes in atmospheres: proceedings of the fifth international held at Garmisch-Partenkirchen (Germany), 2–7 September 1974 pp 45-52.

Hans Volland, Handbook of atmospheric electrodynamics, t.1, CRC Press, 1995.

One day unitary variation of electric field tension as a function of Greenwich time: ocean surface (*1*), poles (*2*) and area of thunderstorms (*3*).

R. Feynman, R. Leighton and M. Sans. The Feynman lectures on physics. V. 2. Electricity and Magnetism. Addison-Wesley Publishing company, Inc. Reading, Massachusetts, Palo Alto, London, 1964.

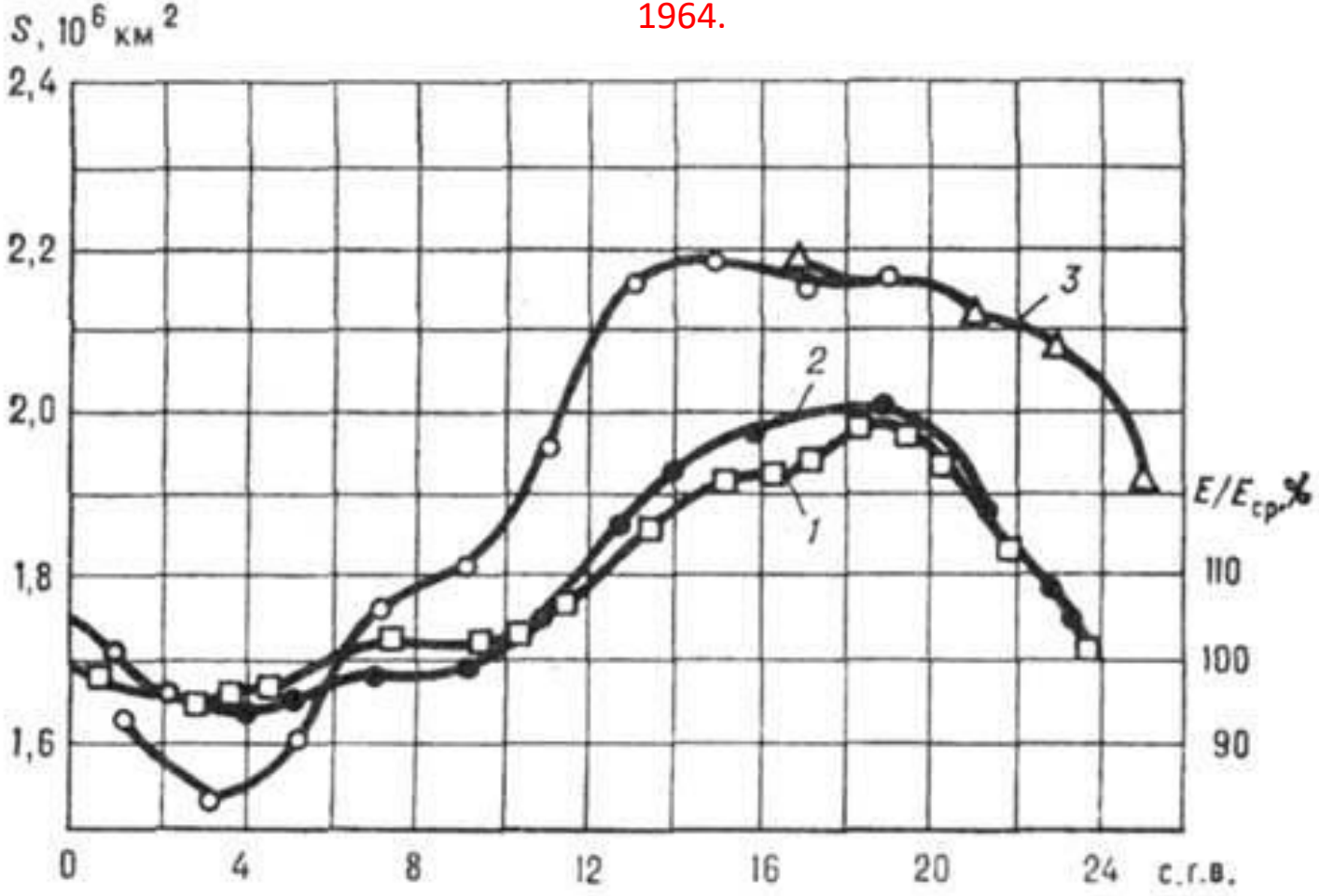

Abnormal daily wave of «good weather field» in mountain valley

A. S. Lidvansky, N. S. Khaerdinov

Institute for Nuclear Research, Moscow

VII Russian Proceedings of Conference on athmospheric electricity, September, 24-28, 2012, S-Petersburg, Russia, p. 155-157

Earth electric field at BNO in good weather 19, 20, 21, 22, 23, 27 September 2007. Local time. Averaging on 20sc.

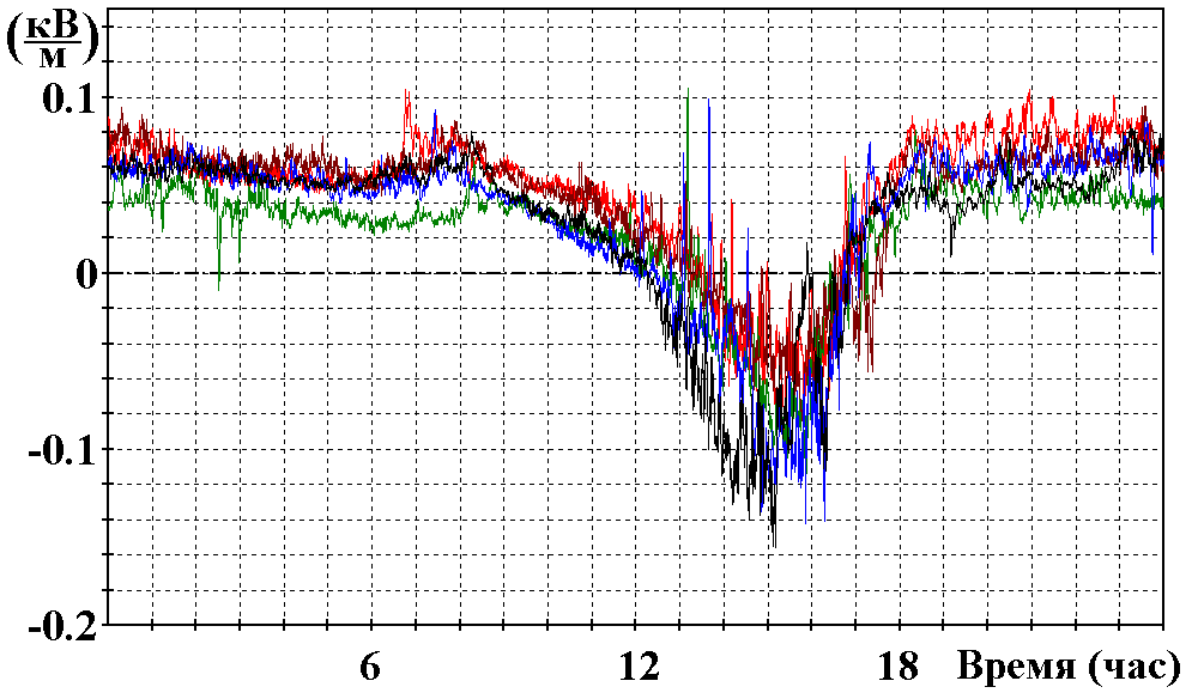

Baikal lake expedition INR RAS

GEOPHISYCAL MOORING

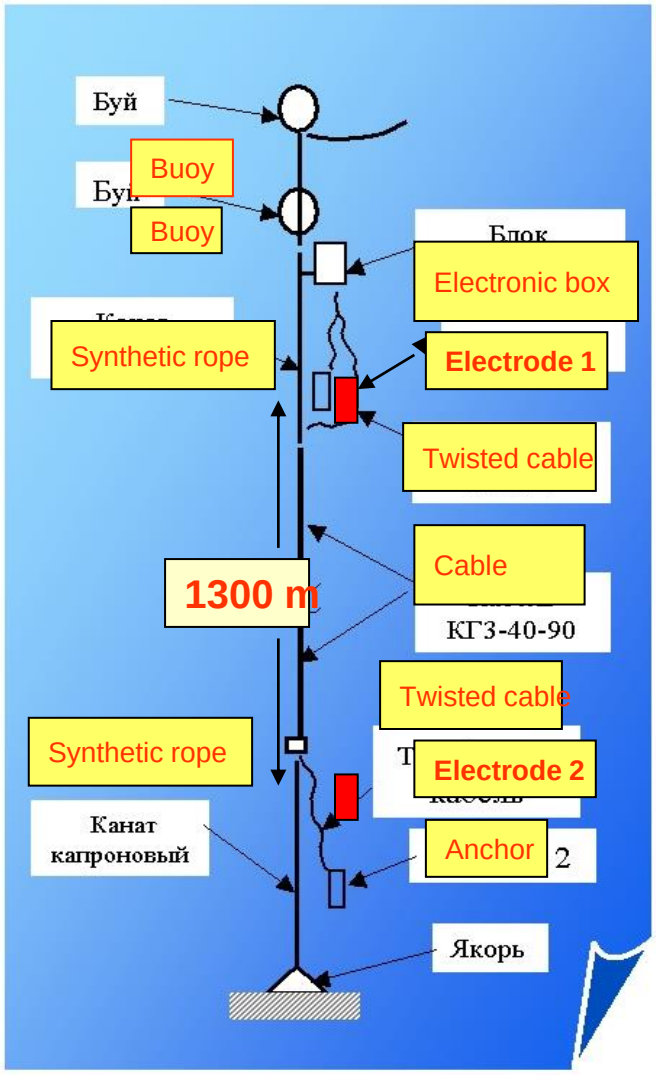

Surface – bottom electric potential difference

22 – 30 August 2008 year.

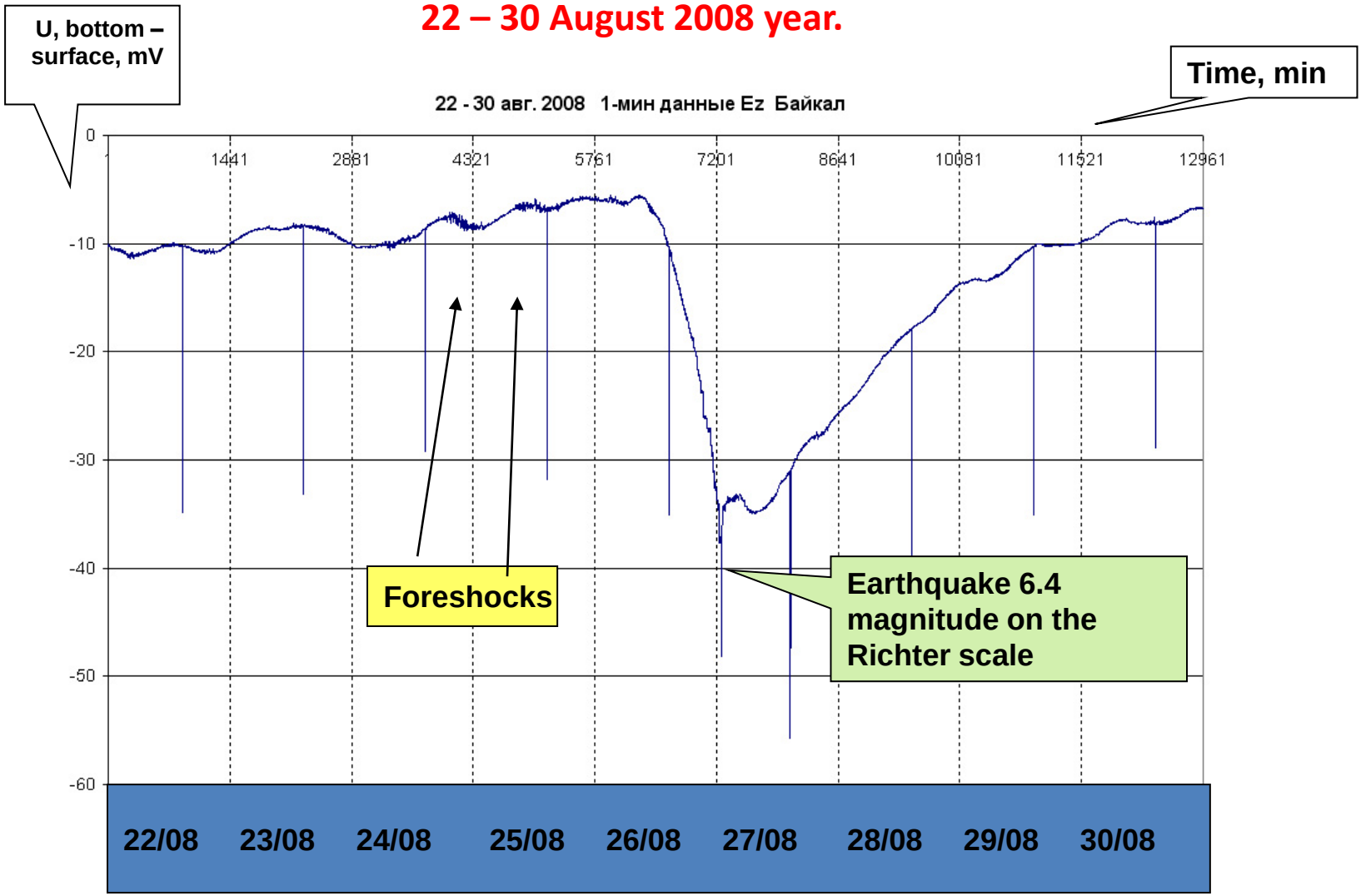

Observation of exceeding positive ions concentrations in under ground rooms by use of Air ions counter «Сапфир 3М»

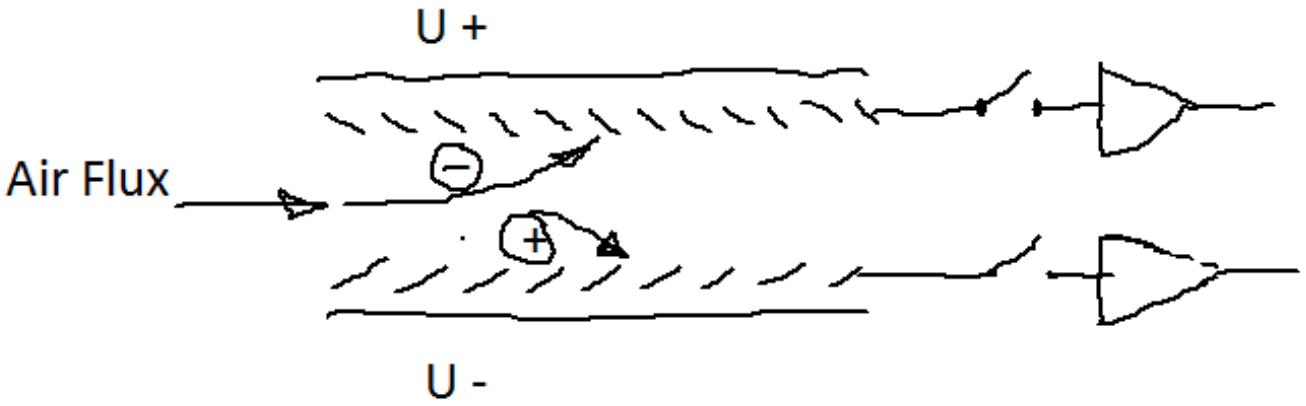

Air ion counter is in INR underground lab. (Moscow)

Number of positive ions - $5 \cdot 10^6$ ion/cm^3

Air ions in underground laboratories.

- At underground lab. of Baksan Neutrino Observatory we found the air ions in amounts up to 3 000 000 ions/cm^3
- In Moscow in non ventilated underground rooms - up to 10 000 000 ions/cm^3

Proceedings of ICRC 2011. Vol.11, 467-470

32ND INTERNATIONAL COSMIC RAY CONFERENCE, BEIJING 2011

Measurement of Low Energy Cosmic Radiation with the Water Cherenkov Detector Array of the Pierre Auger Observatory

HERNÁN ASOREY[1] FOR THE PIERRE AUGER COLLABORATION[2]
[1]*Centro Atómico Bariloche (CNEA), U. N. de Cuyo and U. N. de Río Negro, Bariloche, Río Negro, Argentina*
[2]*Observatorio Pierre Auger, Av. San Martín Norte 304, 5613 Malargüe, Argentina*

The Surface Detector Array

One of the 1 660 water-Cherenkov detectors (WCD) of the Pierre Auger Observatory, located near Malargüe, Argentina (69.3° W, 35.3° S, 9.5 GV) at 1400 m a.s.l.

- 3 000 km^2 array
- 1 660 water-Cherenkov detectors (WCD) (16 600 m^2 of detection area)
- triangular grid with 1 500 m spacing
- Cherenkov detector:
  - 12 m^3 of high purity water
  - three 9" photomultipliers (PMT)
  - Detection of $e^{\pm}$ and γ: calorimetric
  - $\mu^{\pm}$ signals: proportional to track length.

Low energy cosmic ray measurements using individual detectors

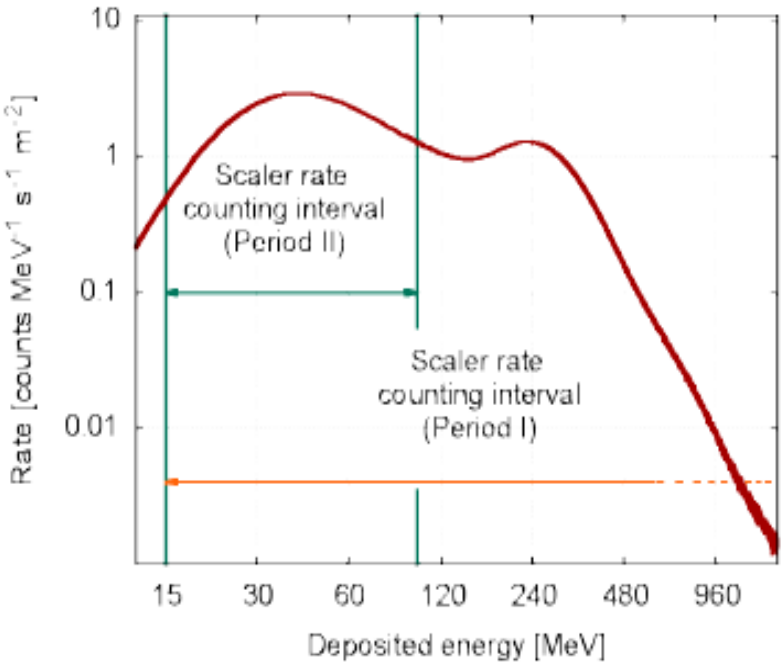

Charge histogram of the signals of one PMT, with the corresponding counting intervals of the scaler mode:

- Period I (orange): $15 \leq (E_d/\mathrm{MeV}) < \infty \rightarrow 380\ \mathrm{m^{-2}\ s^{-1}}$
- Period II (green): $15 \leq (E_d/\mathrm{MeV}) \leq 100 \rightarrow 200\ \mathrm{m^{-2}\ s^{-1}}$

Scaler mode

- Counting event rate between two thresholds;
- period I: Mar to Sep 2005, period II: After Sep 2005.
- rate excess → search for astrophysical transients:
  - Gamma Ray Bursts
  - Forbush decreases
  - Soft Gamma Repeaters

Histogram mode

- Every WCD constantly records one-minute histograms of signals (amplitude and total charge).
- 2$^{\mathrm{nd}}$ peak → (1.03 ± 0.02) of the energy deposited (E_d) by a vertical muon ($E_d \simeq 240$ MeV).
- $\sim$ 10 one-minute histograms are registered at the central DAQ every minute.

Chile Feb 2010 earthquake

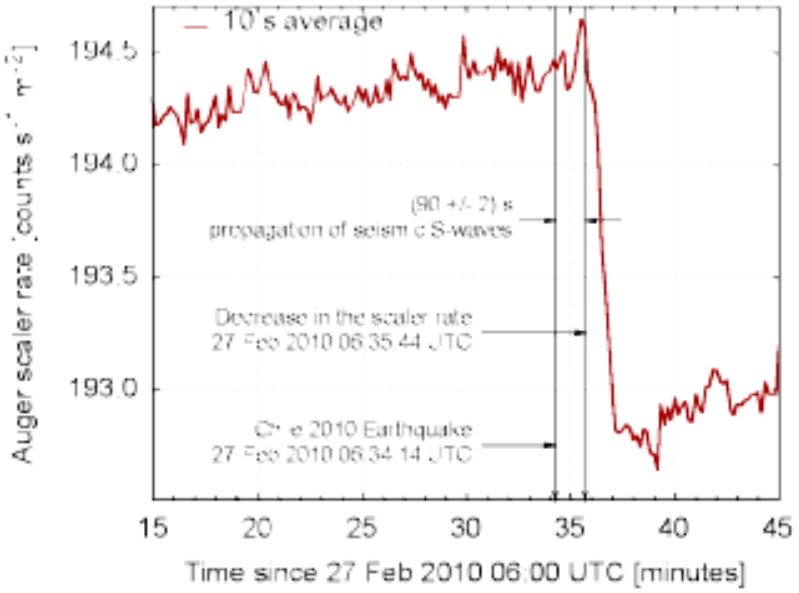

- Magnitude 8.8 on Richter scale
- epicentre at 300 km SW from array
- seismic S-waves propagation observed
- 24σ decrease, recovery time: 6 hours

Воронки на Ямале

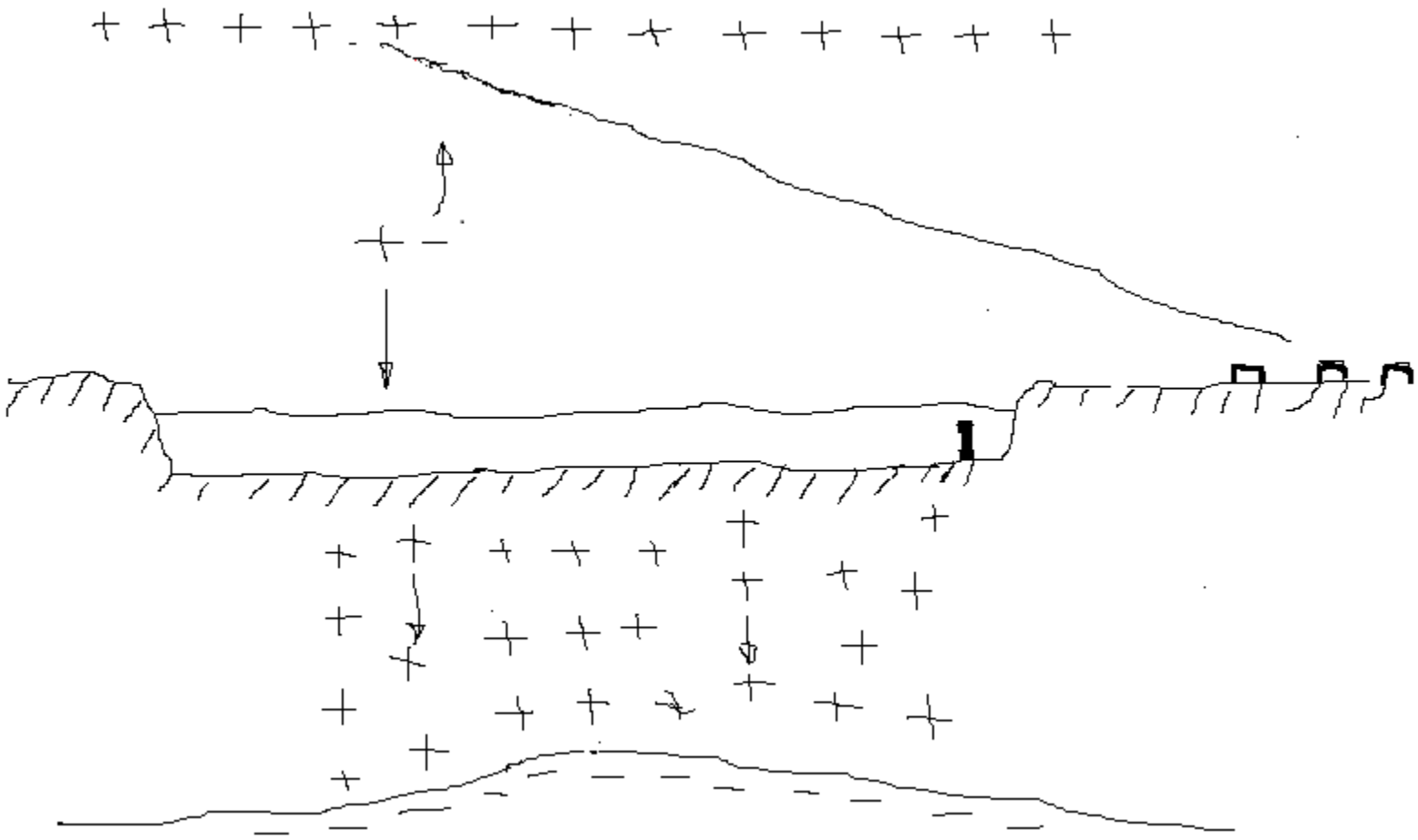

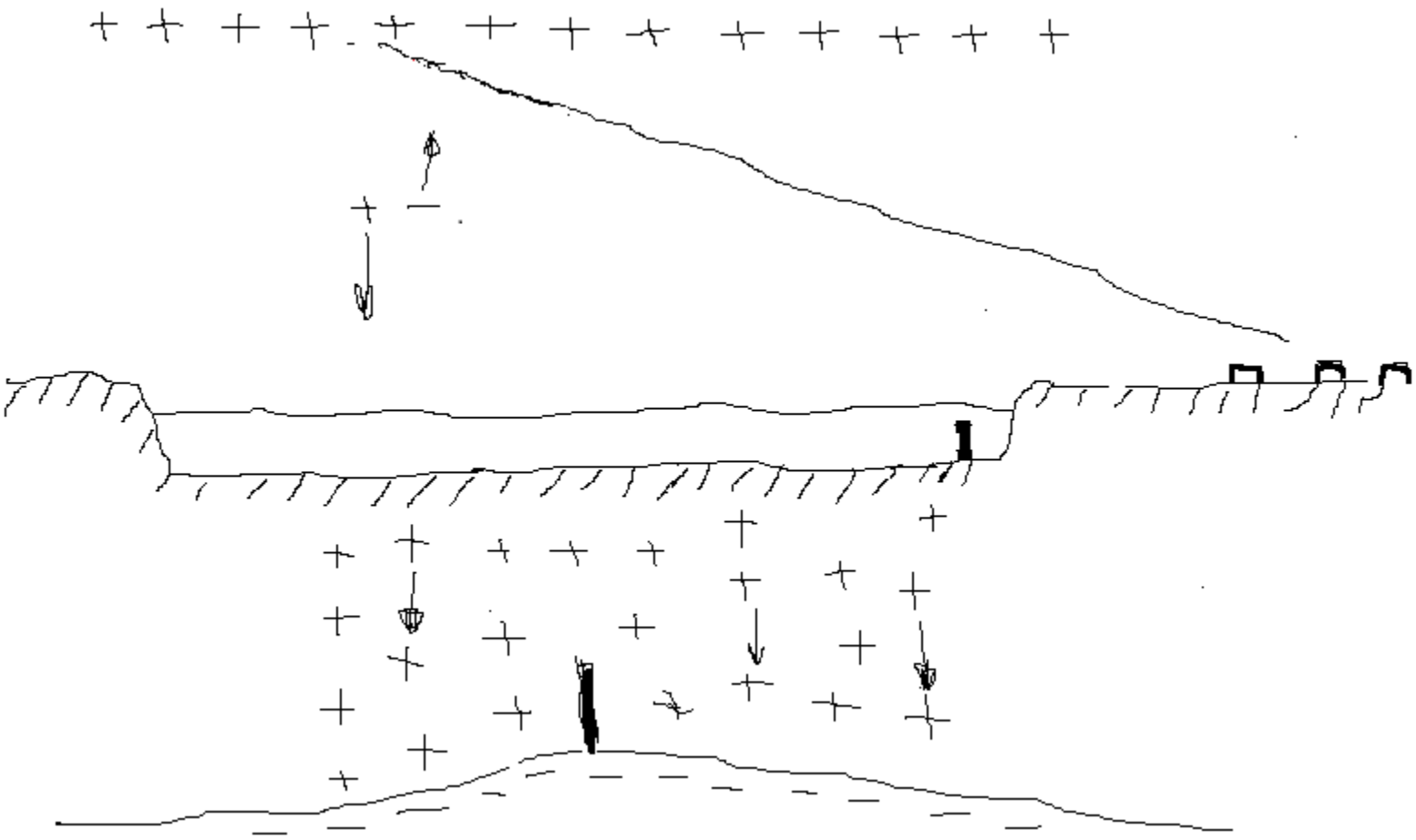

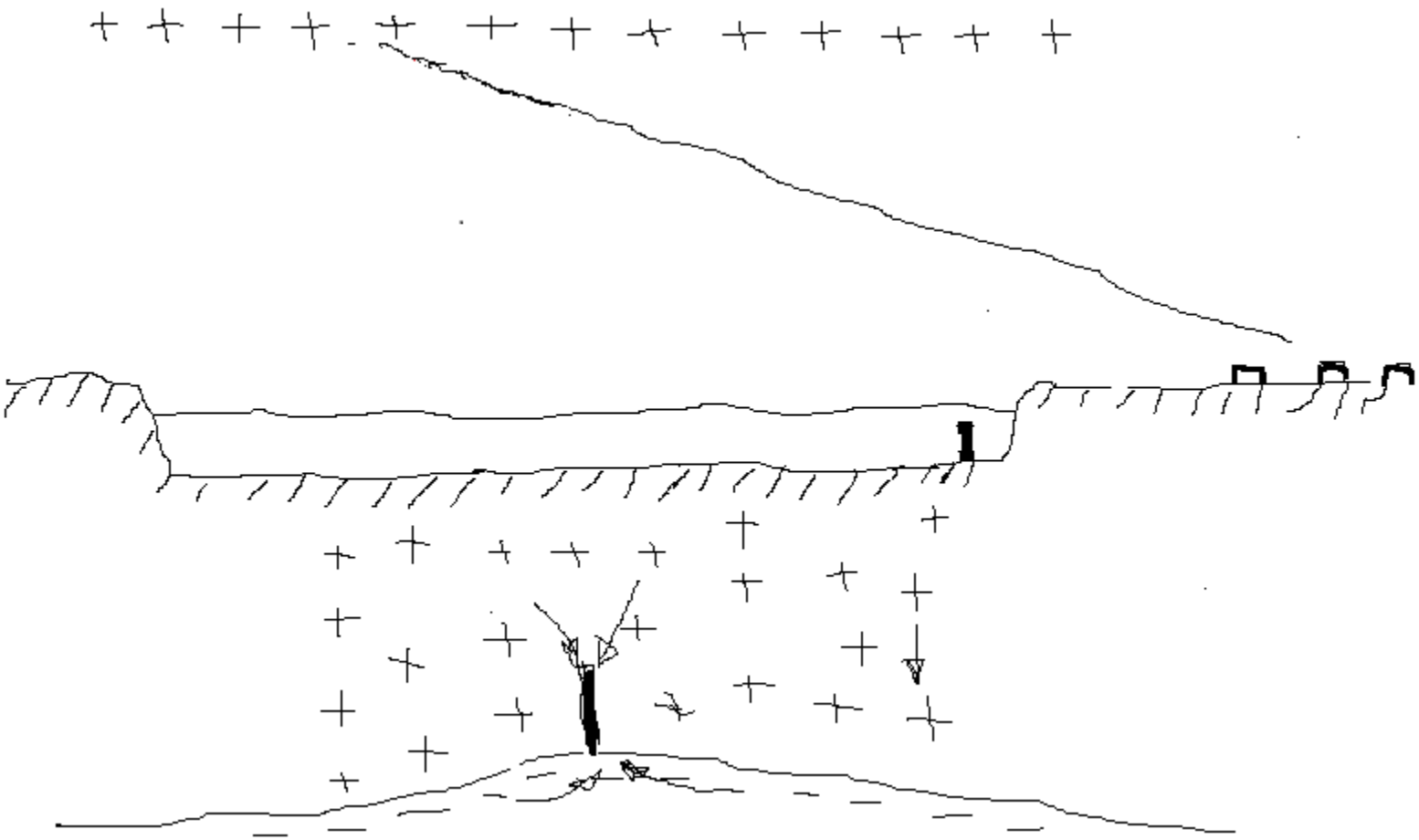

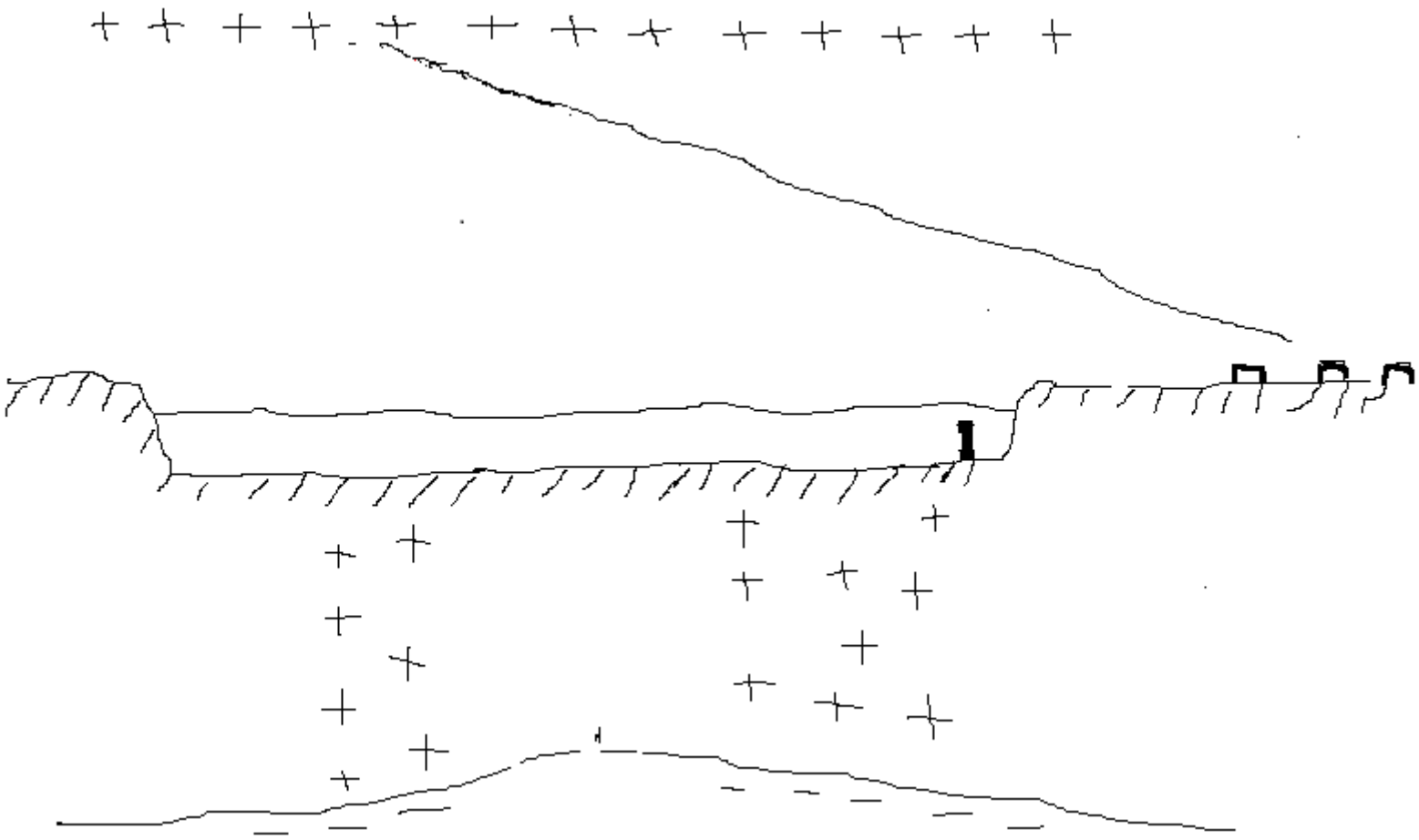

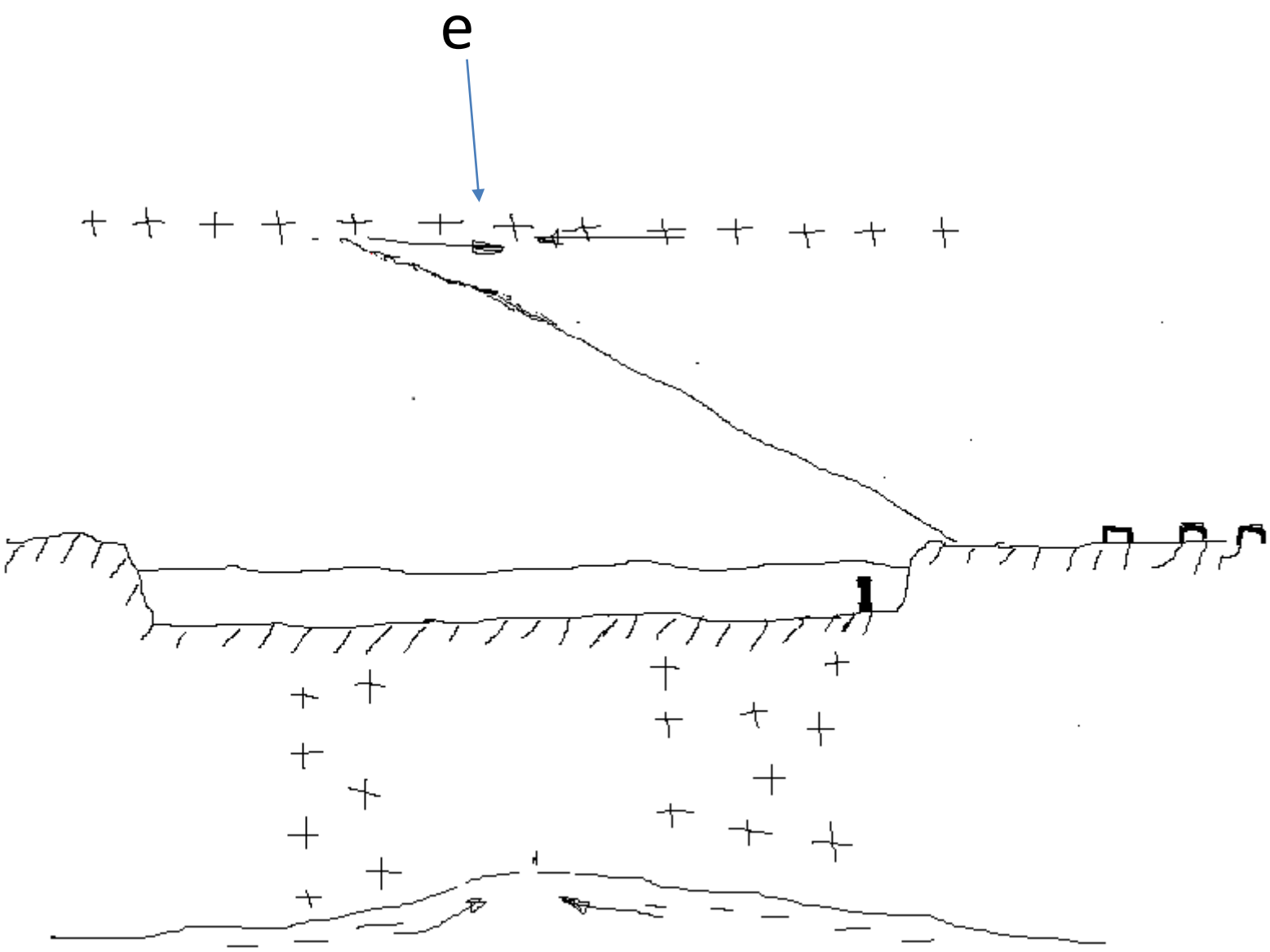
e

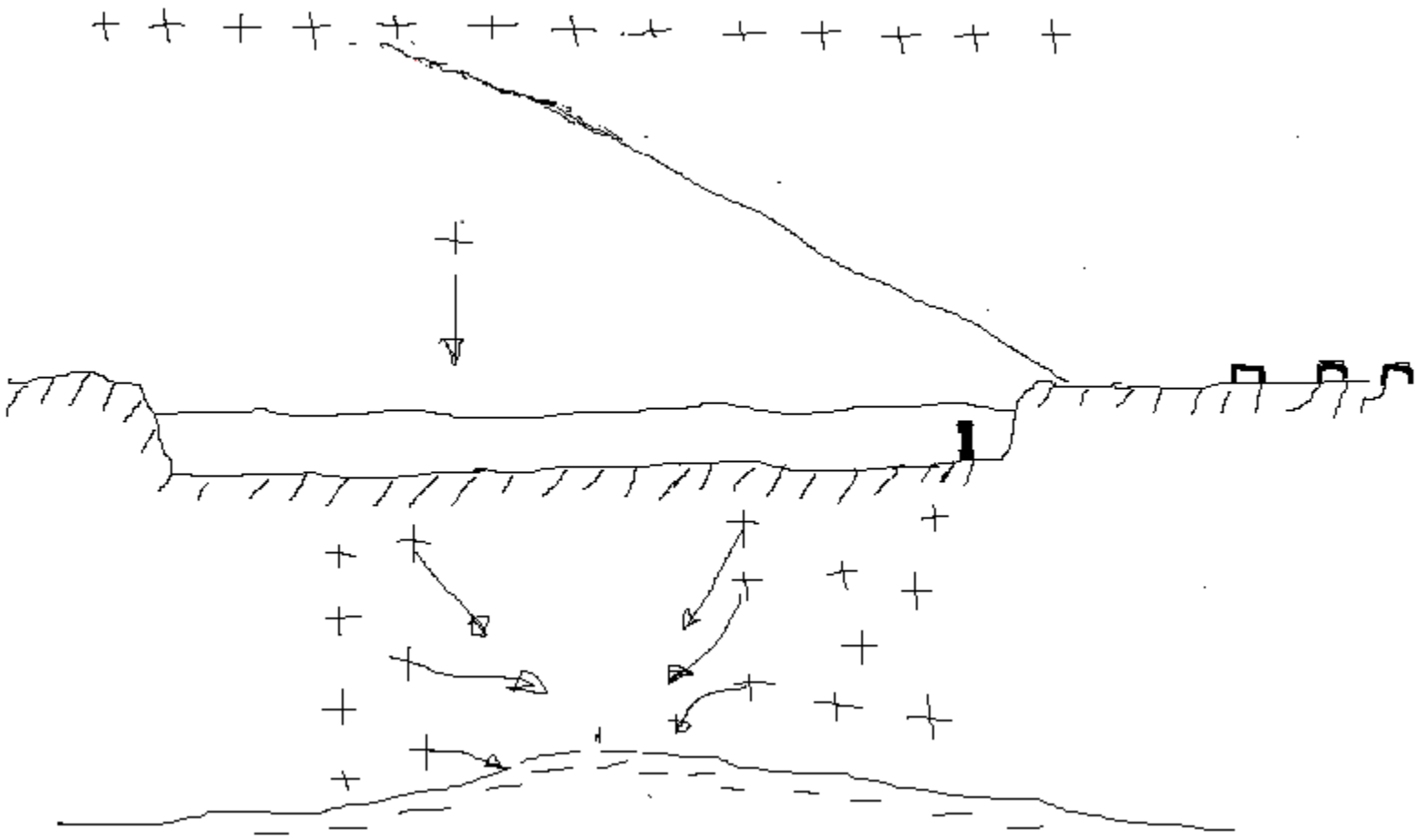

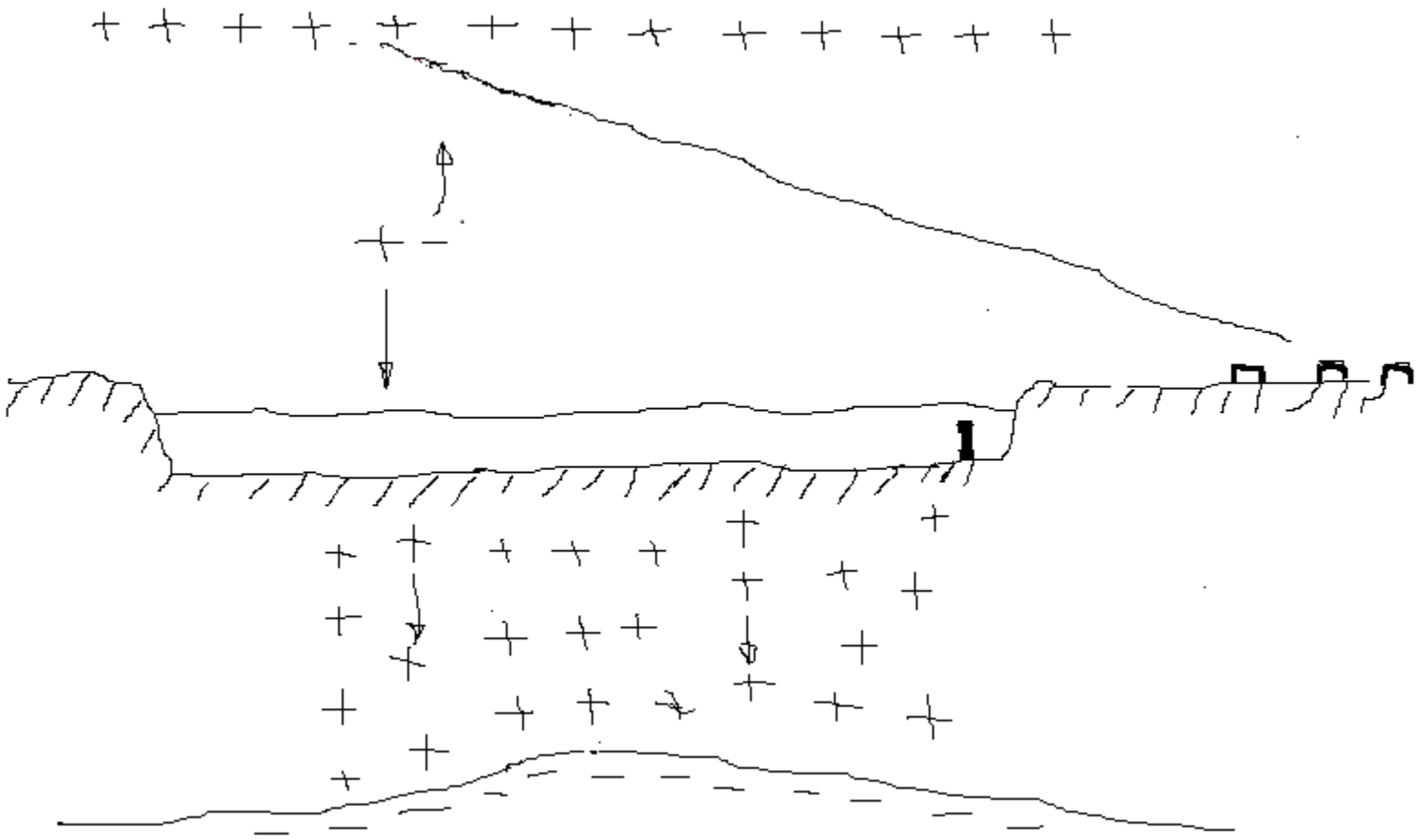

Earthquake in framework of HE model.

- Underground discharge could be a reason of earthquake.
- Vertical proton currents could be increased before the earthquake. They are precursors of earthquake.
- At the moment of earthquake the recombination of positive and negative charges could take place under the Earth crust.
- Negative charge is reconstructed in 100 sec, but total charge of the crust could be reconstructed sufficiently longer – up to several days, what causes increasing of Earth electric field in atmosphere on factor 100 or more.

Unitary electric field variation in framework of HE model.

- It might be explained by the air masses going up when heating by the Sun in regions of rifts, say Pacific region. In Pacific region the noon happens at the moment when in Greenwich 6 a.m.

Global map of the flow of heat, in mWm^{-2}, from Earth's interior to the surface. Higher heat flows are observed at the locations of mid-ocean ridges, and oceanic crust has relatively higher heat flows than continental crust.

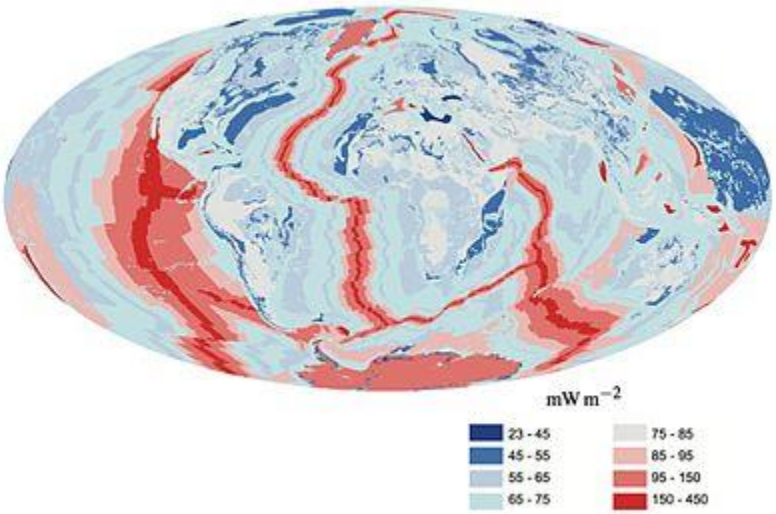

New

- 300 TW
- We observed the predicted fact: The Earth crust (continents and ocean) saturates by positive ions (protons).
- New Earth electric field Новая модель model on the base of HE model is the instrument for earthquake predictions.

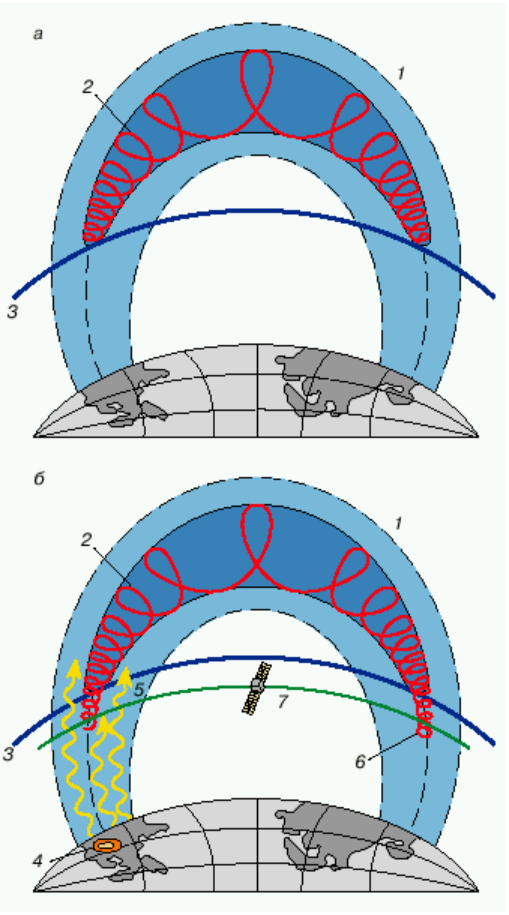

Рис. 5. а) - стационарная траектория заряженной частицы в радиационном поясе: 1 - геомагнитное поле, 2 - траектория частицы, 3 - нижняя граница радиационного пояса; б) - высыпания частиц из СЭМИ радиационного пояса после взаимодействия с ЭМИ сейсмического происхождения: 1 - геомагнитное поле, 2 - траектория частицы, 3 - нижняя граница радиационного пояса, 4 - очаг землетрясения, 5 - электромагнитное излучение, 6 - высыпающиеся частицы, 7 - траектория спутника.

Высыпание высокоэнергичных электронов НЕ модель

- Причина – скопление положительно заряженных ионов в ионосфере над областью землетрясения
- Высыпание может начаться раньше (часы) землетрясения и будет продолжаться долго (десятки часов) до рассасывания скопления ионов
- НЕ модель – инструмент для исследования Бразильской анамалии.

Прохождение южно-бразильской магнитной аномалии

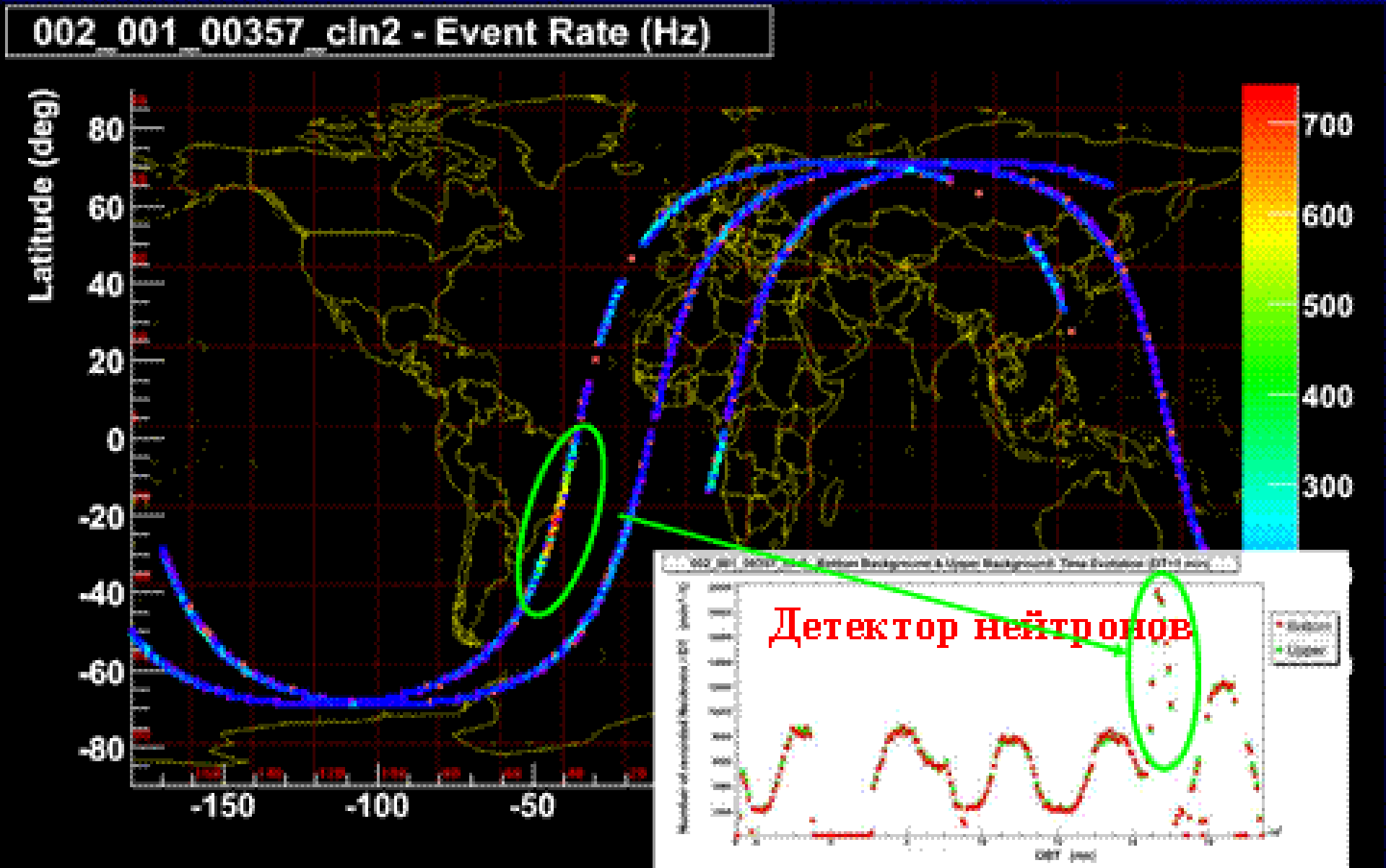

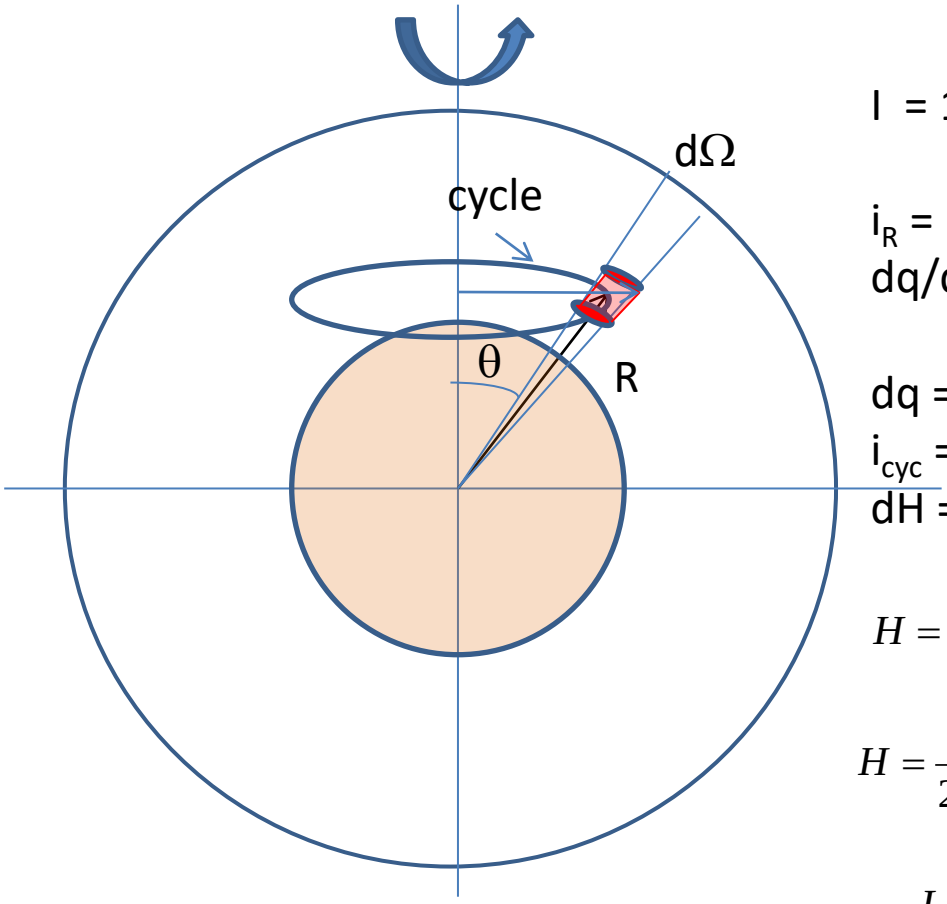

I = 1800 A

$i_R = I/4\pi\, d\Omega$

$dq/dR = i_R / v$

$dq = I/4\pi v\, d\Omega dR$

$i_{cyc} = dq/T$, T – day

$dH = i_{cyc}/2R\sin\theta$

$$H = \frac{I}{4\pi}\frac{1}{Tv}\frac{1}{2}\int\frac{d\Omega dR}{R\sin\theta}$$

$$H = \frac{I}{2vT}\int_0^{\pi/2}\frac{d\theta}{\sin\theta}\int_{R1}^{R2}\frac{dR}{R}$$

$$H = \frac{I}{2vT}\ln\frac{R2}{R1}\ln\left|tg\frac{\pi}{4}\right|$$

$$H = H_+ - H_- = C\left(\frac{1}{v_+} - \frac{1}{v_-}\right), C = 0.00378$$